

**Evaluation of UV-PCO Technology and By-Products Generation in  
Full-Scale Open Test Rig**

Donya Farhanian

A Thesis

in

The Department

of

Building, Civil and Environmental Engineering

Presented in Partial Fulfillment of the Requirements

for the Degree of Master of Applied Science at

Concordia University

Montreal, Quebec, Canada

August 2012

© Donya Farhanian 2012

# Concordia University

## School of Graduate Study

This is to certify that the thesis prepared

By: **Donya Farhanian**

Entitled: **Evaluation of UV-PCO Technology and By-Products Generation in Full-Scale Open Test Rig**

And submitted in partial fulfillment of the requirements for the degree of

### **Master of Applied Science**

complies with the regulations of the University and meets the accepted standards with respect to originality and quality.

Signed by the final examining committee:

<u><b>Dr. C. Mulligan</b></u>	Chair
<u><b>Dr. L. Wang</b></u>	Examiner
<u><b>Dr. H. D. Ng</b></u>	Examiner
<u><b>Dr. F. Haghightat</b></u>	Supervisor

# **ABSTRACT**

## **Evaluation of UV-PCO Technology and By-Products Generation in Full-Scale Open Test Rig**

**Donya Farhanian**

The quantity of the outdoor air for building ventilation has a direct negative effect on the building energy cost and the environment. Also, there are plenty of pollutants in an indoor environment which affect building occupants' health and comfort. This is one of the concerns in design of sustainable buildings which leads to a balancing act between indoor air quality (IAQ) and energy cost.

Ultraviolet photocatalytic oxidation (UV-PCO) is regarded as one of the salient technologies for decomposition of pollutants, especially volatile organic compounds (VOCs) and a viable alternative to activated carbon filters. Majority of the previous research on UV-PCO was performed in an ideal bench top reactor and in ppm range of VOCs. Also, limited research has been devoted to investigate the generation of UV-PCO toxic by-products while this issue is one of the main drawbacks in design of sustainable buildings.

The objectives of this study were to: (1) Develop a methodology for determining the performance of UV-PCO technology using full scale experimental set-up; (2) Qualification and quantification of generated by-products; (3) Comparing UV-PCO performance either in presence or absence of ozone, and (4) Investigating the impact of operational parameters.

Results showed UV-PCO method has better performance in presence of ozone using VUV lamps, although some by-products generated only in presence of ozone. It was found that among tested VOCs, ethanol and 1-butanol generated more by-products, especially acetaldehyde. Some toxic compounds including formaldehyde and acetaldehyde were generated in all cases. Increment of flow rate and relative humidity, decreased the UV-PCO performance for ethanol oxidation. System performance was significantly improved by increasing the number of reactors.

To my husband and my parents

## ACKNOWLEDGMENT

First of all, I wish to express my gratitude appreciation and respect to my supervisor, Dr. Fariborz Haghighat, for his continuous support, inspiration and valuable guidance during my graduate study. I would also like to acknowledge his efforts for establishing a very friendly and stimulating atmosphere in the Indoor Air Cleaning Group.

My sincere appreciation extends Dr. Chang-Seo Lee who served as an unofficial co-advisor and offered many enlightened ideas and comments, invaluable feedbacks, creative innovativeness, valuable discussions and constructive suggestions and help throughout this project.

I am thankful for the financial support by the Natural Science and Engineering Research Council of Canada (NSERC) and Circul-aire Inc.

Very special thanks go out to my colleagues in our research group: Lexuan Zhong, Alireza Aghighi and Mitra Bahri who their valuable assistance and friendship means a lot to me.

It gives me immense pleasure to thank my parents for their perpetual love and encouragement. Nothing I say can do justice to how I feel about their support. I feel very lucky to have a family that shares my enthusiasm for academic pursuits.

I am indebted to my husband Walid Masoudimansour and I owe my heartfelt thanks and love to him for his personal dedication, enthusiasm in sharing his knowledge and providing valuable feedback and cooperation at various stages of this work.

Lastly, I want to thank God for the endless supply of hope that provided me with courage and guidance throughout my life and academic studies.

# TABLE OF CONTENT

<b>ABSTRACT</b> .....	<b>iii</b>
<b>ACKNOWLEDGMENT</b> .....	<b>v</b>
<b>LIST OF FIGURES</b> .....	<b>x</b>
<b>LIST OF TABLES</b> .....	<b>xiii</b>
<b>LIST OF ABBREVIATIONS</b> .....	<b>xiv</b>
<b>LIST OF SYMBOLS</b> .....	<b>xvi</b>
<b>CHAPTER 1 INTRODUCTION</b> .....	<b>1</b>
1.1 BACKGROUND .....	1
1.1.1 <i>Indoor Air Quality</i> .....	2
1.1.2 <i>Air Cleaners</i> .....	5
1.1.2.1 <i>Mechanical filters</i> .....	5
1.1.2.2 <i>Ultraviolet germicidal irradiation (UVGI)</i> .....	7
1.1.2.3 <i>Electronic air cleaner</i> .....	7
1.1.2.4 <i>Solid sorbents</i> .....	8
1.1.2.5 <i>Ozone generators</i> .....	9
1.1.2.6 <i>Photocatalytic oxidation</i> .....	9
1.2 RESEARCH OBJECTIVES .....	10
1.3 THESIS OUTLINE AND PUBLICATIONS .....	11
<b>CHAPTER 2 LITERATURE REVIEW</b> .....	<b>12</b>
2.1 INTRODUCTION .....	12
2.2 PHOTOLYSIS .....	12
2.2.1 <i>Direct UV Photolysis</i> .....	13
2.2.2 <i>Sensitized Photolysis</i> .....	14
2.3 PHOTOCHEMICAL OXIDATION WITH OZONE.....	14
2.4 PHOTOCATALYTIC OXIDATION (PCO).....	17

2.4.1	<i>Photocatalytic Oxidation Mechanism</i> .....	19
2.4.2	<i>Photocatalytic Oxidation Advantages</i> .....	22
2.4.3	<i>Photocatalytic Oxidation Disadvantages</i> .....	23
2.5	CATALYST.....	23
2.5.1	<i>Modification of Photocatalyst</i> .....	26
2.5.2	<i>Catalyst Deactivation and Regeneration</i> .....	28
2.6	UV-LIGHT LAMPS .....	30
2.7	INTERMEDIATES AND BY-PRODUCTS .....	31
2.8	OPERATIONAL PARAMETERS AFFECTING PCO PROCESS .....	33
2.8.1	<i>Humidity</i> .....	33
2.8.2	<i>Oxygen Content</i> .....	35
2.8.3	<i>Temperature</i> .....	36
2.8.4	<i>Flow Rate</i> .....	37
2.8.5	<i>Light Intensity</i> .....	38
2.8.6	<i>Presence of Other Compounds</i> .....	39
2.8.7	<i>Pressure</i> .....	40
2.9	RELATED WORKS.....	41
<b>CHAPTER 3 EXPERIMENTAL SET-UP AND METHODOLOGY .....</b>		<b>44</b>
3.1	INTRODUCTION .....	44
3.2	CHEMICALS AND REAGENTS .....	44
3.3	GENERATION SET-UP OF REAGENTS .....	46
3.4	ANALYTICAL INSTRUMENTS.....	47
3.4.1	<i>High-Performance Liquid Chromatography (HPLC)</i> .....	48
3.4.2	<i>Auto-Sampler</i> .....	50
3.4.3	<i>Multi-Gas Photoacoustic Detector</i> .....	50
3.4.4	<i>Ozone Analyzer</i> .....	50
3.5	INSTRUMENT CALIBRATION.....	50
3.5.1	<i>Sampling Pumps Calibration</i> .....	51

3.5.2	<i>Multi-Gas Photoacoustic Detector</i>	51
3.5.3	<i>HPLC Calibration</i>	52
3.6	DUCT TEST RIG SPECIFICATIONS	53
3.7	ENVIRONMENTAL CONDITION MEASUREMENT	60
3.8	EXPERIMENTAL METHODOLOGY AND PROCEDURE	60
3.8.1	<i>Removal Efficiency</i>	62
3.8.2	<i>Net By-product Concentration</i>	63
<b>CHAPTER 4 EXPERIMENTAL RESULTS AND DISCUSSION</b>		<b>64</b>
4.1	INTRODUCTION	64
4.2	UV-PCO PERFORMANCE AND BY-PRODUCTS GENERATION USING DIFFERENT CLASSES AND CONCENTRATIONS OF VOCs	64
4.2.1	<i>Alcohol VOCs</i>	64
4.2.2	<i>Alkane VOCs</i>	69
4.2.3	<i>Ketone VOCs</i>	73
4.2.4	<i>Aromatic VOCs</i>	76
4.2.5	<i>All Groups of VOCs</i>	80
4.3	PARAMETRIC STUDY OF THE UV-PCO SYSTEM	82
4.3.1	<i>Repeatability Test</i>	83
4.3.2	<i>Concentration Effect</i>	83
4.3.3	<i>Effect of Relative Humidity</i>	83
4.3.4	<i>Effect of Flow Rate</i>	85
4.3.5	<i>Effect of Number of Lamps (Irradiance)</i>	87
4.3.6	<i>Removal Efficiency Improvement</i>	88
<b>CHAPTER 5 CONCLUSIONS AND FUTURE WORK</b>		<b>90</b>
5.1	SUMMARY	90
5.2	CONCLUSIONS AND MAJOR FINDINGS	90
5.3	LIMITATIONS OF THE PRESENT STUDY	94
5.4	RECOMMENDATIONS FOR FUTURE WORK	94

<b>References .....</b>	<b>96</b>
<b>Appendix A: VOCs Injection Rate Calculation Using Syringe System Injection...</b>	<b>104</b>
<b>Appendix B: HPLC and B&amp;K Calibration Equations .....</b>	<b>105</b>
<b>Appendix C: Ozone Concentration in Downstream of Ducts.....</b>	<b>106</b>
<b>Appendix D: Light Intensity of the UV-lamps in Catalyst Surface.....</b>	<b>109</b>

## LIST OF FIGURES

Figure 1-1 Mechanical filter and their installation .....	6
Figure 2-1 Mass transfer mechanism in UV-PCO process .....	20
Figure 2-2 Photocatalytic oxidation molecular process .....	21
Figure 2-3 Structures of rutile and anatase types of TiO <sub>2</sub> .....	24
Figure 2-4 Band gaps and VB and CB edges of common semiconductors and standard redox potentials versus NHE (NHE: normal hydrogen electrode) of the (O <sub>2</sub> /O <sub>2</sub> <sup>•-</sup> ) and (•OH/¯OH) redox couple .....	26
Figure 2-5 Schematic diagrams of the beam techniques. ....	28
Figure 2-6 Catalyst deactivation: a) Sintering b) Fouling or coking c) Poisoning ....	29
Figure 2-7 Water and oxygen molecules adsorb at different active sites. ....	36
Figure 2-8 Schematic diagram of UVPCO reactor showing arrangement of four photocatalytic monoliths and three banks of three UVA lamps .....	42
Figure 3-1 Low concentration generation system setup .....	47
Figure 3-2 High-performance liquid chromatography (HPLC).....	49
Figure 3-3 a)Supelco Lp-DNPH b) Lp-DNPH cartridges Ozone Scrubber (KI Ozone scrubber) .....	49
Figure 3-4 High flow rate sampling pump calibration setup. ....	51
Figure 3-5 Multi-gas photoacoustic detector calibration set-up. ....	52
Figure 3-6 Duct test rig picture .....	54
Figure 3-7 Duct apparatus dimensions .....	54
Figure 3-8 a)Open test rig apparatus schematic diagram b)Different parts of each duct	55
Figure 3-9 UV-lamps and their configuration .....	56
Figure 3-10 Catalyst substrate A consists of TiO <sub>2</sub> coated on fiber glass.....	57

Figure 3-11 Catalyst substrate B consists of TiO <sub>2</sub> coated on the activated carbon. ....	57
Figure 3-12 Filters of multi mix chemical media of activated carbon and chemically impregnated alumina for adsorbing VOCs and aldehydes. ....	58
Figure 3-13 Ozone scrubber screen made of MnO <sub>2</sub> catalyst. ....	58
Figure 3-14 a) Cross section tubes, b) Sampling port setup. ....	59
Figure 4-1 Removal efficiency of ethanol in each duct. ....	65
Figure 4-2 Removal efficiency of 1-butanol in each duct. ....	65
Figure 4-3 Formaldehyde generation in ethanol experiments in each duct. ....	66
Figure 4-4 Acetaldehyde generation in ethanol experiments in each duct. ....	67
Figure 4-5 Formaldehyde generation in 1-butanol experiments in each duct. ....	67
Figure 4-6 Acetaldehyde generation in 1-butanol experiments in each duct. ....	67
Figure 4-7 Propionaldehy degeneration in 1-butanol experiments in each duct. ....	68
Figure 4-8 Butyraldehyde generation in 1-butanol experiments in each duct. ....	68
Figure 4-9 Removal efficiency of n-hexane in each duct. ....	70
Figure 4-10 Removal efficiency of n-octane in each duct. ....	70
Figure 4-11 Formaldehyde generation in n-hexane experiments in each duct. ....	71
Figure 4-12 Acetaldehyde generation in n-hexane experiments in each duct. ....	71
Figure 4-13 By-product generation in n-octane experiments in each duct. ....	72
Figure 4-14 Removal efficiency of acetone in each duct. ....	73
Figure 4-15 Removal efficiency of MEK in each duct. ....	73
Figure 4-16 Formaldehyde generation in acetone experiments in each duct. ....	74
Figure 4-17 Acetaldehyde generation in acetone experiments in each duct. ....	74
Figure 4-18 Formaldehyde generation in MEK experiments in each duct. ....	75

Figure 4-19 Acetaldehyde generation in MEK experiments in each duct. ....	75
Figure 4-20 Removal efficiency of toluene in each duct. ....	76
Figure 4-21 Removal efficiency of p-xylene in each duct. ....	77
Figure 4-22 Formaldehyde generation in toluene experiments in each duct. ....	78
Figure 4-23 Acetaldehyde generation in toluene experiments in each duct. ....	78
Figure 4-24 Crotonaldehyde generation in toluene experiments in each duct. ....	78
Figure 4-25 Formaldehyde generation in p-xylene experiments in each duct. ....	79
Figure 4-26 Acetaldehyde generation in p-xylene experiments in each duct. ....	79
Figure 4-27 Crotonaldehyde generation in p-xylene experiments in each duct. ....	79
Figure 4-28 Removal efficiency of tested VOCs. ....	81
Figure 4-29 Generated by-products of test VOCs with 500 ppb concentration. ....	82
Figure 4-30 Effect of relative humidity on removal efficiency of ethanol in each duct. ...	84
Figure 4-31 Formaldehyde generation in different relative humidity in each duct. ....	84
Figure 4-32 Acetaldehyde generation in different relative humidity in each duct. ....	85
Figure 4-33 Effect of flow rate on removal efficiency of ethanol in each duct. ....	86
Figure 4-34 Effect of flow rate on formaldehyde generation in photocatalytic oxidation of ethanol in each duct. ....	86
Figure 4-35 Effect of flow rate on acetaldehyde generation in photocatalytic oxidation of ethanol in each duct. ....	87

## LIST OF TABLES

Table 1-1 Different classes of VOCs and their possible emission sources.....	3
Table 1-2 Reported air quality in different modes of public transportation ( $\mu\text{g}/\text{m}^3$ ).....	4
Table 2-1 ISO standard on determining solar irradiances .....	30
Table 2-2 Light source employed in photo catalytic reactors.....	31
Table 3-1 Physical specification of challenge gases.....	45
Table 3-2 Possible emission sources and potential health casualties of selected VOCs ..	46
Table 4-1 Environmental test conditions for ethanol and 1-butanol experiments.....	65
Table 4-2 Environmental test conditions for n-hexane and n-octane experiments.....	69
Table 4-3 Environmental test conditions for acetone and MEK experiments.....	73
Table 4-4 Environmental test conditions for toluene and p-xylene experiments. ....	76
Table 4-5 Environmental conditions and removal efficiency for the repeatability experiments.....	83
Table 4-6 Removal efficiency and concentration of generated by-products for each duct in irradiance experiments.....	87
Table 4-7 Configuration of reaction section in each duct in irradiance experiments. ....	88
Table 4-8 Configuration and description of the reaction section in removal efficiency improvement experiment. ....	89
Table 4-9 Removal efficiency and by-products concentration of removal efficiency improvement experiment. ....	89

## LIST OF ABBREVIATIONS

ASHRAE	American Society of Heating, Refrigerating, and Air-Conditioning Engineers
AOP	Advanced Oxidation Process
ARELs	Acute Reference Exposure Levels
BL	Black Light
BLB	Black Light Blue
B &K	Bruel & Kjaer
CB	Conduction Band
cfm	Cubic Feet per Minute
DAS	Data Acquisition System
DCAA	Dichloroacetic Acid
EPA	Environmental Protection Agency
FPM	Foot per Minute
FTIR	Fourier-Transform Infrared Spectroscopy
GAC	Granular Activated Carbon
GC/MS	Gas Chromatography/Mass Spectroscopy
GC-FID/MS	Gas Chromatograph/ Flame Ionization Detector /Mass Spectroscopy
HEPA	High Efficiency Particulate Air
HVAC	Heating, Ventilating and Air-Conditioning
IAQ	Indoor Air Quality
ISO	International Organization for Standardization
IR	Infrared Radiation
MEK	Methyl Ethyl Ketone
NHE	Normal Hydrogen Electrode
OEHHA	Office of Environmental Health Hazard Assessment
PC	Personal Computer
ppb	Parts per Billion
ppm	Parts per Million

ppmv	Parts per Million by Volume
ppbv	Parts per Billion by Volume
PTFE	Polytetrafluoroethylene
PCE	Perchloroethylene
PCO	Photo-Catalytic Oxidation
PAS	Photo-Acoustic Spectroscopy
PTR-MS	Proton Transfer Reaction Mass Spectrometer
RH	Relative Humidity
SEM	Scanning Electron Microscope
SBS	Sick Building Syndrome
TVOC	Total Volatile Organic Compound
TEAM	Total Exposure Assessment Methodology
TCE	Trichloroethylene
TEAM	Total Exposure Assessment Methodology
TPO	Temperature-Programmed Oxidation
TPH	Temperature-Programmed Hydrogenation
TeCE	Tetrachloroethylene
UHP	Ultra High Performance
UV	Ultraviolet
UV-PCO	Ultraviolet Photo-Catalytic Oxidation
UVGI	Ultraviolet Germicidal Irradiation
UV-LED	Ultraviolet Light-Emitting Diode
UVC	Ultraviolet C
VB	Valance Band
VOC	Volatile Organic Compound
VUV	Vacuum Ultraviolet
WHO	World Health Organization

## LIST OF SYMBOLS

<u>English Symbols</u>	<u>Description</u>
[A]	Concentration of the Acceptor
$C$	Concentration
$C_{up,t}$	The Upstream Challenge Gas Concentration (ppb) as a Function of Time
$C_{down,t}$	The Downstream Challenge Gas Concentration (ppb) as a Function of Time
$c_A$	Concentration of the Organics
$C_{up}$	The Upstream Generated By-Product Concentration (ppb)
$C_{down}$	The Downstream Generated By-Product Concentration (ppb)
cfm	Cubic Feet per Minute
$D$	Electron Donor
$E_t$	Efficiency at Time $t$
eV	Electron Volt
g	Gram
$G_a$	The Net Production of Generated By-Product (ppb)
h	Hour
$I_m$	Average Number of Einsteins Absorbed by the Absorbing Species per Unit Volume and Unit Time
$k$	Constant
keV	Kilo-electron Volt
K	Degree Kelvin
L	Liter
mM	Millimole
$m^2$	Square Meter

$m^3$	Cubic Meter
mW	Milliwatt
nm	Nanometer
Pa	Pascal
psia	Pounds per Square Inch Absolute
$Q$	Airflow Rate
$T$	The Elapsed Time (min)
W or w	Watt
$\mu\text{g}$	Microgram
$\mu\text{w}$	Microwatt

# CHAPTER 1 INTRODUCTION

## 1.1 BACKGROUND

People's everyday life is tightly tied to the environment, and among all the component of the environment, air, water and soil are the most important, and this urges more care and attention for them. Air is the most important one among these three parameters, thus more attention and consideration are needed to keep it clean.

Considering the population of the world and amount of time people spend in an indoor environment and growth of new chemical materials such as detergents, petrochemical products, etc. which are used in everyday life, clean indoor air is one of the most important factors for building occupants' health and comfort.

There are lots of strategies to improve the quality of air, especially indoor air; however, there are some questions to be answered. Are these methods economical? Do these methods destroy pollutants completely or just transfer them from one phase to another, and postpone pollutants emission into air? Can these methods completely remove the pollutants or parts of them? Are they efficient for long term application?

For conservation of energy and subsequently reducing energy cost, people seal their houses tightly, and use construction materials with good insulation. Moreover, they reduce infiltration of fresh air, hence, natural ventilation decreases and, subsequently, gaseous pollutants which are generated continuously increase (Birnie et al., 2006; Tompkins et al., 2005a).

### 1.1.1 Indoor Air Quality

Indoor environments are non-industrial areas such as inside of dwellings, offices, aircrafts, vehicles, metros, trains, etc. (Wang et al., 2007). Indoor air has a complex mixture of contaminants which vary over time based on the place and even temperature and humidity of the building.

Indoor air pollutants can be classified into two main groups: First, particles such as dust, mist, pollen and bioaerosols; and second, gaseous pollutants including volatile organic compounds (VOCs), combustion gases and radioactive gases. VOCs are a group of chemical gases with carbon and hydrogen atoms in chain or ring forms. Also their vapor pressure is higher than 1 Pa at room temperature and their concentrations are different based on the environment. In old buildings, the mean concentration of each VOC is lower than  $50 \mu\text{g}/\text{m}^3$ , but higher than  $5 \mu\text{g}/\text{m}^3$ ; this concentration is higher in new and lower in public buildings (Brown et al., 1994). The U.S. Environmental Protection Agency (EPA) in Total Exposure Assessment Methodology (TEAM) studies declared that typical VOCs concentration was 2 to 5 times higher than outdoors (U.S. EPA, 2009; Birnie et al., 2006), and since people spend up to 80% of their life indoors (around 60% in residential and 20% in other places), worryingly, health problems can affect people's life (Waki et al., 1995). VOCs cause sick building syndrome (SBS) which is related to the occupants' comfort and health (Wang et al., 2007). Minnesota Department of Health (2009) reported that several factors such as air volume in the building, off-gassing production rate of VOCs, the ventilation rate in the building, VOCs outdoor concentration, and the time people spend in an indoor activity affect VOCs level in an indoor environment. Table 1-1 shows different classes of VOCs and their sources.

Table 1-1 Different classes of VOCs and their possible emission sources (Cheng and Brown, 2003).

VOC class	Environment and sources
Aliphatic and cyclic hydrocarbons	1, 2, 4, 5, 7, 9–11
Aromatic hydrocarbons	1–7, 9, 11, 12
Aldehydes	1–12
Terpenes	1–4, 7–10
Alcohols	1–9, 11
Esters	1, 2, 4, 7–9
Halocarbons	1, 2, 7, 11
Glycols/glycolethers/glycolesters	1–4, 7, 9
Ketones	1–4, 6–12
Siloxanes	11
Alkene	2, 7
Organic acids	2, 3, 7–9, 11
Ethers	9
Other VOCs	1, 2, 4, 7, 11

1: Established buildings, 2: new and renovated buildings, 3: school, 4: new car interiors, 5: carpets, 6: floor coverings, 7: wood-based panel and furniture, 8: solid woods, 9: paints, 10: cleaning products, 11: unflued gas heaters and electric ovens, 12: office equipment.

VOCs with the most concentration in aircrafts are acetone and ethanol, in subways m-/p-xylenes and in residential and office buildings ethanol, limonene, acetone, toluene, and methylene chloride (Wang et al., 2007). VOC emission is very important since it causes production of photochemical oxidants such as ozone and peroxyacetyl nitrate. These oxidant compounds are produced in the presence of sunlight irradiation and existence of  $\text{NO}_x$ , and cause significant problems such as toxicity and odor, depletion of the stratospheric ozone layer and finally global warming (Alberici and Jardim, 1997). In most of the cases, the emission of VOCs causes localization of pollution problems (Bouzaza et al., 2006). Public transport vehicles are classified as indoor environments, and VOCs in these environments are of greater concentration than others. Some of the most common VOCs in these places are shown in Table 1-2.

Table 1-2 Reported air quality in different modes of public transportation ( $\mu\text{g}/\text{m}^3$ ) (Wang et al., 2007).

Chemical	Aircraft	Train	Bus	Subway
Acetaldehyde	4.4–45.9			
Acetone	21.0–167.7	49–92	30–73	30–92
Benzene	0–7.3	2–4	2–6	4–7
2-Butanone	3.4–17.9	3–11	4–18	4–17
Ethanol	154–3625	170–1700	50–260	130–300
Formaldehyde	1.7–9.5	17–9.5		
<i>n</i> -Hexane		0–3	2–6	0–6
Limonene	4.3–61.9	1–17	190–490	1–6
Methylene chloride (dichloromethane)	3.1–121.6			
Naphthalene	0–1.8			
2-propanol (isopropyl alcohol)	12–92.7	0–33	7–63	9–23
Propionaldehyde	1.5–5.1			
Tetrachloroethylene	32–13			
Toluene	4.7–86.5	7–54	15–39	13–27
<i>m/p</i> -Xylenes	2.0–12.5	3–9	6–48	5–50
<i>o</i> -Xylene	0–2.7			

Exposure to high concentrations of some VOCs for a long time causes damage to some vital organs such as liver, kidney, and central nervous system, or in extreme cases cancer. Moreover, short time exposure can cause eye, nose and throat irritation, headache, nausea, vomiting, dizziness, fatigue, allergic skin reaction, and worsening of asthma symptoms (Minnesota Department of Health, 2009; U.S. EPA. 2009).

For improvement of indoor air quality, several solutions exist which can be classified into three major groups:

- ✓ Controlling contaminant sources.
- ✓ Increasing air change and ventilation in the building and dilution of indoor air with outdoor to decrease pollutants.
- ✓ Using portable air cleaners for rooms or even in duct system for the entire house.

But controlling pollutant sources is almost impossible. In the modern world, people's demand for detergents, odors and paints are increasing. On the other hand, building materials are mentioned as the largest source of VOCs in an indoor area especially in new buildings (Wang et al., 2007). On the other hand, increasing air exchange or ventilation rate has some disadvantages; it does not remove pollutants and just transfers them to the outdoors. Also it increases the cost of heating and cooling, and finally outdoor air may bring undesirable pollutants indoor. Therefore, in recent years, air cleaning technologies have gained significant attention.

### **1.1.2 Air Cleaners**

Heating, ventilation and air-conditioning (HVAC) system by controlling the air temperature and humidity provides an indoor environment in which the occupants are thermally comfortable. This is a cost demanding process, and therefore, air cleaner systems must be designed to take this into account. Air cleaners with different technologies such as mechanical filters, electronic air cleaners, ion generator adsorbents or reactive adsorbents for gaseous pollutants are used for indoor buildings. Removing the sources of pollutants is not feasible; increasing ventilation and air change is not economical, while removing pollutants with some air cleaners is feasible and economical. Each air cleaner is designed for specific purposes and with a special technology. Based on their technologies, air cleaners are classified as the following (U.S. EPA, 2007):

#### **1.1.2.1 Mechanical filters**

This type can be used either as a portable device or in duct system in buildings with central air conditioning or heating system. There are several forms of this type of filter

such as flat or panel filters, pleated or extended surface filters, or high efficiency particulate air (HEPA) filters, Figure 1-1.

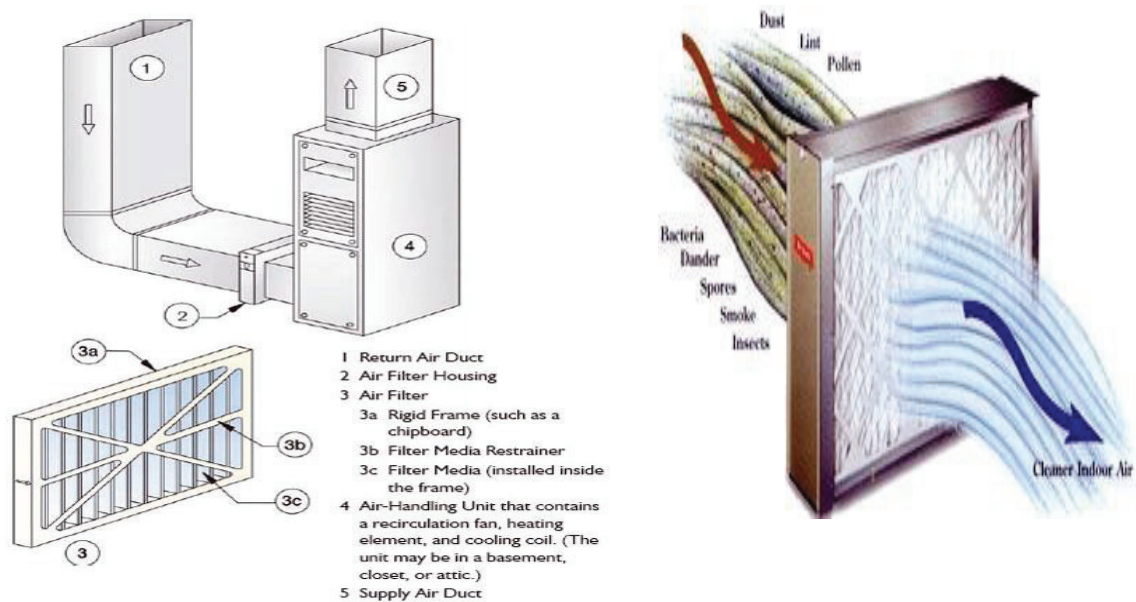


Figure 1-1 Mechanical filter and their installation (<http://store.airmechanical.com/air-cleaner-filters/bryant-cartridge-filter-filbbcar0020.html>), (<http://www.epa.gov/iaq/pubs/residair.html#summary>).

Flat or panel filters are made of coarse glass fibers, coated animal hair, vegetable fibers, synthetic fibers (polyester or nylon), synthetic foams, metallic wools, or expanded metals and foils which sometimes are treated with viscous substances such as oil, which helps particles to stick to the fibers. Also it can be made of permanent electrically charged materials such as resin wool, a plastic film or a fiber called “electret,” or an electrostatically sprayed polymer. As a result of static charge, particles stick to them. This filter has a low pressure drop and is efficient in attracting small particles. Pleated or extended surface filters have greater surface area with packed and dense media made of fiber mats, bonded glass fibers, synthetic fibers, cellulose fibers, wool felt, and other cotton-polyester material blends without a large pressure drop. This type is more efficient than the flat type. The HEPA filter is a filter with an extended surface consisting of sub-

micron glass fibers. Since this filter can remove suspended particles such as bacteria and air born particles, it is more efficient than the two other types, but this filter provides a good environment for microorganisms to live and multiply, and during the replacement in most of the cases these particles go back into the air (Lam, 2007).

#### **1.1.2.2 Ultraviolet germicidal irradiation (UVGI)**

In this process, lamps and ozone generators are commonly used for elimination of bacteria but this method is not efficient for airborne fungal and toxic chemicals deactivation. Also UV-irradiation, in some cases, causes skin irritation. In addition, ozone, which is produced during this process, causes respiratory diseases (Lam, 2007). In this technology, low pressure mercury vapor UV lamps with 253.7 nm wavelength are used. These lamps change microorganism's DNA by destructing their cell structure; therefore, it destroys the cells. UVGI lamps are located in the air duct of an HVAC system downstream of the filter or cooling coil of upstream or even in a portable air cleaner in the downstream of the filter. Based on the literature, efficiency of the UVGI cleaners in killing microorganisms is different based on UV irradiation dosage. For most of the microorganisms, including some viruses and most mold and bacterial spores, high UV irradiation is required. Additionally, relative humidity, temperature, air velocity, and duct reflectivity are other elements that affect the performance of this type of air cleaners.

#### **1.1.2.3 Electronic air cleaner**

Charged particles can be trapped in electrical fields. This type of air cleaner can be used as a portable cleaner with fans or in heating or air conditioning systems. Common types of air cleaners with this technology are electrostatic precipitators or charged-media filters

which have series of charged media which collect particles on the fibers. Ion generator air cleaner does not have collecting plates, and produce ions using UV light. Ions stick into the particles and give them charge to adhere into some surfaces such as walls, furniture, etc. or even join the other charged particles to settle down. Although, this type is more efficient in particle removal, it cannot remove gases or odors. On the other hand, as a result of high voltage usage in this method, ozone is produced as a by-product, and its concentration is increased in the environment which is risky to people's health. In addition, ozone can react with other environmental chemical compounds such as air fresheners, deodorizers, certain paints, polishes, wood flooring, and carpets. Therefore, it produces more harmful by-products such as formaldehyde, ketones, and organic acids which, more adversely, affect people's health (Menzies et al., 1999).

#### **1.1.2.4 Solid sorbents**

Solid sorbents like zeolites, activated aluminum, and specially activated carbon with different packing density can be used for removal of gaseous pollutants especially VOCs (Haghighat et al., 2008). However, performance of air cleaners based on these materials depends on the physical, chemical, and concentration of the pollutants and sorbent, air flow rate in sorbent bed, configuration and depth of sorbent bed in the device and also the quantity of the sorbent and its porosity. Activated carbon is a popular sorbent for gaseous pollutants especially hydrocarbons and non-polar gases, but it is not efficient for VOCs with low molecular weight. Another sorbent for removing particular pollutants is chemisorbing impregnated with active chemical materials. Impregnated activated aluminum with potassium permanganate ( $\text{KMnO}_4$ ) has been used for low molecular weight gases such as formaldehyde (Thad, 2001). Moreover, zeolites commonly are used

for indoor polar gases treatment such as benzene, n-hexane and formaldehyde (Chin et al., 2006). Also, the lifetime of the sorbent and its capacity for removing pollutants is a major problem in air cleaners design; also pollutants are just moved from one media to another media which needs to be regenerated every so often.

#### **1.1.2.5 Ozone generators**

Ozone-generator air cleaners are based on capability of ozone for reaction with either biological or chemical compounds. But ozone itself is an irritant compound and causes asthma attacks, chest discomfort, and irritation of the nose, throat, and trachea; and generally adversely affects humans' health. Moreover, it can produce some harmful compounds as a result of partial oxidation of chemicals; therefore, the EPA does not find these air cleaners safe and effective (ASHRAE Handbook 2008).

#### **1.1.2.6 Photocatalytic oxidation**

In recent years, photocatalytic oxidation (PCO) and ultraviolet photocatalytic oxidation (UV-PCO) has attracted great interest as new promising methods. The former method is usable under visible light while the latter needs UV light. However, both of them need verification to be used widely.

Although UV-PCO technology was first used for water treatment, its application in air purification is more attractive than water treatment based on the following reasons (Ray, 2000): air purification needs lower UV- adsorption, prevention of reverse recombination of electron/hole pairs and radicals as a result of higher mobility of reactants in the gas-phase, presence of oxygen as an oxidant in an adequate amount in air, and lack of bicarbonate and carbonate in the gas-phase.

Although there are some air cleaners with UV-PCO technology in the market; however, still there are lots of unknown issues related to this technology such as the efficiency of this type of air cleaners for one pass and for long time usage, knowledge about operational parameters such as temperature, flow rate, etc., production of intermediates and by-products and their toxicity, and relationship between intermediates production and catalyst deactivation. Thus, more investigation is needed prior to the large scale application of this technology.

## **1.2 RESEARCH OBJECTIVES**

There are some challenges in applications of UV-PCO air cleaner in an industry, and researchers are trying to overcome the limitations mentioned in previous paragraph. This research focuses on this subject and the followings are the objectives of this study:

- ❖ Developing an experimental methodology for investigation of UV-PCO performance and removal efficiency using one pass in the duct system for each group of VOCs (including alkanes, ketones, alcohols, and aromatic) in an indoor range concentration.
- ❖ Qualification and quantification of generated by-products for each VOCs group in different range of concentration (including alkanes, ketones, alcohols, and aromatic) during UV-PCO process.
- ❖ Impact of operational parameters such as light intensity, wavelength, humidity, air flow rate etc. on the UV-PCO removal efficiency and quality and quantity of generated by-products using ethanol as a target pollutant.

- ❖ Evaluation of UV-PCO performance and by-product generation in the presence and absence of ozone (using VUV and UVC lamps).

### 1.3 THESIS OUTLINE AND PUBLICATIONS

The rest of this work is organized as follows:

Chapter 2 explains the fundamentals of UV-PCO technology and provides critical reviews of previous studies on VOCs mineralization using UV-PCO technology; characteristics and removal performance of this technology along with generated by-products and effect of operational parameters. Chapter 3 describes the experimental set-up and methodology. Moreover, details of set-up design, experimental procedure, target pollutants, chemical generation system, sampling, and analysis instruments are provided in this chapter. Chapter 4 illustrates and discusses the experimental results stemming from this research. Chapter 5 provides the conclusion of this study and recommendations for future work.

The results of this research have been published/submitted to the following conferences/journals:

- Farhanian, D., Haghghat, F., Lee, C.S., Zhong, L., Lakdawala, N., “Investigation of Ultraviolet Photocatalytic Oxidation by-Products”, Accepted in ASHRAE Cold Climate HVAC Conference, 2012.
- Lee, C.S., Zhong, L., Farhanian, D., Flaherty, Ch., Haghghat, F., “Development of a parallel test system for the evaluation of UV-PCO systems”, Accepted in ASHRAE Cold Climate HVAC Conference, 2012.
- Farhanian, D., Haghghat, F., “Ultraviolet Photocatalytic Oxidation Performance Using UVC and VUV lamps” Submitted to CLIMA 2013 International Conference, 2012.
- Farhanian, D., Haghghat, F., Lee, C.S., Lakdawala, N., "Performance of Ultraviolet Photocatalytic Oxidation Air Cleaner: Parametric Study", to be submitted to the International Journal of Atmospheric Environment.

# CHAPTER 2 LITERATURE REVIEW

## 2.1 INTRODUCTION

PCO is one of the benign environmental processes and it is claimed as decisively cost effective technology. This technology is a subdivision of Advanced Oxidation Process (AOP). There are some processes which are similar to PCO such as UV photolysis, UV photo-oxidation in presence of oxidants such as ozone, hydrogen peroxide and hydroxyl radicals (Ray, 2000). Some physical-chemical and biotechnological methods have been used for removal of VOCs before UV-PCO technology but some of their limitations and handicaps made them hardly usable. Although this process is new but at least 400 papers, reports, and patents are published annually in this field which illustrates its importance and applicability. Numerous studies were done in UV-PCO; however, most of them are in part-per-million (ppm) ranges not sub-ppm or part-per-billion (ppb) levels which are applicable for indoor environments (Wang et al., 2007).

Photocatalytic oxidation has a great potential for degradation of organic compounds and bio-aerosols (i.e., bacteria and viruses) (Chin et al., 2006; Frazer, 2001). PCO is used in a large number of studies for water treatment while its application in air purification is new.

## 2.2 PHOTOLYSIS

Photo-dissociation, photolysis, or photodecomposition is a chemical reaction of some chemical compounds, in this case VOCs. Photolysis occurs when VOCs are exposed to UV-light irradiation and produce some intermediate.

Also, photolysis can take place for decomposition of inorganic material for instance ozone and nitrogen. Photolysis classified as direct UV photolysis and sensitized photolysis (Ray, 2000).

### 2.2.1 Direct UV Photolysis

Direct photooxidation occurs in the presence of photons while there is no photocatalyst in the system. Photolysis was investigated for several VOCs such as alkenes group including TCE, PCE (Bhowmick and Semmens, 1994; Yung-Shuen and Young, 1998) and aromatics such as benzene, toluene, xylene (Wekhof, 1991). Photolysis of aromatic compounds increases by having either greater molecule size or alkyl groups. For the majority of VOCs except trichloroethylene (TCE) and tetrachloroethylene (TeCE) direct photolysis is very small in comparison with the case where they are exposed to a photocatalyst. For TCE and TeCE direct photolysis under 254 nm wavelengths led to higher degradation similar to that in the exposure of photocatalyst, but under black light lamp direct photolysis is less than catalyst exposure; this is due to ozone existence in the 254 nm system (Alberici and Jardim, 1997). For direct photolysis 4 eV to 7 eV or 175 nm to 300 nm radiation are necessary and this process mathematically expressed by the following equation (Ray, 2000):

$$-\frac{dc_A}{dt} = \Phi I_m$$

Equation 2-1

where:

$c_A$  = concentration of the organics (ppb).

$\Phi$  = quantum yield of the reaction.

$I_m$  = average number of Einsteins absorbed by the absorbing species per unit volume and unit time (Einstein is one mole equal to Avogadro's number of photons and  $\lambda$  is the wavelength of the light)

### 2.2.2 Sensitized Photolysis

This type of photolysis is based on the energy transfer of photochemically excited molecule to an acceptor from. The acceptor can be oxygen or a transient reactive form of it, like single oxygen atoms. Degradation rate for sensitized photolysis can be expressed as Equation 2-2 (Ray, 2000).

$$\text{Rate} = k [A]$$

Equation 2-2

where  $k$  is a constant containing the concentration of the sensitizer and the light absorption rate, likewise triplet energy transfer terms and triplet quantum yield (in a sensitized reaction, triplet is a common excited state).  $[A]$  is the concentration of the acceptor. In this process if during the experiment the concentration of the sensitizer changes, the expression of reaction rate becomes much more complex.

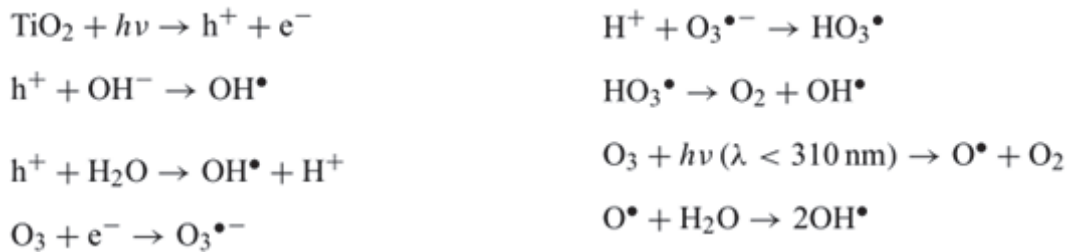
## 2.3 PHOTOCHEMICAL OXIDATION WITH OZONE

Ozone is an unstable tri-atomic molecule form of oxygen. Therefore, it reacts with other compounds in the environment. It usually breaks down to an oxygen molecule ( $O_2$ ) and highly reactive single oxygen ( $O_1$ ) atom.

Three common ozone production methods include:

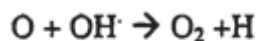
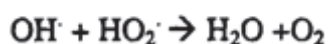
1. Hot spark
2. Ultraviolet light
3. Cold plasma

The second method is more applicable for photochemical reaction purification for indoor air, since it utilizes Ultraviolet germicidal lamps. Ozone, itself, is one of the most risky by-products and WHO (World Health Organization) recommends that the level of ozone concentration in indoor environment should be as low as 0.05 ppmv. Ozone causes the following reactions (Pengyi et al., 2003):

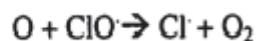


Ozone is one of the species which increases VOCs degradation and is observed during n-octane photo oxidation (Wang et al., 2007), and toluene mineralization (Pengyi et al., 2003). Zhang and his colleagues (2003) observed that ozone plays a prohibitory role for catalyst deactivation and by adding ozone to toluene, conversion rate increases. When concentration of toluene increases from 5 ppmv to 20 ppmv, conversion decreases in the following order for different systems:  $\text{O}_3/\text{TiO}_2/\text{UV} > \text{O}_3/\text{UV} > \text{TiO}_2/\text{UV}$ . In  $\text{O}_3/\text{UV}$  process, conversion decreases linearly in this concentration range. The presence of  $\text{TiO}_2$  catalyst accelerates the reaction; however, in the  $\text{TiO}_2/\text{UV}$  system, conversion rapidly dropped due to catalyst deactivation (Pengyi et al., 2003).

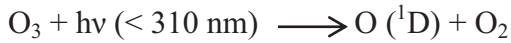
In a comparison between 254 nm germicidal lamps and 365 nm black light lamps, during toluene photodegradation, it was found that in 254 nm wavelengths, in all 3 systems of O<sub>3</sub>/UV, TiO<sub>2</sub>/UV, and O<sub>3</sub>/TiO<sub>2</sub>/UV toluene conversion is higher. This significant difference is due to two reasons: first, difference in irradiation intensity which is 58 w/m<sup>2</sup> for 254 nm, while it is 30 w/m<sup>2</sup> for 365 nm wavelengths; which causes more photon excitation. Second, ozone decomposition in 254 nm UV-lamp is more efficient than 365 nm UV-lamp; subsequently more hydroxyl radicals are produced as a result of ozone decomposition (Pengyi et al., 2003). In O<sub>3</sub>/TiO<sub>2</sub>/UV process, either less hazardous compounds or lower residual ozone is detectable. Ozone consumption in this process is due to the following reactions: first, ozone either as a hydroxyl radical scavenger or electron acceptor, and second ozone decomposition by UV-light. Ozone can react with OH radicals and consume them according to the following reactions (Buckley and Birks, 1995).



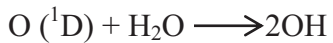
Shen and Ku (2002) during TCE photo-degradation observed this phenomenon too. They reported that ozone existence decreases removal efficiency, because it reacts with hydroxyl radicals and causes less conversion in O<sub>3</sub>/TiO<sub>2</sub>/UV system in comparison with the sum of TiO<sub>2</sub>/UV and O<sub>3</sub>/UV systems. They found that ozone in chlorinated compounds undergo according to the following reactions:



Cl radicals increase the rate of degradation by inducing chain reactions. Single oxygen, which is an important oxidant atom, is produced as a result of ozone photolysis according to the following reactions (Buckley and Birks, 1995).



And, if it reacts with water molecules in the air, two hydroxyl radicals are formed.



There is always a competition between O (<sup>1</sup>D) and Cl radicals in chlorinated systems (Ray, 2000).

Ozone residue also can be affected by relative humidity and flow rate. Relative humidity is related to water vapor content in the system and therefore ozone consumption is linked with it. Flow rate causes dilution or concentration of ozone molecules, therefore, ozone retention time in the system changes. One of the problems of using germicidal UV-lamps which produce ozone is that in the O<sub>3</sub>/TiO<sub>2</sub>/UV system, there is always some residual ozone, and since ozone is a harmful compound for health, this compound should not exist in high concentration in indoor areas.

## **2.4 PHOTOCATALYTIC OXIDATION (PCO)**

In the early 1970's, during water cleavage on TiO<sub>2</sub> electrodes, photocatalytic oxidation was discovered by Fujishima and Honda. This method was used first in 1977 for water treatment by Frank and Allen's research (1977) in cyanide decomposition in an aqueous TiO<sub>2</sub> suspension. However, since the suspended catalyst (TiO<sub>2</sub> in this case) should be filtered, immobilized TiO<sub>2</sub> catalyst was developed. Considering the ability of this

technology for removal of the organic pollutants, a new application for this method in air purification has gained interest (Waki et al., 1995). Dibble and Raupp (1992) are the first researchers who applied PCO for air purification and they did some experiments in TCE as a first VOC which was remediated by this process.

In the photocatalytic oxidation method, as the name implies, photon, catalysts and also an oxidant component are involved. This method works in existence of heterogeneous catalyst, UV-light or even, in some cases, visible light. From the molecular point of view, PCO mechanisms are explained based on the band gap model. In this model, electrons from valance band (VB) are transferred into the conduction band (CB) via irradiation of UV-light. VB is introduced as the highest energy band occupied by electrons and CB is defined as the band without electrons and hence the lowest energy (Xu and Schoonen, 2000). VB/CB band prepare electron/hole pairs, which may precede redox (reduction/oxidation) reactions if they have enough potential; if VB holes and CB electrons have more positive potential than adsorbed compound and more negative potential than adsorbents respectively. Otherwise, recombination of electron/hole pairs occur and thereupon thermal or light energy is released (Demeestere et al., 2007). The number of electron/hole pairs is related to the intensity of the UV-lamps and VOCs electronic properties (Ray, 2000). As mentioned before, VB/CB potential plays a basic role in progress of redox (reduction and oxidation) reaction, considering 3.2 eV energy band gap, near ultraviolet (UV) photons with  $\lambda \leq 388$  nm necessary for the promotion of the electrons and electron/hole pairs regeneration (Demeestere et al., 2007). Charge separation causes oxidation of both organic and water molecules and reduction of oxygen molecules which lead to redox reactions (Demeestere et al., 2007). Water molecules

which exist in the air produce some oxidizing agents which are called reactive oxygen species such as oxygen ( $O_2$ ), peroxide ( $O_2^{-2}$ ), superoxide ( $O_2^-$ ), and hydroxide ( $OH^-$ ) (Waki et al., 1995). In this process, electrons enter water and change it to hydroxyl radicals which can cause decomposition of organic materials. When electrons are transferred into water, electrons from pollutants can fill the empty place, then, oxygen molecules give their electrons to these holes producing  $O^+$  ions. UV or visible light provides required energy for electron movement. The main products in PCO process are  $CO_2$  and water. Moreover, HCl in the chlorinated VOCs and sulfate in sulfurous VOCs are formed in complete mineralization. However, as a result of partial oxidation, some intermediate and by-products are formed. UV-PCO research areas include different conditions of pollutants such as gas-phase concentrations of both ppbv and ppmv levels, oxygen content between 0% and 100%, light intensities from  $0.1 \text{ mW/cm}^2$  to  $4300 \text{ W/cm}^2$ , diversity in reactor configurations, relative humidity between 0% and 100%, temperatures ranged from  $5 \text{ }^\circ\text{C}$  to  $400 \text{ }^\circ\text{C}$  and different types of catalysts which result removal efficiencies between 1% to 99%. This differences cause inconceivable comparison (Demeestere et al., 2007).

#### **2.4.1 Photocatalytic Oxidation Mechanism**

The PCO gas-solid phase mechanism from the mass transfer point of view on the porous heterogeneous photocatalyst can be explained by Figure 2-1 (Fogler, 2006). The mass transfer mechanism is consisted of the following steps:

1. Advection.

2. Diffusion of the reactant(s) (e.g., species A) from the bulk of the fluid into the catalyst external surface.
3. Diffusion of the reactant(s) from the external surface of the catalyst to vicinity of the internal catalyst surface.
4. Adsorption of the reactant(s) into the internal catalyst surface and its porosity and settling into the active sites.
5. Reaction of reactants with oxygen and hydroxyl molecules on the catalyst active sites (A  $\longrightarrow$  B).
6. Diffusion of the products from the catalyst interior surface (porosities) into the external surface.
7. Diffusion of the products from the external surface of the catalyst into the fluid bulk.

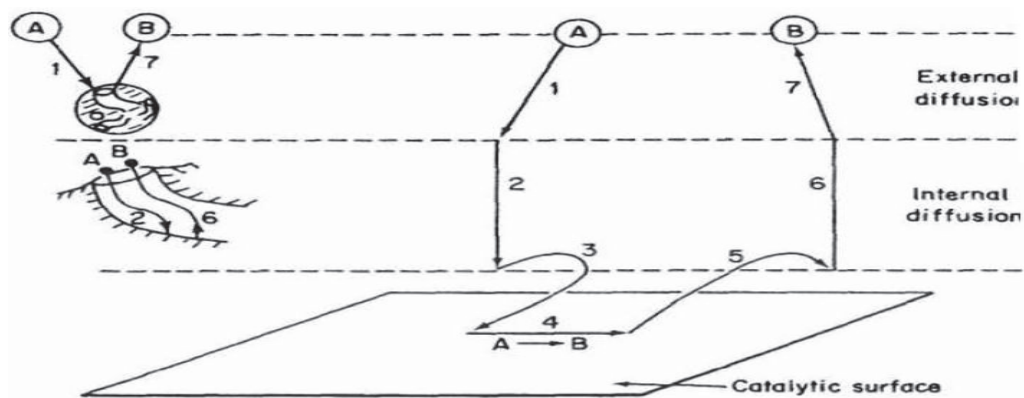


Figure 2-1 Mass transfer mechanism in UV-PCO process ( Fogler, 2006).

On the other hand, PCO process includes the following reactions (Zhong et al., 2010):

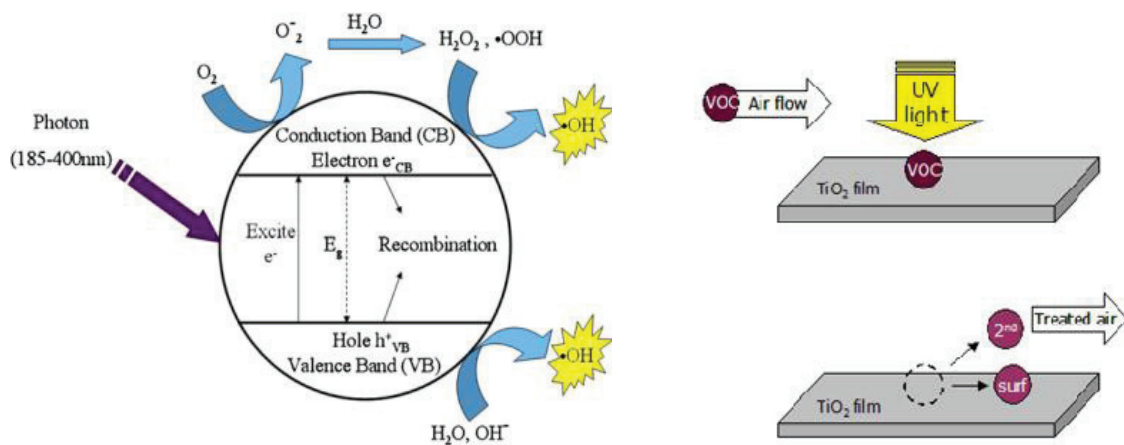
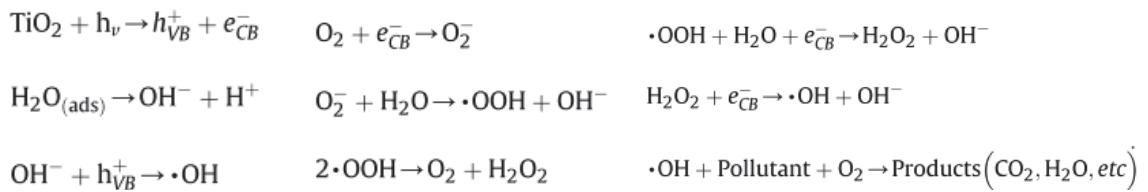


Figure 2-2 Photocatalytic oxidation molecular process (Zhong et al., 2010).

Based on Bickley and Jayanty's research (1974)  $\text{TiO}_2$  has more  $\text{Ti}^{+3}$  sites which are responsible for hole-traps and cause adsorption of more oxygen molecule and therefore production of  $\text{O}_2^-$ . Since electrons and holes recombined in this method, it causes inefficiency and waste of photons' energy, which is a limiting factor in the PCO process, and every effort which decreases recombination of holes and electrons increases PCO efficiency (Hugo et al., 2005). Electrons participate in the reaction with any type of halogenated organic compound present in air and produce another type of radicals for redox reaction. However, oxygen molecules are the best scavenger for electrons and other type of radicals kinetically cannot compete with hydroxyl radicals. On the other hand, reduction reaction has more important role compared to oxidation (Demeestere et al., 2007). During photo-degradation charge transfer occurs in adsorbed species and photocatalyst surface (Wang et al., 2007). Degradation is a combination of adsorption

and desorption parameters, but a lower adsorption constant does not always mean lower degradation. For example, TCE has a lower adsorption constant but is more degradable than toluene (Bouzaza et al., 2006).

#### **2.4.2 Photocatalytic Oxidation Advantages**

The PCO method has several advantages. For example (Bellu et al., 2007):

- There is no consumption of expensive oxidizing chemicals; the oxidant is atmospheric oxygen and the catalyst is non-hazardous.
- The photo catalytic reaction may be driven by the natural UV component of sunlight.
- No chemical additives, such as auxiliary fuel, are required.
- There is a high quantum yield for gas phase reactants (low-intensity UV lamps).
- The catalyst is inexpensive (titanium dioxide).
- PCO is applicable to a large number of organics.
- PCO is effective for low concentrations of pollutants.
- This method works in humid conditions.
- Catalyst activity is not destroyed by chlorinated organic.
- Low maintenance is required and it has long service life.
- Gaseous pollutants are destroyed instead of transferring them to another media.

- PCO has minimum pressure drop in the system.
- This process consumes low power and subsequently it is cost effective.

### **2.4.3 Photocatalytic Oxidation Disadvantages**

Photocatalytic oxidation method also has some disadvantages which are as follows:

- Production of some hazardous intermediates and by-products.
- Catalyst deactivation.

## **2.5 CATALYST**

In 1921 the first report regarding photoactivity of some compounds was published. Gravelle and his colleagues (1971) were pioneers in gas-solid heterogeneous photocatalysis applications. Some of the most common photocatalysts include TiO<sub>2</sub>, ZnO, ZrO<sub>2</sub>, SnO<sub>2</sub>, WO<sub>3</sub>, CeO<sub>2</sub>, Fe<sub>2</sub>O<sub>3</sub>, Al<sub>2</sub>O<sub>3</sub>, ZnS and CdS (Hoffmann et al., 1995). Catalyst has a critical role in pollutant destruction and removal efficiency of VOCs in PCO process highly depends on it. Thus, amount of catalyst should be sized up based on the amount of pollutants entering the photo-reactor. Since the input air volume to the reactor is high, catalyst activity should be high enough to mineralize pollutants; therefore, in most cases even small amounts of catalyst with high activity is enough for large volume of polluted air. High activity of catalyst leads to better electron/hole pair generation and it is not necessary to provide more UV-light, consequently decreasing the cost of the process.

In the literature,  $\text{TiO}_2$  and  $\text{ZnO}$  are the foremost among photocatalysts for PCO process. The surfaces of these two catalysts are hydrophilic and highly covered by water molecules existing in the air (Peral and Ollis, 1997) and they have the following favorable conditions compared to other catalysts (Zou et al., 2006):

1. Photo active near UV illumination and able to utilize visible and/or near-UV light.
2. Biologically and chemically inert and chemically stable.
3. Photo stable (i.e. not liable to photo corrosion).

$\text{TiO}_2$  exists in three forms in nature: rutile, anatase and brookite. The most common form for reaction as a catalyst is anatase, and also its combination with rutile. Commercial form of  $\text{TiO}_2$  is Degussa P25 which is provided by flame pyrolysis and is used widely for air purification. This type of catalyst has 70% anatase and 30% rutile and particle size of 300 nm with  $50 \text{ m}^2\text{g}^{-1}$  surface area (Mo et al., 2009). Catalyst composition and structure immensely affect its performance. The most important parameters which affect catalyst activity are its surface area, porosity, pore size and amount of active sites in the surface of the catalyst (Kittrell et al., 2006).

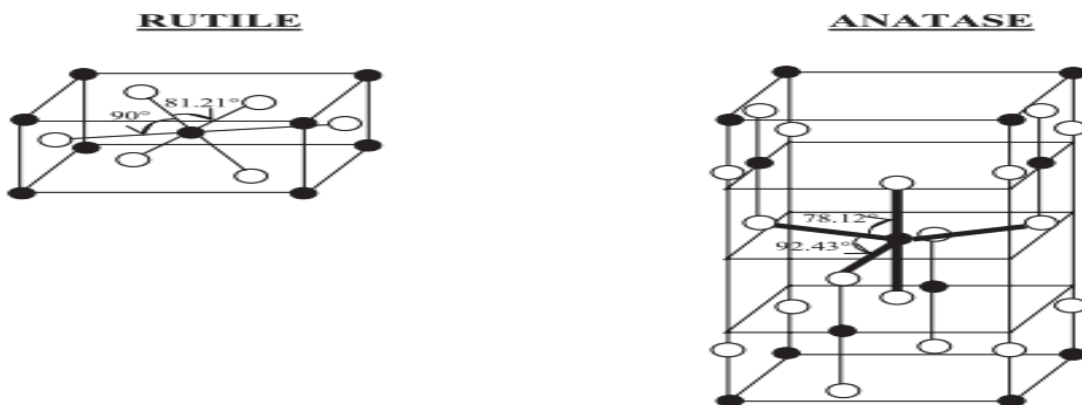


Figure 2-3 Structures of rutile and anatase types of  $\text{TiO}_2$  (Linsebigler et al., 1995).

TiO<sub>2</sub> catalyst shows selectivity to some VOCs and this is one of the challenges in PCO application in a mixture of VOCs. For instance, it has poor reactivity to acetone and toluene compared to TCE (Avila et al., 1998; Hager and Bauer, 1999).

As it can be seen in Figure 2-4, both anatase and rutile TiO<sub>2</sub> crystalline phase have more positive potential than other catalysts for hydroxyl radicals which can carry out redox reaction. Since negative potential of rutile is lower than O<sub>2</sub>/O<sub>2</sub><sup>•-</sup>, compared to anatase, converting oxygen to superoxide radicals is performed by anatase CB electrons and not by rutile CB electrons. In most cases, combination of these two crystalline phases is used to increase catalyst activity. Accordingly, TiO<sub>2</sub> Degussa P25, consisting of 70% –80% of anatase and 20% –30% of rutile, is an applicable photo catalyst (Bhatkhande et al., 2002; Sattler and Liljestrand, 2003). On the other hand, the negative potential of the anatase crystalline phase is close to (O<sub>2</sub>/O<sub>2</sub><sup>•-</sup>). Therefore, combining percentages of other catalyst such as ZnO and ZnS can improve catalyst negative potential (Demeestere et al., 2007). ZnO is one of the photocatalysts that has almost the same band gap energy as TiO<sub>2</sub>, but it is not stable and can be deactivated by converting to the Zn(OH)<sub>2</sub> on the surface of the catalyst during OH radical attendance in the environment. In some cases the combination of TiO<sub>2</sub> and ZnO is used as a photocatalyst. Some of the other photocatalysts are not applicable because of photoanodic or photocathodic corrosion such as metal sulfide and iron oxide polymorphs. Another problem which is associated with using other catalyst is the lower surface potential (Lam, 2007).

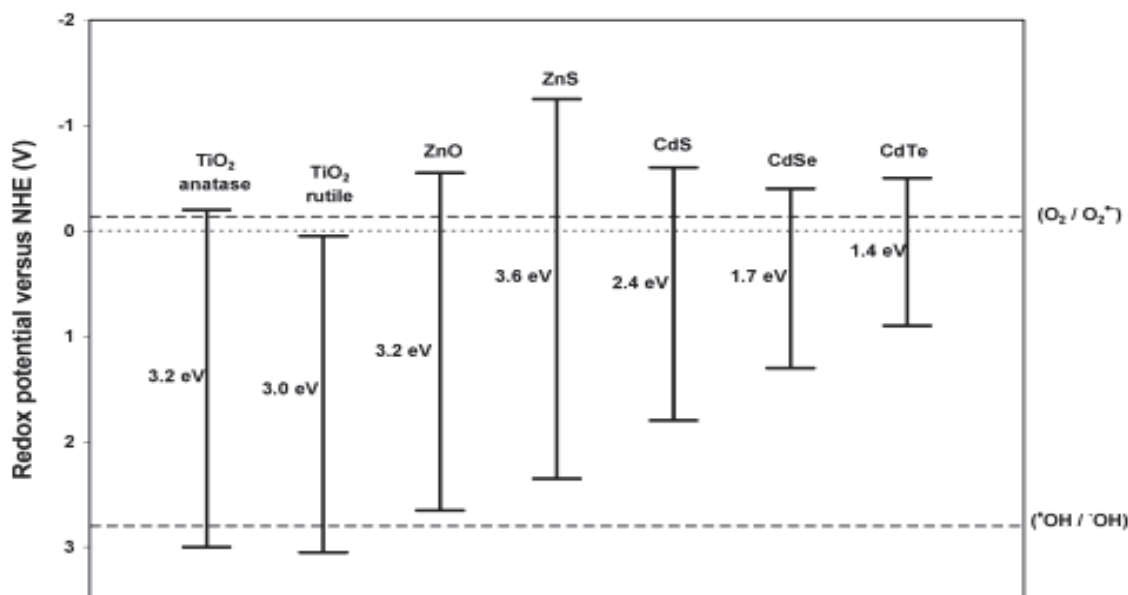


Figure 2-4 Band gaps and VB and CB edges of common semiconductors and standard redox potentials versus NHE (NHE: normal hydrogen electrode) of the  $(O_2/O_2^{\cdot-})$  and  $(^{\cdot}OH/^{\cdot}OH)$  redox couple (Demeestere et al., 2007).

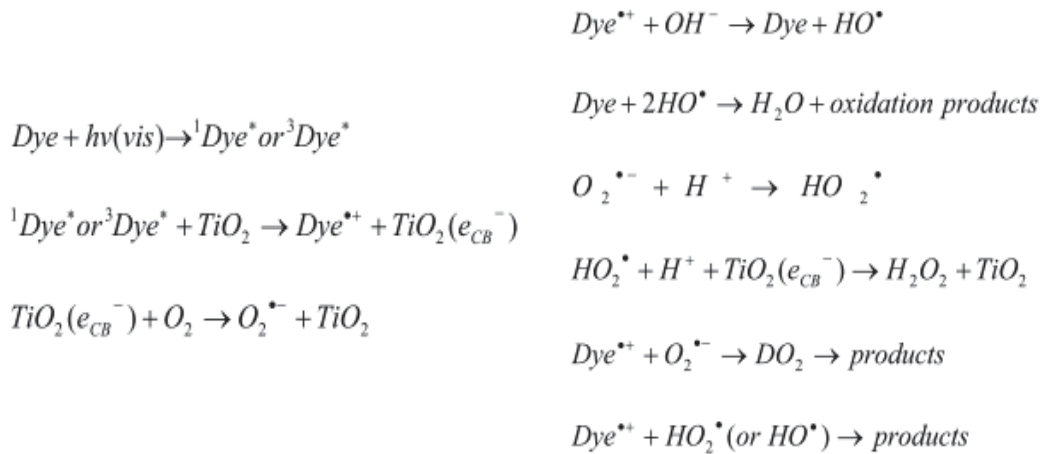
### 2.5.1 Modification of Photocatalyst

In PCO process, the activity of the photocatalyst depends on the electron/hole pair separation and capability of catalyst in adsorption of gaseous VOCs, and modification of catalyst activity should be in improvement of these aspects (Mo et al., 2009). Many studies were done to improve photocatalyst activity by localizing electrons and prepare a photocatalyst which is active even in the visible light range. The followings are some of the methods for improvement of the photocatalyst:

**Metal and Ion Doping:** One of the efficient methods is coupling  $TiO_2$  with transient metal ions such as V, Cr, Mn, Fe, Co, Ni, or Cu (Anpo and Takeuchi, 2003). These metal ions provide recombination sites for photogenerated charge carriers. Also doping metal ions into  $TiO_2$  structure hinders catalyst deactivation (Mo et al., 2009). Augmenting number and strength of acid sites in the  $TiO_2$  catalyst surface increase catalyst activity (Muggli et al., 2002). For applicability of  $TiO_2$  in the visible range, some anions such as

$N^{3-}$ ,  $C^{4-}$ ,  $S^{4-}$  or halides such as  $F^-$ ,  $Cl^-$ ,  $Br^-$ , and  $I^-$  are doped into  $TiO_2$  structure to narrow band gap (Belver et al., 2006a). Unfortunately, there is not enough research for investigation of N doped  $TiO_2$  catalysts in indoor pollutant levels and most of the studies are in ppm range (Wang et al., 2007). Li et al. (2005) have mentioned that if lanthanide ions such as  $La^{3+}$ ,  $Eu^{3+}$ ,  $Pr^{3+}$ ,  $Nd^{3+}$ , and  $Sm^{3+}$  are incorporated into the  $TiO_2$  matrix, they can promote chemical and physical adsorption ability of catalyst for organic compounds.

**Photosensitized Oxidation:** In this process electron is injected from the excited dye molecules onto the  $TiO_2$  conduction band. The dye is converted to the cationic dye radicals ( $Dye^{*+}$ ) and it can react with hydroxyl ions in the reaction environment (Lam, 2007).



**Metal Ion Implantation:** Implantation of metal ions into the  $TiO_2$  structure can be done by injecting the ion beam into the catalyst sample. There are low/middle/high acceleration energies for doping ions during interaction with the catalyst surface; low: 0.2-2 keV which causes formation of thin film on the top surface of the sample by deposition of metal ions, middle: 5-30 keV which embeds metal ions to the surface atoms

of the catalyst samples, high: 50-200 keV which leads to deep bulk implementation of metal ions by bombarding them into the catalyst (Yamashita and Anpo, 2004).

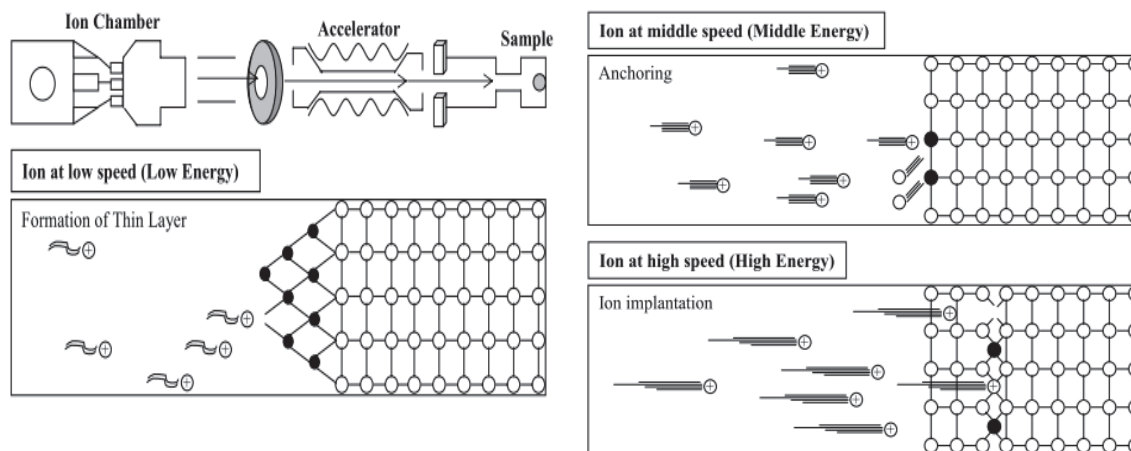


Figure 2-5 Schematic diagrams of the beam techniques (Yamashita and Anpo, 2004).

### 2.5.2 Catalyst Deactivation and Regeneration

Catalyst deactivation is a process in which the activity of the catalyst decreases, and it is classified as the following (Fogler, 2006):

**Deactivation by sintering (sintering or aging):** this type of deactivation is due to loss of active sites in the surface. This happens at very high temperature or irradiation, and may occur either by crystal agglomeration and growth of the metals deposited on the support of the catalyst or by narrowing or closing the pores inside the catalyst pellet.

**Deactivation by poisoning:** When some poisoning molecules chemisorbed in the catalyst surface irreversibly, the number of active sites decreases. Therefore, fewer compounds can react to produce the main product and in some cases impure products are formed. This process causes catalyst deactivation and is called poisoning deactivation.

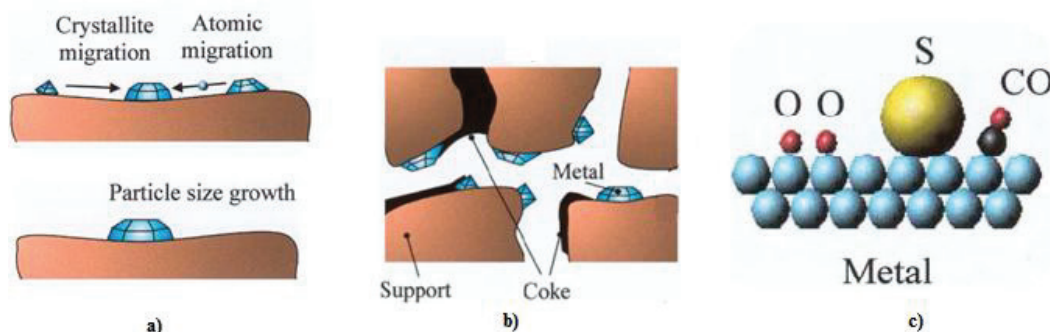


Figure 2-6 Catalyst deactivation: a) Sintering b) Fouling or coking c) Poisoning.

**Deactivation by coking or fouling:** This deactivation is due to the production of carbon compounds such as hydrocarbons,  $\text{CO}_2$ , and  $\text{CO}$  in the catalyst surface. In this process pores are blocked.

It has been reported that catalyst deactivation in PCO process is due to reduction of catalyst active sites and this phenomenon happens as a result of the following reasons (Mo et al., 2009): Formation of intermediates or by-products which blocks the active sites which is observed during mineralization of toluene and dimethylsulfide, and trichloropropene; photopolymerization of some species especially due to the lack of water such as benzene; mineralization of the substrate with a well-fixed species including nitrogen and sulphur; oxidation and accumulation of inorganic compounds such as N and S in the surface and blocking pores as a result of fouling.

For treatment of the deactivated catalyst several methods were tested: First, changing the structure of the catalyst and combining it with other compounds to avoid or even hinder the catalyst deactivation. For instance, some work was done to speed up poisonous intermediates removal from the  $\text{TiO}_2$  catalyst. One method is loading platinum on the  $\text{TiO}_2$  structure which is tested in toluene photodegradation. However, in this method, a lower oxidation rate is achieved (Wang et al., 2007). The second method is injection of

some chemicals onto the catalyst surface such as injection of a vaporized H<sub>2</sub>O<sub>2</sub> solution (Piera et al., 2002), using chlorine radicals (d'Hennezel et al., 1998; Blount and Falconer, 2002) or ozone-purging with water vapor (Wang et al., 2003). The third technique is thermal method for burning and oxidizing surface species and removing them from the catalyst surface. The final method is performed by irradiation of UV-light into the catalyst surface for complete photocatalytic oxidation of surface species.

## 2.6 UV-LIGHT LAMPS

UV-light is a component of a UV-PCO system, and different types of UV- lamps based on their wavelengths were used. Since in PCO method catalysts must produce electrons for the reactions, electrons from valance band have to be excited. This is done by irradiation from light source into catalyst surface. The electromagnetic spectrum of ultraviolet light can be subdivided into different bands which are described in Table 2-1.

Table 2-1 ISO standard on determining solar irradiances (ISO-DIS-21348).

<i>Name</i>	<i>Abbreviation</i>	<i>Wavelength range (nanometers)</i>	<i>Energy per photon</i>
<b>Ultraviolet A, long wave, or black light</b>	UVA	400 nm – 315 nm	3.10 – 3.94 eV
<b>Near</b>	NUV	400 nm – 300 nm	3.10 – 4.13 eV
<b>Ultraviolet B or medium wave</b>	UVB	315 nm – 280 nm	3.94 – 4.43 eV
<b>Middle</b>	MUV	300 nm – 200 nm	4.13 – 6.20 eV
<b>Ultraviolet C, short wave, or germicidal</b>	UVC	280 nm – 100 nm	4.43 – 12.4 eV
<b>Far</b>	FUV	200 nm – 122 nm	6.20 – 10.2 eV

For emission of UVA spectrum, black light (or “BL”) and black light blue (or “BLB”) lamps are designed. Ozone is produced at 185 nm wavelength and in these types of lamps light below 240 nm does not pass through the glass; therefore, no ozone molecules are produced (Hoffmann et al., 1995). 320 nm – 400 nm UV-light wavelength ranges are sufficient for electron promotion and catalyst activation. However, the best UV-light for UV-PCO process is 254 nm + 185 nm radiations, since in this range of irradiation, more

reactive species as a result of ozone existence were formed in the system, and due to photochemical oxidation and photocatalytic oxidation on the TiO<sub>2</sub> catalyst, higher efficiency rate for VOCs was observed (Jeong et al., 2004). Typical UV-lamps include low and medium pressure mercury lamps with 254 nm output and less (<15%) 185 nm emission. New Xenon plasma flash lamps which have wavelengths < 250 nm are suitable for photolysis compared to the other types of lamps. Another technology in light source is argon ion laser with 330 nm and 360 nm emissions (Nimlos et al., 1993). The other UV source for PCO applications is Ultraviolet Light-Emitting Diode (UV-LED) which has some benefits such as long-lasting, robustness, small size and high efficiency are its benefits (Chen et al., 2005). Common light sources which are used in the literature are provided in Table 2-2.

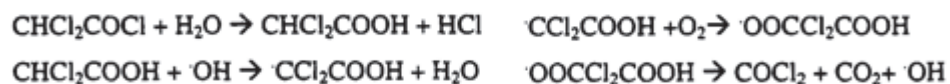
Table 2-2 Light source employed in photo catalytic reactors (Hoffmann et al., 1995).

Type	Nominal Power (W)	Irradiation	Manufacturer	Reference
Xe lamp	990	0.96 kW m <sup>-2</sup>	Ushio Electronics Co.	Kaneco et al. (1999)
UV lamps	4	0.3 mW cm <sup>-2</sup> ; 365 nm peak	GE	Muggli et al. (1998)
Hg lamp	125	Not measured; light pass through Corning 7-60 optical filter (300 nm < λ < 400 nm); 365 nm peak	Philips (HPK)	d'Hennezel et al. (1998)
UV lamps	4, 6, 8, 12, 40	variable, typically 2-10 mW cm <sup>-2</sup> at and near surface of bulb.	WIKO (Japan) GTE Sylvania	Zorn et al. (2000), Wolfrum et al. (1997)
Hg-Xe	N/A	1 mW cm <sup>-2</sup> at the surface of the thin-film photocatalyst	Hayashi Tokei, Luminar Ace 210	Noguchi et al. (1998)

## 2.7 INTERMEDIATES AND BY-PRODUCTS

When emission of light into the catalyst surface starts, some reactions including isomerization, rearrangement, bond cleavage, or intermolecular chemical reactions

occur. Therefore, in addition to CO<sub>2</sub> and H<sub>2</sub>O as the main products, some by-products are formed. By-products or intermediates are produced during partial oxidization of compounds which can settle on the catalyst surface or present in the gas phase. Generation of by-products is one of the challenges in full scale usage of PCO due to the possibility of some more toxic VOCs generation as compared to the parent compounds. For instance, during mineralization of TCE and PCE some by-products such as dichloroacetyl chloride (DCAC), trichloroacetaldehyde, and trichloroacetic acids are formed while the DCAC toxicity is 40 times higher than TCE (Ray, 2000). DCAC also can be hydrolyzed under water vapor existence to form dichloroacetic acid (DCAA) based on the following reactions (Hung and Marifas, 1997; Bhowmick and Semmens, 1994):



Although some of the reports asserted no intermediate detection in concentration up to 80 ppmv, other researchers identified numerous intermediate formations (Cao et al., 2000; Einaga et al., 2001; Ao and Lee, 2003). In some cases, production of intermediates causes the delay in estimated half-life, and this is due to competition between intermediates and initial compounds for finding active sites and reaction (Chang et al., 2003).

Most common intermediates due to organic compounds photo-degradation in the atmosphere are carbonyl compounds, especially different forms of aldehyde which are highly toxic. As a result of photo-oxidation of these compounds, secondary compounds such as peroxyacetyl nitrates are formed which have more toxicity than parent compounds (Carlier and Mouvier, 1986). In most papers it is mentioned that more intermediates were

formed under the germicidal lamp source compared to the black-light source (Mo et al., 2009). Oxidation process in PCO is due to either addition of the oxidant into the chemical structure or substitution. In the first case, some compounds such as chlorine or ozone are added in the double bond of olefin and in the second case some oxidizer atoms such as hydroxyl radicals replace some atoms in the compound (Ray, 2000). In some cases production of heavier VOCs compared to the parent compounds were observed. Hung and Marifas (1997) observed production of VOCs with higher molecular weights during photodegradation of some reactants such as hexa-chloroethane, penta- chloroethane, 1,1,2,2-tetrachloroethane. Photocatalytic oxidation of epoxide can form epoxy carbonyls during PCO process which can react with ozone and hydroxyl radicals to form smaller molecules (Ray, 2000).

During acetone photo-memorization at conversion of 5-20% of acetone no intermediates are formed (Chang et al., 2003), while Xu and Raftery (2001) observed surface intermediates such as diacetone alcohol, mesityl oxide, formic acid, propylene oxide and acetic acid using solid-state in situ solid-state nuclear magnetic resonance spectroscopy. Jacoby et al. (1996) worked on benzene photodegradation, and they identified phenol, hydroquinone and/or benzoquinone, and malonic acids as possible intermediates.

## **2.8 OPERATIONAL PARAMETERS AFFECTING PCO PROCESS**

### **2.8.1 Humidity**

Relative humidity (RH) plays a twofold role in the PCO process. In some cases, it decreases degradation, and in other cases increases mineralization. The RH effect depends on water vapor concentration, and affects VOCs mineralization either based on

water concentration or the type of VOCs and their amount which participates in the reaction. RH provides hydroxyl radicals to expedite degradation and specific amount of it is necessary for providing required hydroxyl radicals. Therefore, in some cases researchers have reported that increasing RH causes high elimination of VOCs. When amounts of hydroxyl radicals increase more than the required amount; the degradation rate decreases due to competition between water vapors with other VOCs for catching active sites. Moreover, when saturation occurs in the reaction environment, none of the water molecules abandon their places (Wang et al., 1999; Demeestere et al., 2007). Hydroxyl radicals also play a basic role in distribution of intermediates and progress of side reactions. Besides, it is important in catalysts lifetime. For example, Dibble and Raupp (1992) asserted water vapor necessity for long term activity of the catalyst during trichloroethene degradation while Hager and Bauer (1999) and Hegedüs and Dombi (2004a) observed no catalyst deactivation of tri- and tetrachloroethene in dry air conditions.

In high RH, water vapor adsorbs on the catalyst surface to enhance partial oxidized compound degradation and does not allow parent VOCs to oxidize due to competition between pollutants and water vapor for catching catalyst active sites. This process is desired, since it regenerates the catalyst. On the other hand, this process decreases parent VOCs degradation and hence removal efficiency. Some observations confirm this idea and some of them are in contrast with it. For example, Vorontsov and his coworkers (2001, 2003a) asserted mineralization of 2-phenethyl-2-chloroethylmercurization is higher at RH = 38% than at RH = 1.4%. Also, they observed different compounds during degradation of diethyl sulfide at RH  $\geq$  13% compared to RH = 2%, less CO<sub>2</sub> is produced

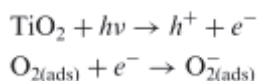
and catalyst is deactivated faster. Despite these different observations, explanation of less catalyst deactivation at low RH is possible since when RH is low, lower amounts of •OH are produced and consequently smaller amounts of VOCs are degraded. Therefore, less carbon or other materials accumulate on the catalyst surface to deactivate it.

Amama et al. (2004) found out that the optimum relative humidity for TCE and methanol photodegradation is 25%. In acetone degradation, when water vapor is increased from 18.7 mM to 417 mM, acetone degradation is increased too, while any further increases in water vapor decrease the oxidation rate. If relative humidity increases from 0% to 60%, a tenfold increase in CO<sub>2</sub> and a fourfold increase in benzaldehyde production are observed during toluene (80 ppm) photodegradation (Larson and Falconer, 1997).

### 2.8.2 Oxygen Content

The oxygen compound is one of the necessities for the PCO reaction and without oxygen, PCO reaction does not happen. It accepts electrons and promotes the oxidation part (Chang et al., 2003). Teichner et al. (1985) reported O<sub>2</sub><sup>-</sup> and O<sup>-</sup> surface species as a result of TiO<sub>2</sub> illumination and afterwards O<sub>3</sub><sup>-</sup> was found.

In acetone photo-degradation an increase of oxygen content from 0% to 5% increases conversion from 20% to 70%. On the other hand, the reaction constant increases with the increase of oxygen from 0% to 20%. Existence of oxygen molecules decreases the chance of electron/hole pair recombination by catching electrons and forming O<sup>2-</sup> (Chang et al., 2003).



It was observed that during TCE photodegradation, increasing oxygen concentration more than 10,000 ppmv did not affect photo-degradation compared to the water vapor. Since adsorption sites for these molecules and their radicals are different, thus, despite the increase in water vapor, oxygen molecules neither decrease nor increase the photodegradation rate. Figure 2-7 represents water and oxygen molecules in the catalyst active sites during TCE mineralization (Ma and Ku, 2006; Kim et al., 2002; Hung and Marifas, 1997).

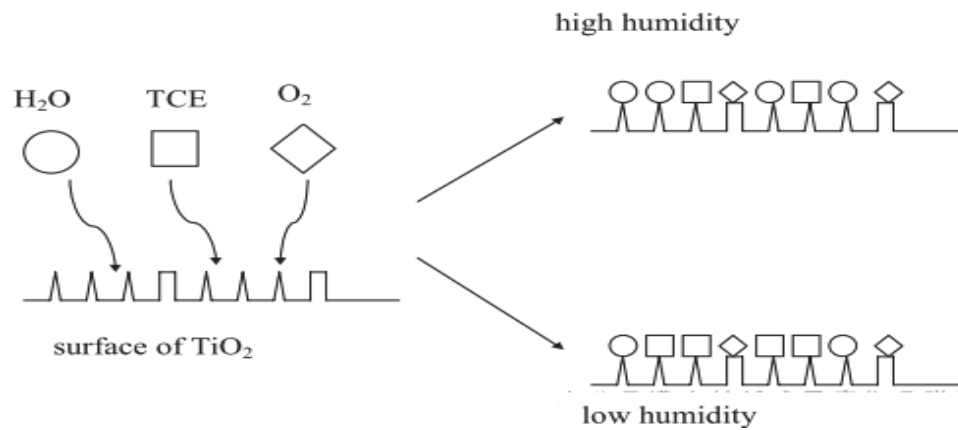


Figure 2-7 Water and oxygen molecules adsorb at different active sites (Ma and Ku, 2006).

### 2.8.3 Temperature

The PCO process is done in an indoor temperature. However, generally, altering the temperature affects VOCs adsorption–desorption and even chemical conversion (Demeestere et al., 2007). Adsorption is an exothermic process while desorption is an endothermic process and UV-PCO reaction also can be exothermic or endothermic which depends on the VOC type. Therefore, increasing or decreasing the temperature has different influences on the removal efficiency (Doucet et al., 2006). Also, the temperature affects the product distribution by changing adsorption–desorption equilibrium and also the rate of product formation (Demeestere et al., 2007). Kim et al. (2002) reported that VOCs adsorption might be rate limiting at high temperatures while products desorption

may be rate limiting at lower temperatures. Raise of temperature increases product desorption while decreases the rate of adsorption. Avila et al. (1998) and Sánchez et al. (1999) observed that trichloroethene removal is nearly constant up to 125 °C while it decreased at a higher temperature. In acetone degradation increasing the temperature causes better oxidation for acetone, whereas, the catalyst became yellow at 120 °C and by increasing it to 163 °C, it became brown (Xu and Raftery, 2001).

Although PCO can occur at room temperature, the acetone reaction rate constant increases if the temperature increases from 30 °C to 77 °C and consequently, the rate of reaction increases. Furthermore, above 100 °C the reaction constant decreases, thus degradation of acetone decreases (Chang et al., 2003). Hager and Bauer (1999) studied the effect of temperature on toluene mineralization by performing tests at the temperature range of 278 K to 348 K at 6 L/h flow rate and injection rate of 18.7 g/m<sup>3</sup>. Based on their observations, the maximum conversion is in 298 K which promoted the PCO process at room temperature is more economic and efficient. Although, increment of temperature changes degradation from marginal to significant, due to adsorption/desorption limitation in some ranges, it decreases the photodegradation. For example, TCE conversion improved by increasing the temperature but decreased at temperatures above 125 °C (Sánchez et al., 1999).

#### **2.8.4 Flow Rate**

Flow rate plays an important role in VOCs degradation since a low flow rate causes high retention time, conversion is more than 80% while at high flow rate conversion decreases to less than 30% (Bouzaza et al., 2006). For application of high flow rate in a UV-PCO system, multi-pass recirculation is the best choice for increasing residence time of VOCs

in the system. At low flow rate, VOC removal efficiency increases but kinetic parameters do not change while in a very high flow rate, since the retention time is very short, reaction is not complete. A moderate flow rate did not show any changes in the degradation (Demeestere et al., 2007)

### **2.8.5 Light Intensity**

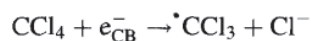
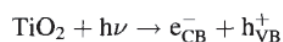
Since photons cause electron excitation and then redox reaction, light intensity is a substantial issue in PCO process. Electron/hole pair generation or recombination is directly related to light intensity and light wavelength. Light intensity affects removal efficiency in two ways (Demeestere et al., 2007):

- a) First order regime: in this process electron/hole pairs consumption is faster than their recombination which is at high concentration of VOCs and low light intensity.
- b) Half order regime: this process happens at high light intensity and low concentration of VOCs and recombination persists.

Lamp intensity affects PCO performance, and the degradation rate increases with enhancement of light intensity. For instance, in TCE degradation rate vs. intensity, at low concentration, the conversion rate showed square-root dependency to light intensity while at high concentration it is linear. At high intensity, mass transfer limitation controls degradation rate, and recombination of hydroxyl radicals occurs. Both of these issues decrease quantum yield (Ray, 2000). Ohko et al. (1998) investigated 2-propanol and found out that at  $10^4$ - $10^6$   $\mu\text{w}/\text{cm}^2$  intensity, mass transfer controls the process, whereas in the 1-1000 ppm concentration range, the light intensity controls the process.

## 2.8.6 Presence of Other Compounds

The types of reactant have a critical role in the operational condition for complete mineralization. Different structures of VOCs photodegradation were investigated by researchers and they observed that the presence of some compounds cause less mineralization while others cause more degradation. For instance, nitrogen containing compounds remediate less than chlorine, sulfur and phosphorus containing components (Waki et al., 1995). Also, since air has a complex mixture of contaminants, some of these compounds can enhance photodegradation of others or decrease them. For example, methanol (1000 ppmv) presence as an electron donor (D) increases CCl<sub>4</sub> conversion from 0% to 10% since it minimizes the undesired electron-hole pair recombination, while O<sub>2</sub> did not show significant effect on the CCl<sub>4</sub> photodegradation (Waki et al., 1995).



In the formaldehyde mineralization, nitric oxide (NO) promotes photodegradation but sulfur ions decrease remediation (Ao and Lee, 2004). The presence of NO promoted the conversion since OH radicals are produced as a result of NO existence in the mixture. But, due to the existence of SO<sub>2</sub> in the mixture, sulfate ions are formed which compete with pollutants for active sites and therefore, inhibit the conversion rate. Halogenated VOCs as sensitizers, which provide radicals, can be used for less or non-degradable compounds. For instance presence of chloroform in 254 nm wavelength and carbon tetrachloride as a reactant causes mineralization of this non-degradable compound (Bhowmick and Semmens, 1994).

Moreover, some contaminants have a twofold role. Lichtin et al. (1996) observed that trichloroethylene inhibited acetone conversion while promoting trichloromethane, dichloromethane and octane degradation. These inhibition/promotion effects can be a result of competition between components for achievement of catalyst active sites or even production of side products which are absorbed on the catalyst surface and block the active sites or they can consume driving radicals of PCO process.

### **2.8.7 Pressure**

Pressure is another parameter which affects the PCO process in gas-phase systems. Pressure reduction in these systems, drastically increases VOCs mineralization. For instance, PCO performance at 6-10 psia is greater than 10-21 psia. This aspect especially in systems with low concentration of VOCs and high water vapor concentration is important (Raupp et al., 1997; and Ray, 2000). Generally, low pressure usage is beneficial for removing diffusional mass transfer limitation in PCO process. In thin film catalyst usage, mass transfer limitation is very important and high flow rate is used for overcoming this problem. In this case, pressure reduction also increases reactant diffusivity although at low pressure always there is a competition between VOCs and water vapor for adsorption on the catalyst surface.

Most of the operational parameters in the UV-PCO system influence each other. For instance, air flow rate affects radical productions which participate into the reaction. In addition, it can affect boundary layer, mass transfer coefficient and also diffusion coefficient of both reactants and products. Temperature induces speed of reaction and also increases adsorption and desorption coefficient.

## 2.9 RELATED WORKS

**Hodgson et al. (2003, 2005, 2005a)** carried out laboratory experiments on two prototype honeycomb monolith UV-PCO devices (12 in. by 12 in.). One had aluminum honeycomb monoliths coated with Degussa P25 TiO<sub>2</sub> impregnated with 3% tungsten oxide (WO<sub>3</sub>). The other had a honeycomb monolith made of an optical polymer and coated with a thin semitransparent silane barrier coat followed by a thin semitransparent TiO<sub>2</sub> film serving as the photocatalyst. They used nine UVA lamps with 46 cm (18 in) long and about 2.8 Watts total UV with peak irradiance at 368 nm, arranged in three banks. The distance between a lamp surface and monolith is about 7 cm (Figure 2-8). They prepared steady state concentrations in a classroom laboratory or a 20 m<sup>3</sup> chamber and the inner duct dimensions of the reactor were 34 cm by 41 cm (13.5in by 16 in). The air flow rate was varied from approximately 175 m<sup>3</sup>/h to either 300 m<sup>3</sup>/h or 600 m<sup>3</sup>/h. They challenged their UV-PCO system with several complex mixtures of ppb level VOCs concentration. For the first device, the oxidation rates of the chemical classes of compounds followed the approximate order of alcohols and glycol ethers (> 70% at the low flow rate of 165 m<sup>3</sup>/h and near 40% at the high flow rate of 580 m<sup>3</sup>/h) > aldehydes, ketones, and terpene hydrocarbons > aromatic and alkane hydrocarbons > halogenated aliphatic hydrocarbons. Formaldehyde, acetaldehyde, acetone, formic acid and acetic acid were identified in these experiments as reaction by-products. The second device had high reaction efficiencies for many VOCs commonly encountered in indoor environments (many alcohols, glycol ethers, formaldehyde, hexanal, etc.), and the external mass transfer might be the rate-limiting step for these highly reactive compounds at low flow rates. Formaldehyde, acetaldehyde and acetone were observed as reaction by-products. In both

cases, no chlorine-containing by-products were reported when the UV-PCO device was challenged by the VOC mixture containing low concentrations of trichloroethene and other chlorinated solvents. In addition, there was no discussion about interference effects among the multiple VOCs.

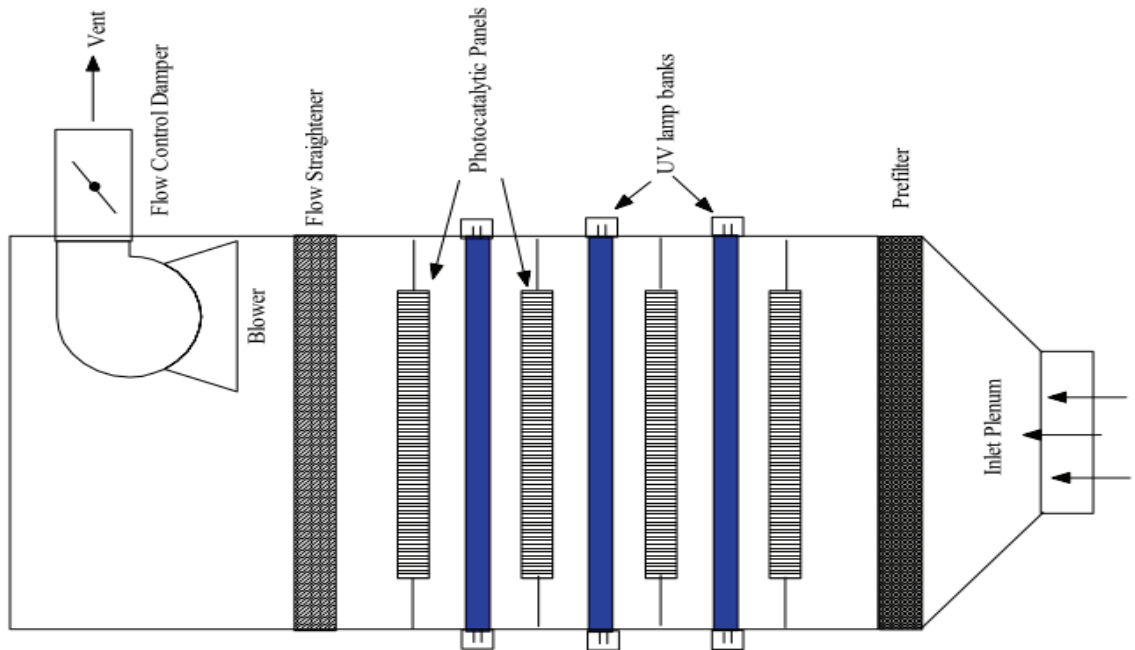


Figure 2-8 Schematic diagram of UVPCO reactor showing arrangement of four photocatalytic monoliths and three banks of three UVA lamps.

**Ginestet et al. (2005)** tested the UV-PCO units with different designs of catalyst inserts, including pleated wire coarse meshes, pleated wire fine meshes and triangular honeycomb monolith. Based on their observations, very low (near zero) removal efficiency of the PCO in units with pleated wire meshes while the triangular monolith unit had a removal efficiency of over 10% under the same test conditions. They conducted further tests for the honeycomb monolith using toluene, acetone and ethanol as test compounds and the test concentration level was 10 ppm. They found that all these compounds could be significantly removed by the PCO unit and formaldehyde and acetaldehyde were the main by-products.

**Sun et al. (2005)** evaluated two UV-PCO units in an aircraft cabin simulator with relative humidity lower than 20% and supply air flow rate and outside air supply rate were controlled at 200 L/s and 2.4 L/s per person respectively. Ethanol, isoprene and toluene oxidation were studied in these units. Generation of formaldehyde and acetaldehyde for both units and generation of methanol for one of the unit were observed.

# CHAPTER 3 EXPERIMENTAL SET-UP AND METHODOLOGY

## 3.1 INTRODUCTION

As mentioned in chapter 1, one of the main objectives of this research is to develop an experimental methodology to evaluate UV-PCO performance and generated by-products using different groups of VOCs. In this part, test rig design, chemical generation system along with gas sampling and analysis instruments are explained.

## 3.2 CHEMICALS AND REAGENTS

More than 300 VOCs have been identified in an indoor environment, and more than 170 of them can be detected in an indoor environment by means of GC/MS or GC-FID/MS (ISO 16000-6:2004(E)). VOCs for this research were selected according to VanOsdell's (1994) specification for target compounds which are as the following:

- ✓ Frequently exist in indoor spaces.
- ✓ Easily can be analyzed.
- ✓ Do not have serious health risks and remarkable safety notifications.
- ✓ Reasonable test performing cost.

Also, target compounds have been chosen based on their high concentration in North American buildings (Hodgson et al., 2005). Most of these compounds have been recommended in the ASHRAE standard 145.1 (2008) and 145.2 (2011).

Based on the above precautions, the following compounds were selected and purchased from Fisher scientific company and all of these chemicals had a purity of 99%. Moreover, for full evaluation of the PCO technology performance and comparing by-products generation, challenge VOCs were chosen from different classes of chemical compounds including aromatics, alcohols, ketones, and alkanes. Besides, at least two compounds from the same chemical class were chosen to compare their by-products and facilitate investigation of their similarity and differences. Table 3-1 lists target compound specifications, and Table 3-2 provides information about the possible sources of these compounds in an indoor environment.

Table 3-1 Physical specification of challenge gases.

<i>Chemical Class.</i>	<i>Compound Name</i>	<i>Molecular Formula</i>	<i>Molecular Weight (g/mol)</i>	<i>Density (g/mL)</i>	<i>Boiling Point (°C)</i>	<i>Vapor Pressure. at 23 °C (mm Hg)</i>	<i>ASHRAE Std 145.1</i>	<i>Toxic Cat.</i>
<i>Aromatic</i>	<i>Toluene</i>	C <sub>7</sub> H <sub>8</sub>	92.14	0.867	110.6	25.64	+	H
	<i>p-Xylene</i>	C <sub>8</sub> H <sub>10</sub>	106.16	0.866	138		+	H
<i>Alkane</i>	<i>n-Hexane</i>	C <sub>6</sub> H <sub>14</sub>	86.18	0.656	69	139.88	+	
	<i>n-Octane</i>	C <sub>8</sub> H <sub>18</sub>	114.23	0.703	125	12.56		
<i>Ketones</i>	<i>2-Butanone (MEK)</i>	C <sub>4</sub> H <sub>8</sub> O	72.11	0.8	79.64	86.95	+	H
	<i>Acetone</i>	C <sub>3</sub> H <sub>6</sub> O	58.08	0.788	56.53	184.5	+	
<i>Alcohol</i>	<i>Ethanol</i>	C <sub>2</sub> H <sub>6</sub> O	46.07	0.785	78.4	44.63	+	
	<i>1-Butanol</i>	C <sub>4</sub> H <sub>10</sub> O	74.12	0.808	117	5.47		

Presence on U.S. EPA Hazardous Air Pollutant lists was indicated by “H”,  
Compounds proposed in ASHRAE Standard 145.1 were included (indicated by “+”)

Table 3-2 Possible emission sources and potential health casualties of selected VOCs.

Chemical Class	Compound Name	Compounds Source	Reported air quality in different modes of public transportation ( $\mu\text{g}/\text{m}^3$ )						Health problems
			Aircraft	Train	Bus	Subway	Residential	Office	
Aromatic	Toluene	Polyurethane foam, aerosols, Paints, adhesives, gasoline, combustion sources	4.7–86.5	7–54	15–39	13–27	12-240	2.1-40	Disorders or diseases of the skin, eye, liver, kidney, nervous system, respiratory and/or pulmonary system, lung.
	P-xylene		2.0–12.5	3–9	6–48	5–50	28-120	1.4-10	
Alkane	n-Hexane	Paints, adhesives, gasoline, combustion products		0–3	2–6	0–6			Causes irritation to eyes, skin and respiratory tract. Disorders of lung, central and peripheral nervous system
	n-Octane						3.6	0.11-13	
Ketones	Butanone (MEK)	Lacquers, varnishes, polish removers, adhesives	3.4–17.9	3–11	4–18	4–17			Affects central nervous system. Causes irritation to nose, throat, eyes, skin and respiratory tract. Disorders of lung.
	Acetone		21.0–167.7	49–93	30–73	30–92			
Alcohol	Ethanol	Aerosols, window cleaners, paints, paint thinners, cosmetics, adhesives	154–3625	170–1700	50–260	130–300		130	Causes severe eye irritation and moderate skin irritation. Disorders of kidneys, heart, central nervous system, liver. Respiratory tract.
	1-Butanol							2.3-63	

### 3.3 GENERATION SET-UP OF REAGENTS

VOCs have low boiling points and they vaporize easily, although there are many generation methods, for instance gas cylinders, diffusion cells, etc., direct vaporization of VOCs is the simplest and most economical way. Since VOCs concentration in an indoor is at the ppb-level, three concentrations which are 250, 500 and 1000 ppb were chosen. Although, in the case of acetone, due to B&K respond limitation chosen concentrations are 500, 1000, 2000 ppb and in the case of 1-butanol due to condensation of 1-butanol in

tubing 250-500, and 800 ppb were chosen. This option provides the possibility of further investigation of UV-PCO performance and by-product generation at different concentrations of VOCs in the contaminated air.

Selected VOCs are liquid at room pressure and temperature. Syringes (Hamilton Company) with compressed air as a carrier gas were chosen. The injection rate was controlled via mass flow control box and mass flow controller transducers (Matheson Gas Products Company). The calculation procedure of the injection rate of VOCs is provided in Appendix A. In Figure 3-1 schematic diagram of this set up is presented. In this setup, target VOCs concentration was controlled via adjusting air flow rate with an air flow controller and KD Scientific Syringe Pumps.

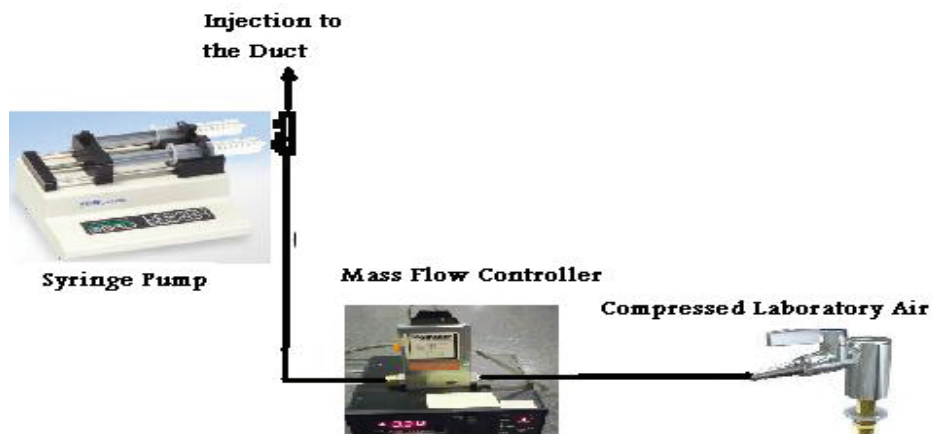


Figure 3-1 Low concentration generation system setup.

### 3.4 ANALYTICAL INSTRUMENTS

Different analytical instruments can be used in UV-PCO tests; for instance gas chromatography/flame ionization detector (GC/FID), gas chromatography/mass spectroscopy (GC/MS), high performance liquid chromatography (HPLC), Fourier-transform infrared spectroscopy (FTIR), temperature-programmed oxidation (TPO) and temperature-programmed hydrogenation (TPH) are instruments for intermediate

identification. FTIR is more applicable for catalyst surface intermediates, however it works efficiently only when the concentration of intermediates is high (Mo et al., 2009). At very low concentrations of intermediates, liquid nitrogen trapping and adsorbent tube were usually used to concentrate these intermediates (Ye et al., 2006). Also, for low concentration of VOCs, Photo-Acoustic Spectroscopy (PAS) and Proton Transfer Reaction Mass Spectrometer (PTR-MS) are applicable for real-time monitoring of VOCs (Obee and Hay, 1997).

#### **3.4.1 High-Performance Liquid Chromatography (HPLC)**

In this research high-performance liquid chromatography (HPLC) was used for analysis of aldehydes and ketones, which is shown in Figure 3-2. Water and acetonitrile with 30% and 70% ratio are used as solvents and a UV-Vis detector as a detector of HPLC. EPA TO-11a method was adopted and aldehydes and ketones were gathered into the cartridge coated with 2, 4-dinitrophenylhydrazine (2, 4-DNPH) (Supelco LpDNPH-SIGMA ALDRICH Company). Lp DNPH cartridges ozone scrubber (KI Ozone scrubber-SIGMA ALDRICH Company) was installed beyond the sampling port and 2, 4 – DNPH cartridge. An ozone scrubber was installed in this connection to prevent ozone from reacting with DNPH solid sorbent. Sampling cartridges were connected to the sampling pump via PTFE tubing. Sampling pumps were calibrated into the required flow rate based on the sampling. The sampling pump flow rate was 1.3 L/min. 2, 4 – DNPH cartridges were extracted with 4 mL of acetonitrile which introduced by micro-volume Bottle dispenser (1-10 ml) (Fisher Scientific co.), into the cartridge. Elute analyzed by high-performance liquid chromatography (HPLC) with ultraviolet detection (Perkin

Elmer Flexar HPLC) and quantification of the elute compounds were verified using HPLC standards and calibration curves.



Figure 3-2 High-performance liquid chromatography (HPLC).

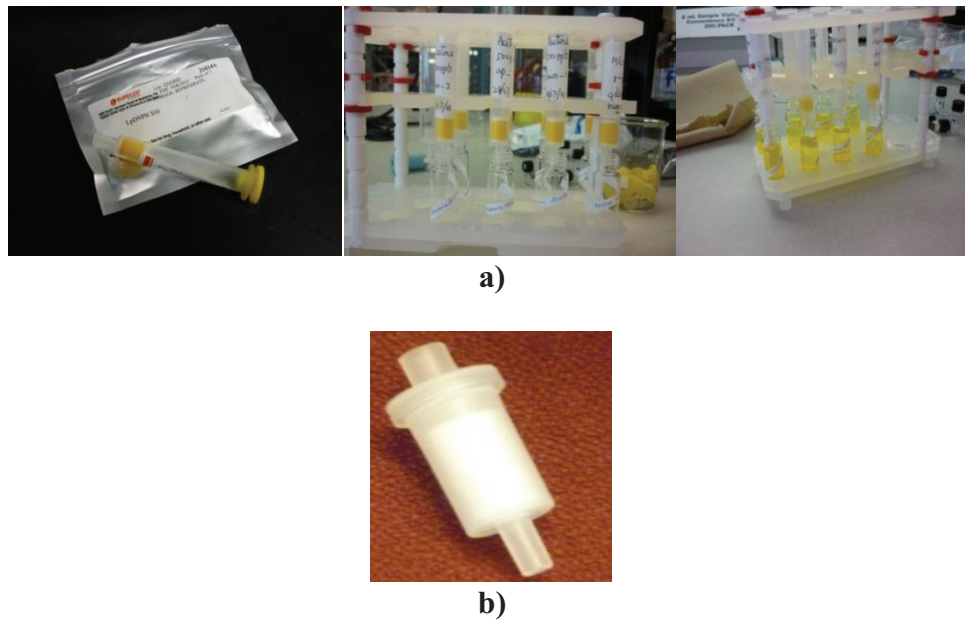


Figure 3-3 a) Supelco Lp-DNPH b) Lp-DNPH cartridges Ozone Scrubber (KI Ozone scrubber).

### **3.4.2 Auto-Sampler**

The CBISS MK3, an 8-channel auto sampler is a third generation computer controlled industrial multiplexor intelligent sampling system (WINCO International) was used to take samples from upstream and downstream of the test rig and send them to a multi-gas photoacoustic detector (Bruel & Kjaer, Model 1302).

### **3.4.3 Multi-Gas Photoacoustic Detector (Bruel & Kjaer, Model 1302)**

A multi-gas photoacoustic detector was applied to measure the concentration of challenged gas in upstream and downstream of UV-PCO reactor. Rather than measuring the concentration directly, this equipment measures the effect of absorbed energy of gas molecule. It irradiates infrared radiation (IR) to gas molecules, and the gas molecules adsorb the IR. After absorbing the IR energy, gas molecules convert it to kinetic energy. Then the resulting energy is converted to sound waves as their amplitude is proportional to the concentration of detected compound by two microphones.

### **3.4.4 Ozone Analyzer**

Multi-Channel Industrial Hygiene Ozone Analyzer Model 465L (Teledyne Technologies Company) is UV photometric ozone monitor which is used for taking samples from upstream and downstream and measuring the ozone concentration.

## **3.5 INSTRUMENT CALIBRATION**

There are a series of calibrations that must be done before the main tests, which are as follows:

### 3.5.1 Sampling Pumps Calibration

Two types of vacuum pumps were used, GILAIR-3 & GILAIR-5 (SENSIDYNE Co.) which used to take samples for HPLC analysis at 1.3 L/min flow rate. The vacuum sampling pumps were calibrated by connecting each pump with the same Lp-DNPH and Lp-DNPH ozone scrubber cartridges and measuring the flow rate with DryCal<sup>®</sup> DC-Lite (Bios International Corporation) and adjusting the flow rate. The calibration was performed three times, and each time the average of 10 readings was taken for vacuum sampling pumps flow rate. Figure 3-4 shows the calibration set-up for aldehyde/ketone sampling pumps.

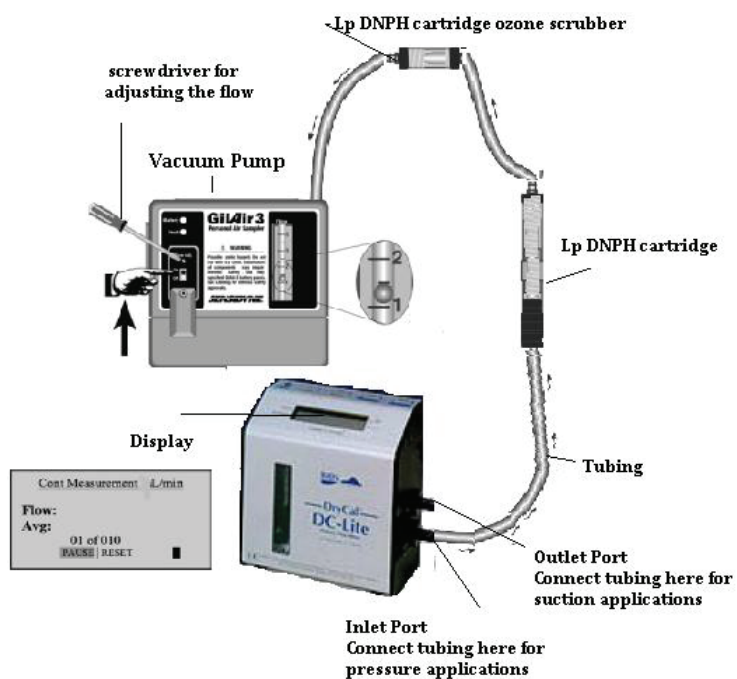


Figure 3-4 High flow rate sampling pump calibration setup.

### 3.5.2 Multi-Gas Photoacoustic Detector (Bruel & Kjaer, Model 1302)

Different VOCs with different concentrations as target compounds are used for the experiments; therefore it is necessary to calibrate B&K before analyzing the samples.

Compressed air at 10.11 L/min flow rate passed through the tubing as a carrier while the flow rate was controlled by mass flow control box and mass flow controller transducers (Matheson Gas Products Company). Each target compound of VOC with known concentration was injected through the septum on the T-joint into the carrier compressed air via Hamilton syringe. Contaminated compressed air total hydrocarbon concentration is monitored by multi gas B&K detector and average of reading was considered as instrument respond for that concentration. Different concentration of each single compound was injected and monitored to have the calibration curves of all the target compounds. Calibration equation of each target compound is given in Appendix B.

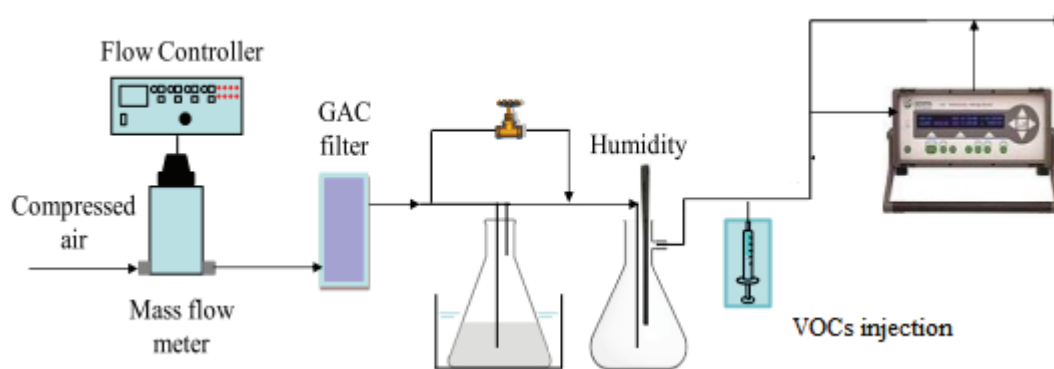


Figure 3-5 Multi-gas photoacoustic detector calibration set-up.

### 3.5.3 HPLC Calibration

HPLC was used to measure by-products generation in UV-PCO system. HPLC calibration was done based on TO-11A method, using 15 compounds carbonyl-DNPH mixtures standard with analytical concentration of 15  $\mu\text{g/ml}$  which is included formaldehyde, acetaldehyde, acrolein, acetone, propionaldehyde, crotonaldehyde, butyraldehyde, benzaldehyde, isovaleraldehyde, valeraldehyde, o-tolualdehyde, m-tolualdehyde, p- tolualdehyde, hexaldehyde, and 2, 5-dimethylbenzaldehyde. Acetonitrile was used for dilution of the standard, and the total amount of standard was 1.5 mL. Four

standard solutions were prepared; dilute solution #1 with 50  $\mu\text{l}$  of standard and 2450  $\mu\text{l}$  of Acetonitrile (concentration of the solution was 2%), dilute solution #2 with 400  $\mu\text{l}$  of standard and 7600  $\mu\text{l}$  of Acetonitrile (concentration of the solution was 5%), dilute solution #3 with 200  $\mu\text{l}$  of standard and 800  $\mu\text{l}$  of Acetonitrile (concentration of the solution was 20%), and dilute solution #4 with 500  $\mu\text{l}$  of standard and 500  $\mu\text{l}$  of Acetonitrile (concentration of the solution was 50%). Injection volumes for all of the dilute solutions were 10  $\mu\text{l}$  and 20  $\mu\text{l}$ . Thus, 3, 6, 7.5, 15, 30, 60, 75, 150 ng mass injected points for each compound were provided for calibration. For repeatability of the injection, each calibration standard was analyzed twice and the average of the two HPLC area respond versus injected mass was plotted. The HPLC equipment generates calibration curves and, during the experiment gives the mass of the recognized compound based on calibration curves. The calibration equations of each compound are listed in Appendix B.

### **3.6 DUCT TEST RIG SPECIFICATIONS**

The test rig is an open duct with four ducts which have the same condition. This design makes it possible to perform four experiments in parallel. The experimental apparatus picture and schematic diagram with dimensions are provided in Figure 3-6 and in Figure 3-7 respectively.



Figure 3-6 Duct test rig picture.

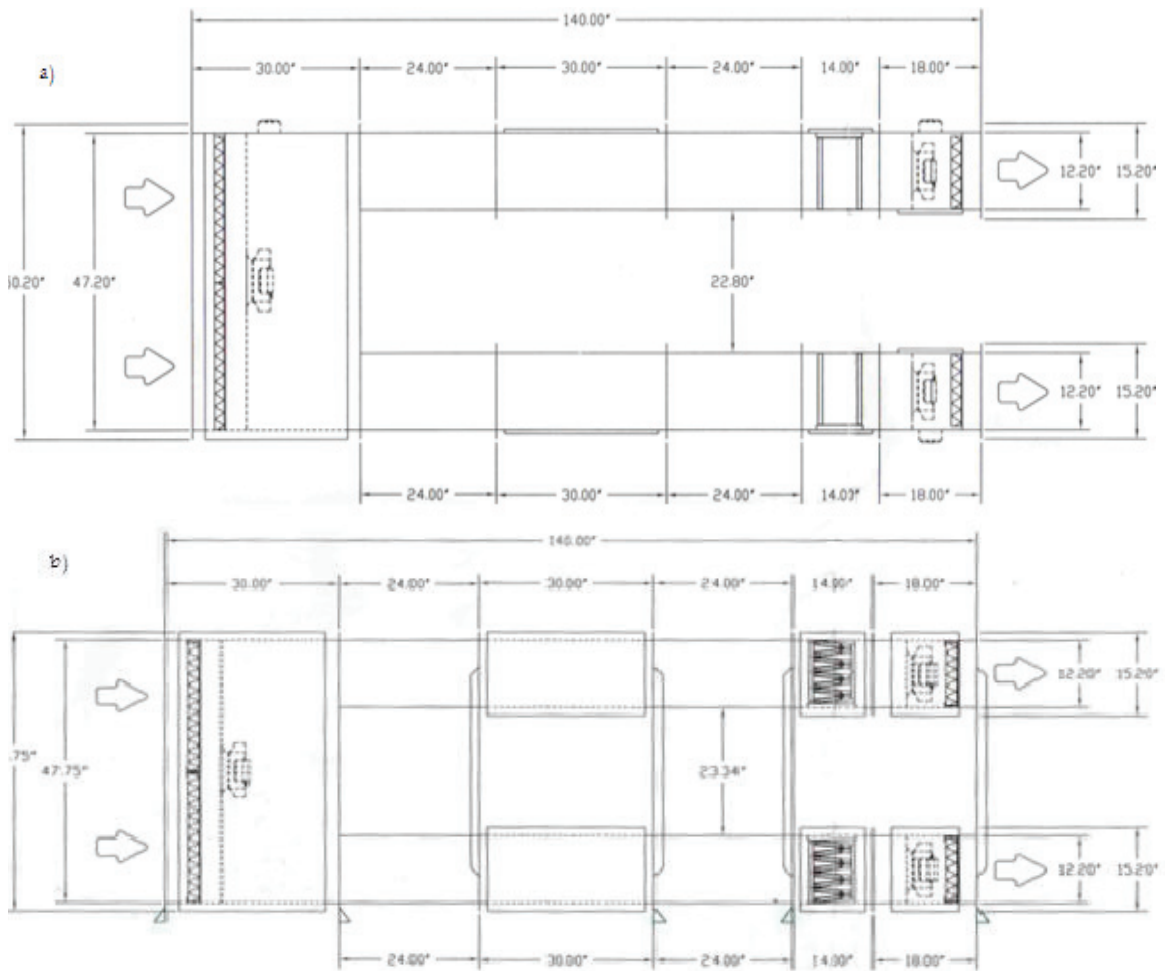


Figure 3-7 Duct apparatus dimensions.

Each duct consists of four main parts: Injection section, upstream, reaction section, adsorption section, and sampling ports. Figure 3-8 shows the schematic drawing of the apparatus with its different parts.

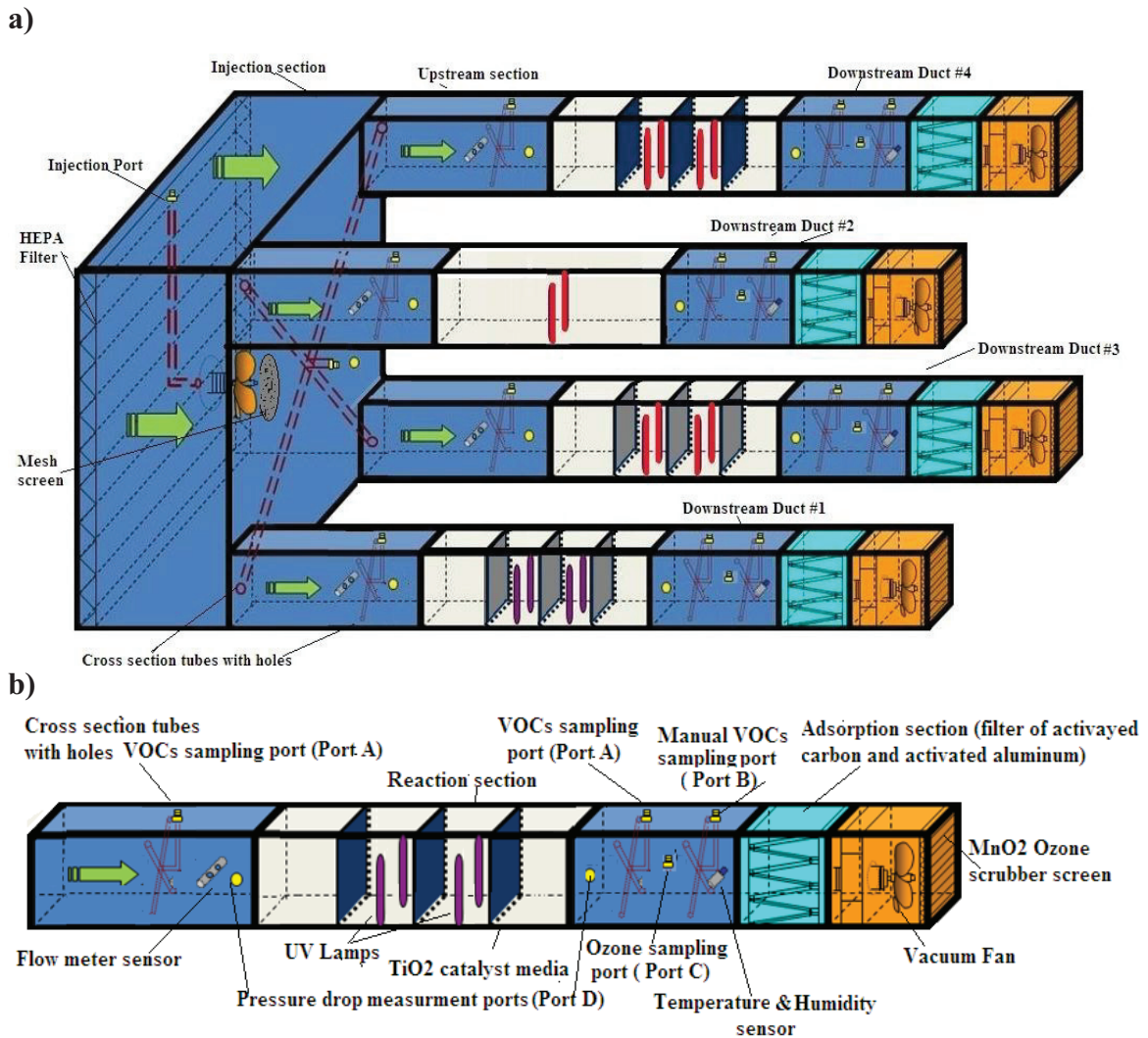


Figure 3-8 a) Open test rig apparatus schematic diagram. b) Different parts of each duct.

**Injection section:** This part is a common section to all the ducts. Laboratory air was sucked into the ducts using radial fans. Particulate filter was installed at the entrance of the duct to remove dust. First, air passes through the filter and mixes with the injected VOCs, and enters the ducts. Since it is necessary to have a uniform VOC concentration in the duct a mesh screen was installed at the duct entrance. One fan in the injection section and four fans in each of the ducts are available. The system was calibrated in order to

have a flow rate of  $0.047 \text{ m}^3/\text{s}$  -  $0.141 \text{ m}^3/\text{s}$  (100 cfm - 300 cfm) in each duct which can be controlled individually. Most of the tests were done at  $0.047 \text{ m}^3/\text{s}$  (100 cfm) flow rate.

**Upstream section:** This section includes cross section tubes with holes. VOCs concentration in upstream was measured from this part. The flow meter sensor is installed to measure and adjust the flow rate.

**Reaction section:** This section consists of UV-lamps and  $\text{TiO}_2$  catalysts. It is possible to change the number of lamps and media in this section. Catalysts media are located 2 inches away from the UV-lamps.

**UV-Lamps:** Two types of UV-lamps were used in the experiments: UVC and VUV lamps with 254 nm wavelength and 185 nm + 245 nm wavelengths, respectively (Figure 3-9). VUV lamps produce ozone as a by-product which reacts with VOCs. Therefore, experiments can be done in the absence and the presence of ozone using UVC and VUV lamps, respectively.

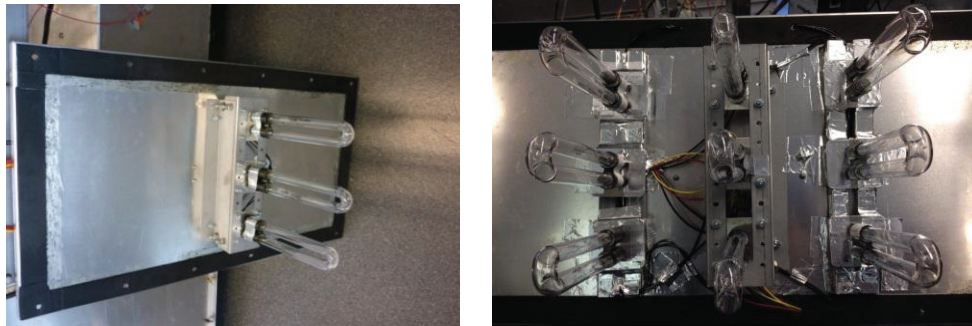


Figure 3-9 UV-lamps and their configuration.

**Catalyst:** Catalyst substrate A consists of  $\text{TiO}_2$  coated on fiber glass and catalyst substrate B consists of  $\text{TiO}_2$  coated on activated carbon. The BET test result shows the BET surface area of the catalyst substrate A and B are  $105.7063 \pm 1.6269 \text{ m}^2/\text{g}$  and  $887.6638 \pm 10.6871 \text{ m}^2/\text{g}$ , respectively. The SEM test results for catalyst substrates A and B are presented in Figures 3-10 and 3-11, respectively.

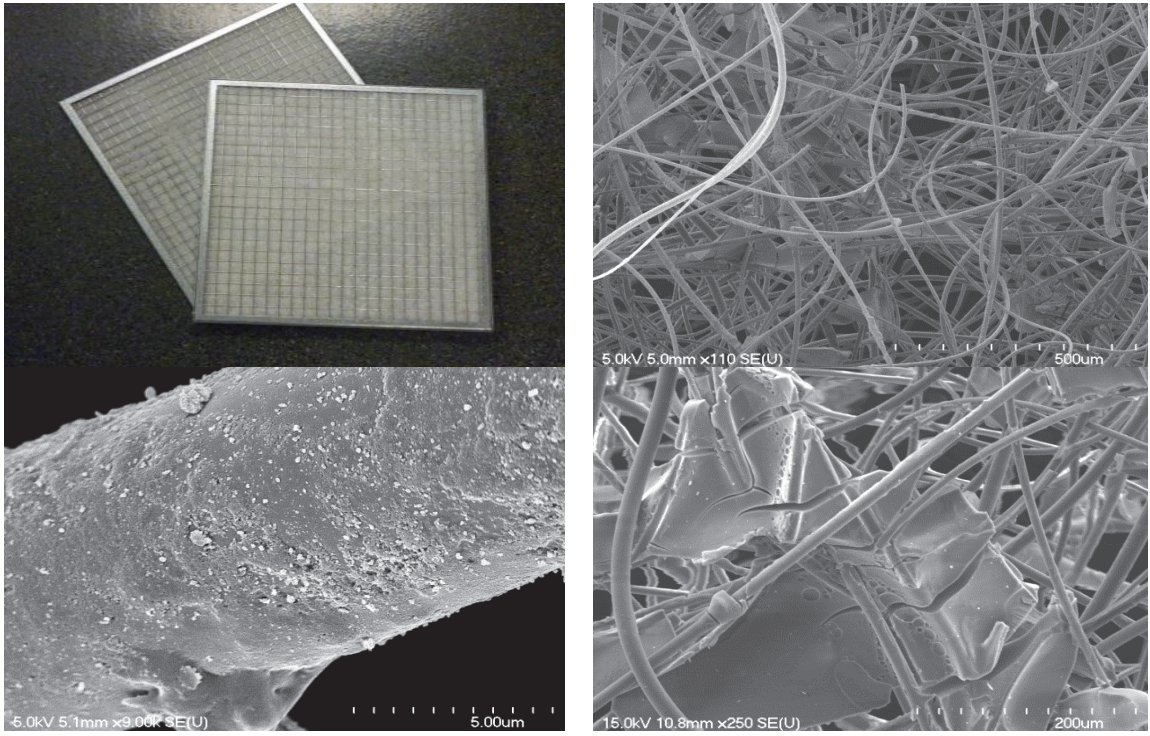


Figure 3-10 Catalyst substrate A consists of  $\text{TiO}_2$  coated on fiber glass.

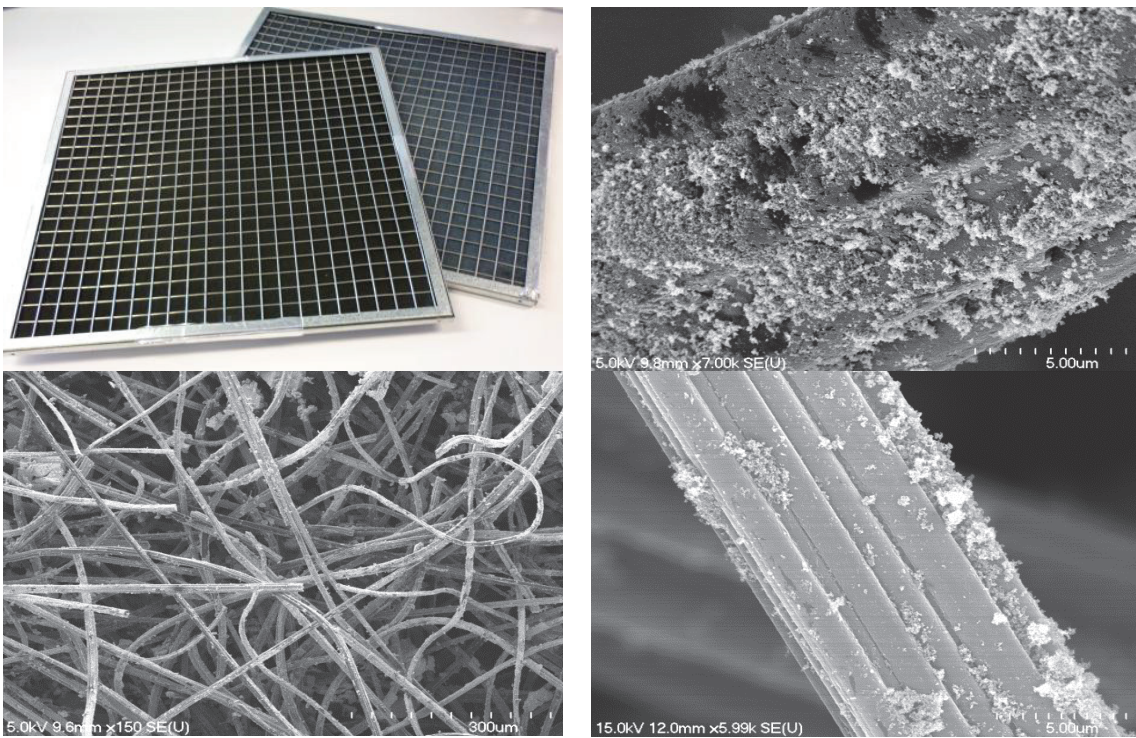


Figure 3-11 Catalyst substrate B consists of  $\text{TiO}_2$  coated on the activated carbon.

**Adsorption section:** Since there are some by-products, un-reacted challenge compounds, and also ozone in the duct, two precautions were considered to make sure that the exhaust air is clean. First, a multi mix chemical media of activated carbon and chemically impregnated alumina (Circul-Aire, Inc.) for VOC adsorption and especially aldehydes was installed before the radial fan at the end of each duct. Second, since in 254 nm +185 nm UV-lamps, ozone concentration was higher than the standard concentration; therefore an ozone scrubber screen made of  $MnO_2$  catalyst was also installed at the exhaust of each duct. Figures 3-12 and 3-13 show these filters and scrubbers.



Figure 3-12 Filters of multi mix chemical media of activated carbon and chemically impregnated alumina for adsorbing VOCs and aldehydes.

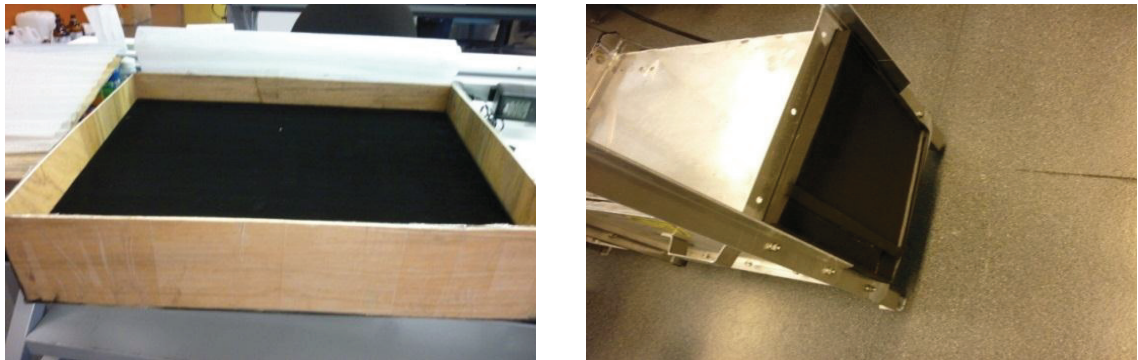


Figure 3-13 Ozone scrubber screen made of  $MnO_2$  catalyst.

**Sampling ports:** There are three types of sampling ports in each duct, which are as follows:

**Ozone sampling port (port C):** these ports are for taking ozone samples automatically. Each channel is connected to the sampling port (Upstream, Downstream Duct #1 to 4 and exhaust) via tubing and it takes samples and analyzes them.

**VOCs sampling port (port A):** these ports which exist in Upstream, before the reaction section, and downstream, after the reaction section, of Duct #1 to Duct #4 are connected to the CBISS MK3 Auto sampler coupled to the multi gas detector (B&K) via tubing. Ports are connected to the cross section tubes with some holes in them to have a uniform concentration of the samples.

**Manual VOCs sampling port (port B):** these ports are for manually taking samples. Since we want to have uniform samples of contaminated air of the duct, cross section tubes with some holes in them are installed inside the duct. These tubes are connected to the sampling port. Contaminated air passes through cross tubes and is gathered by air sampling pumps. In Figure 3-14, cross section tubes and sampling ports set-up are shown.

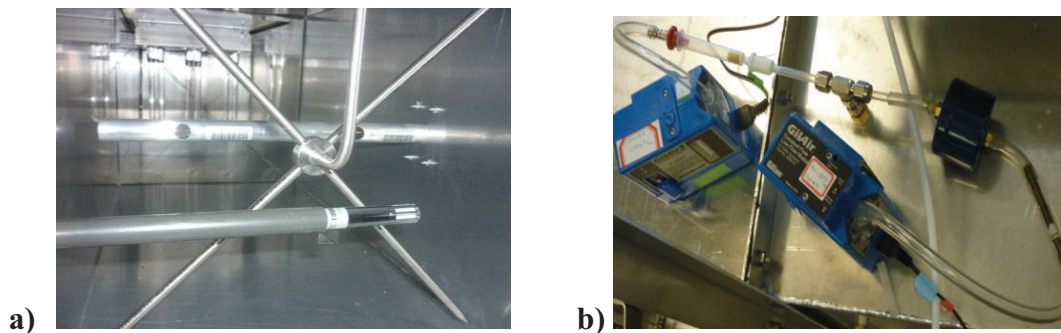


Figure 3-14 a) Cross section tubes, b) Sampling port setup.

**Pressure drop measurement port (port D):** there are two ports in each duct before and after the reaction part to measure the pressure drop.

### **3.7 ENVIRONMENTAL CONDITION MEASUREMENT**

For measuring temperature and relative humidity, Vaisala HUMICAP humidity and temperature transmitter series HMT100 were used in each duct downstream and upstream. Flow rate which can be adjusted by changing the speed of each of the vacuum fans, is measured by electronic low flow (ELF) sensor provided by EBTRON Thermal Dispersion Air flow Measurement Technology Company. The ELF is a factory calibrated from 0 to 3,000 FPM (0 to 15.24 m/s) in highly accurate wind tunnels to NIST traceable volumetric air flow standards to provide typical air flow accuracy of 3% of reading over the entire flow range. These instruments have probes which are mounted in the upstream and downstream at the same section in all of the ducts, and their measured data were transferred into a personal computer (PC) via data acquisition system (DAS) (provided from Agilent 34970 Data Acquisition/Switch Unit). In this system, data were produced by DC voltage difference and converted to temperature in Celsius and percentage of relative humidity by a developed program (Agilent IO Libraries Suite) which was installed in the PC. Analog output range for this instrument is 0-10 V which is sent to the Agilent DAS and measured relative humidity range is 0% to 100% with accuracy of  $\pm 1.7\%$  RH (0% to 90% RH);  $\pm 2.5\%$  RH (90% to 100% RH) and the temperature range is -40 °C to 80 °C (-40 °F to 176 °F) with  $\pm 0.2^\circ\text{C}$  accuracy.

### **3.8 EXPERIMENTAL METHODOLOGY AND PROCEDURE**

Two types of  $\text{TiO}_2$  catalyst substrates were used in this study. Substrate A which consists of  $\text{TiO}_2$  coated on fiber glass, and substrate B which is  $\text{TiO}_2$  coated on activated carbon (Figure 3-10 and Figure 3-11). The experiments were performed with two types of UV-

lamps, UVC and VUV lamps with 254 nm wavelength and 185 nm + 245 nm wavelengths respectively (Figure 3-9). Duct # 1 consisted of two units of PCO- reactors including three catalyst substrates A and two UVC lamps between each two catalyst substrates (total of four lamps). Duct #2 had two VUV lamps. The configuration of the Duct # 3 was as same as Duct # 1 except that instead of UVC; two VUV lamps were installed between each two catalysts (total of four lamps). Duct # 4 was supplied with two PCO reactors including three catalyst substrates B and two VUV lamps between each two catalyst substrates (total of four lamps). The configuration of the lamps and catalyst substrates is provided in Figure 3-8. This configuration made it possible to study the UV-PCO performance of each catalyst in both VUV-lamps with 185 nm + 254 nm and UVC-lamps with 254 nm wavelength. Also, using the proposed configuration, UV-PCO technology in the presence of ozone with VUV lamps can be investigated.

Experiments were performed at a 100 cfm air flow rate through each duct. First UV-lamps were turned on and after stabilization of light intensity and VOCs background measurement (which took 30 minutes), challenge gas was injected into the system from the injection section. Ozone is one of the by-products of UV-PCO using 254 nm + 185 nm wavelength VUV-lamps; Multi-Channel Industrial Hygiene Ozone Analyzer Model 465L was exploited to measure concentration in upstream and downstream of each duct (Port C). Target compound concentration at the upstream and downstream of each duct was measured and recorded with an auto-sampler coupled with a calibrated B&K gas detector (Port A). When the challenge compound concentration at the downstream was stabilized, air samples from the upstream and downstream were taken manually using Sigma Aldrich Supleco Lp-DNPH and KI ozone scrubber cartridges. The sampling

duration with Lp-DNPH cartridges was 1.5 hours at 1.3 L/min flow rate (Port B). High-performance liquid chromatography (HPLC) (PerkinElmer Company) was used for aldehydes and ketones analysis. UV-lamp light intensity was measured by 185 nm sensor (International Light Inc) and 254 nm wavelength sensor (Steril-Aire Company) (Appendix D). After completion of each experiment, when the injection was stopped, the test rig was continued to flush out overnight at the same airflow rate in order to prevent VOC residue in the test rig. Lamps were also remained on for 8-10 hours to activate the catalyst substrates after each experiment.

### 3.8.1 Removal Efficiency

The performance of UV-PCO was quantified by removal efficiency, and it was calculated from the measured upstream and downstream concentrations.

$$\text{Removal Efficiency, } E_t (\%) = \frac{C_{up,t} - C_{down,t}}{C_{up,t}} \times 100 \quad \text{Equation 3-1}$$

where;

$C_{up,t}$  = the upstream challenge gas concentration (ppb) as a function of time.

$C_{down,t}$  = the downstream challenge gas concentration (ppb) as a function of time.

$E_t$  = the removal efficiency as a function of time.

$t$  = the elapsed time (min).

### 3.8.2 Net By-product Concentration

Generated by-products' concentration in these experiments was quantified by comparing concentration of generated compound in upstream and downstream.

Net generated by-products concentration,  $G_a = C_{up} - C_{down}$  Equation 3-2

$C_{up}$  = the upstream generated by-product concentration (ppb).

$C_{down}$  = the downstream generated by-product concentration (ppb).

$G_a$  = the net production of generated by-product (ppb).

# CHAPTER 4 EXPERIMENTAL RESULTS AND DISCUSSION

## 4.1 INTRODUCTION

This chapter reports the experimental results based on the described methodology in chapter 3. Experiments were carried out in two categories: Section 4.2 consists of UV-PCO performance and by-products generation applying different classes and concentrations of VOCs, and section 4.3 includes parametric study of the system using ethanol as a target pollutants in order to more precisely investigate the complexity of the system.

## 4.2 UV-PCO PERFORMANCE AND BY-PRODUCTS GENERATION USING DIFFERENT CLASSES AND CONCENTRATIONS OF VOCS

The UV-PCO system has a different efficiency and by-products due to catalyst substrate specification and type of UV-Lamps. This section reports the results of four groups of VOCs including alcohols, ketones, alkanes, and aromatics. Two compounds from each group with three concentrations were chosen to study the trend of efficiency and generated by-products. Average ozone concentration during the experiments for each duct is presented in Appendix C.

### 4.2.1 Alcohol VOCs

Alcohols with  $C_nH_{2n+1}OH$  formulation are one of the major groups of volatile organic compounds (VOCs) in an indoor environment. Ethanol and 1-butanol were chosen from

this group. Environmental test conditions are presented in Table 4-1. Removal efficiency by the system for each compound in each duct is presented in Figures 4-1 and 4-2.

Table 4-1 Environmental test conditions for ethanol and 1-butanol experiments.

Condition	Flow rate ( CFM )		Relative Humidity ( % )		Temperature ( °C )	
	Ethanol	1-Butanol	Ethanol	1-Butanol	Ethanol	1-Butanol
Upstream	-	-	14.6 ± 1.0	19.8 ± 2.0	25.0 ± 0.1	25.0 ± 0.1
Duct #1	104.7 ± 5.9	106.4 ± 3.7	15.5 ± 0.9	17.8 ± 2.0	25.5 ± 0.3	25.6 ± 0.1
Duct #2	104.6 ± 5.8	105.0 ± 2.3	14.6 ± 0.9	19.3 ± 2.0	25.3 ± 0.1	25.3 ± 0.1
Duct #3	103.6 ± 6.1	103.4 ± 4.5	15.4 ± 0.9	19.1 ± 2.0	24.4 ± 0.1	25.0 ± 0.1
Duct #4	105.3 ± 2.8	99.5 ± 2.6	13.5 ± 0.8	20.0 ± 12.0	25.2 ± 0.1	25.0 ± 0.1

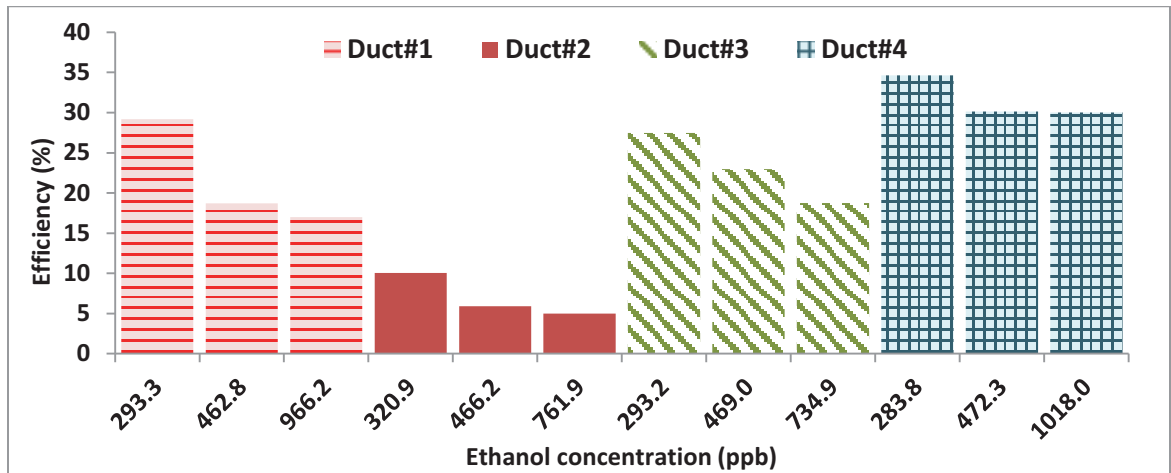


Figure 4-1 Removal efficiency of ethanol in each duct.

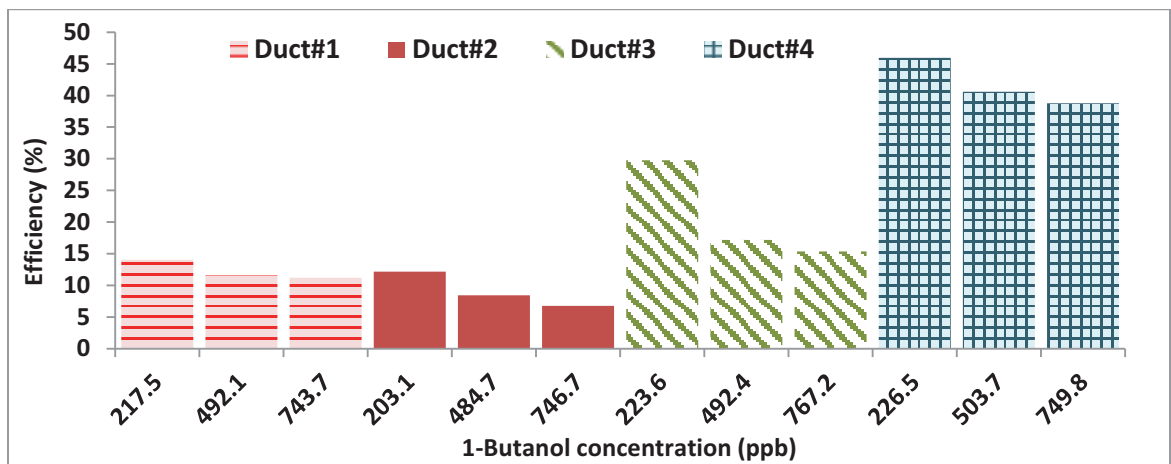


Figure 4-2 Removal efficiency of 1-butanol in each duct.

In ethanol and 1-butanol experiments, removal efficiency of Duct # 4 is higher than the other ducts. Therefore, the catalyst substrate B has a better removal efficiency compared to the catalyst substrate A. Duct # 3 with VUV lamps and almost 1000-1100 ppb ozone concentration shows better removal efficiency compared to the Duct # 1 with UVC lamps and 20 ppb ozone concentration which demonstrates that presence of ozone is in favor of alcohol oxidation. The removal efficiency of Duct # 2 confirms the ozone role in oxidation of alcohol, since the ozone concentration in this duct is 2000 ppb and 700 ppb in the case of ethanol and 1-butanol respectively. The removal efficiency reduces with the concentration increment due to the higher competition between compounds for adsorption on the catalyst surface and oxidation in presence of the UV-lamps. The ozone concentration in 1-butanol degradation is significantly less than ethanol which means the heavier compound has more reaction with ozone compared to the lighter compound (Appendix C). Figures 4-3 to 4-8 provide by-product results for ethanol and 1-butanol experiments.

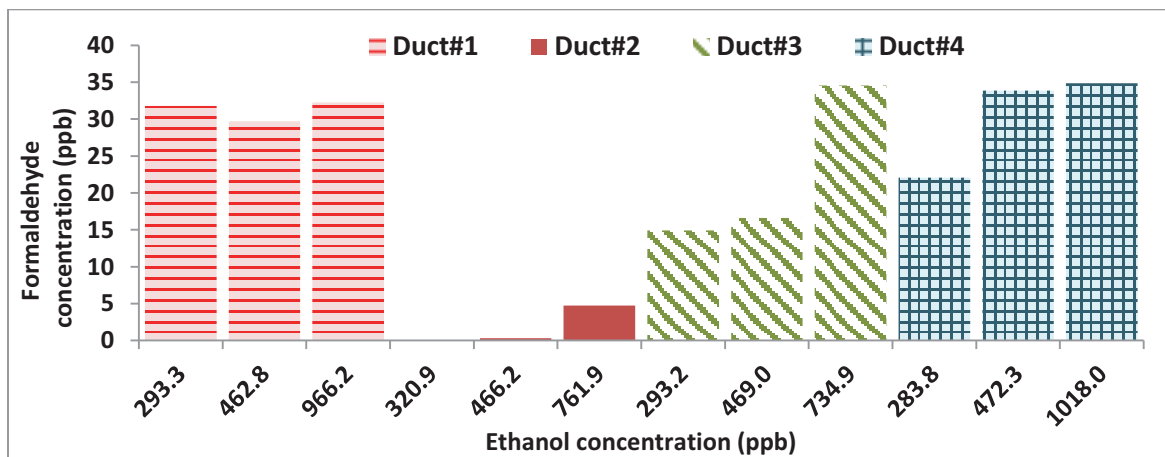


Figure 4-3 Formaldehyde generation in ethanol experiments in each duct.

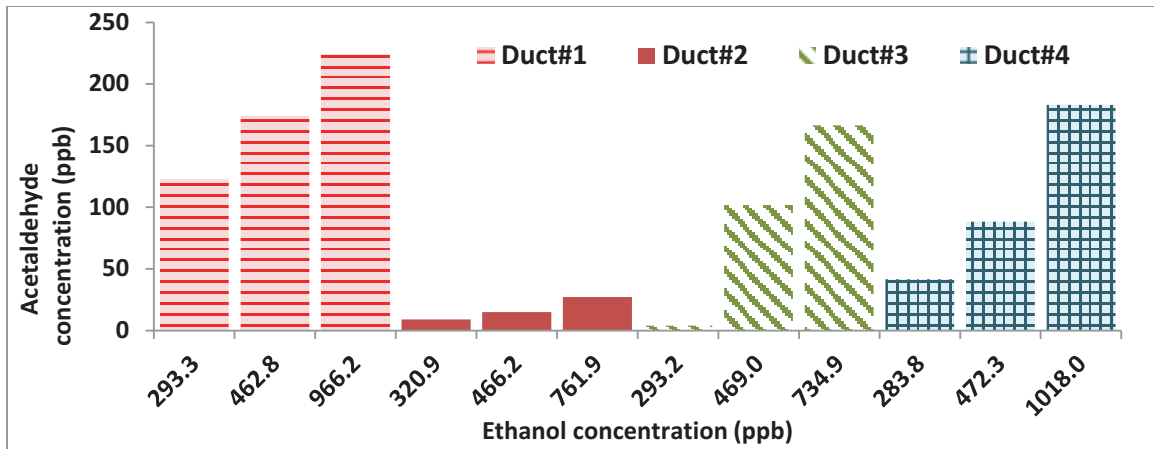


Figure 4-4 Acetaldehyde generation in ethanol experiments in each duct.

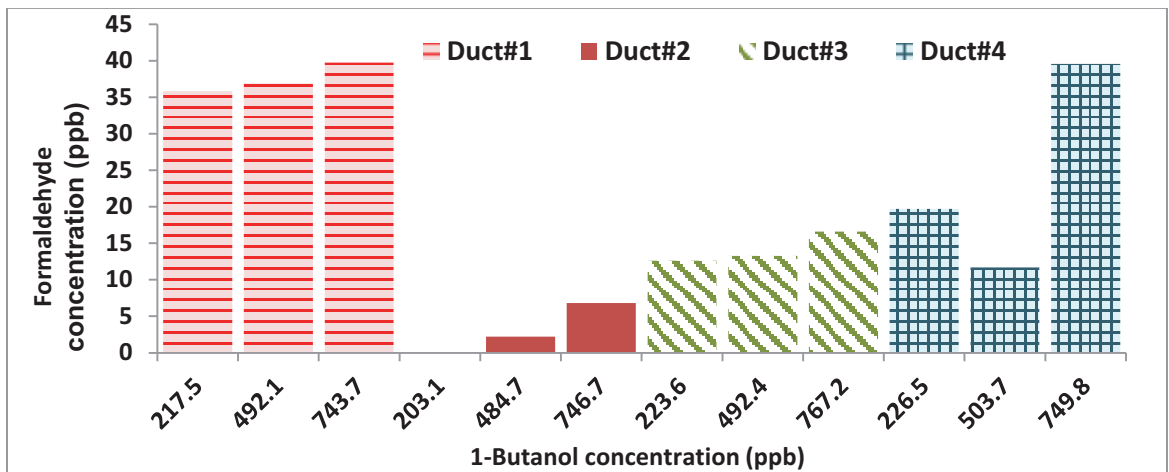


Figure 4-5 Formaldehyde generation in 1-butanol experiments in each duct.

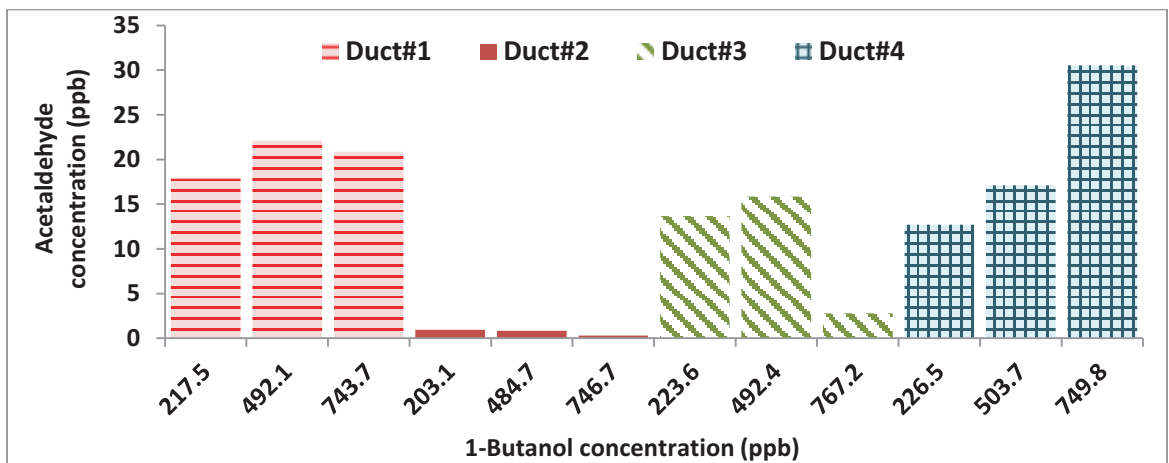


Figure 4-6 Acetaldehyde generation in 1-butanol experiments in each duct.

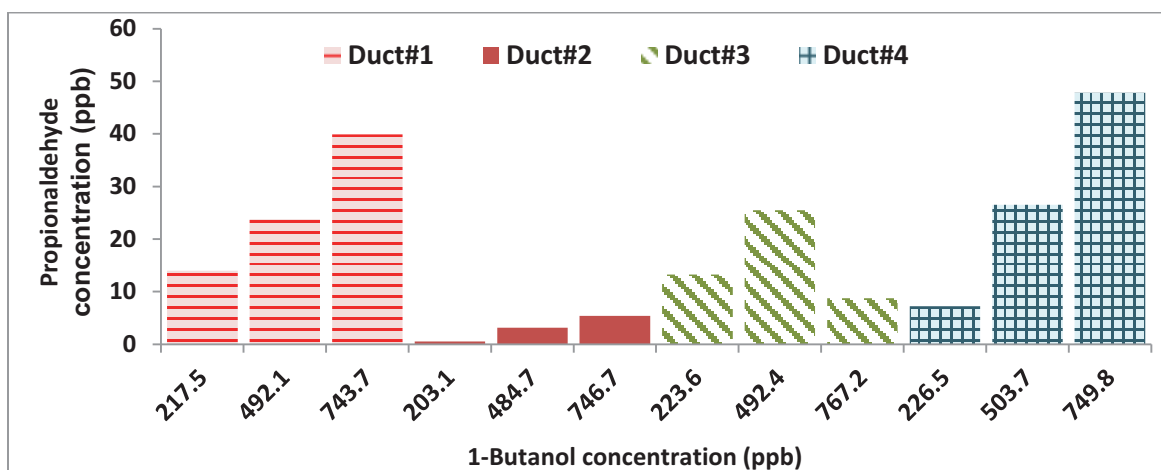


Figure 4-7 Propionaldehyde degeneration in 1-butanol experiments in each duct.

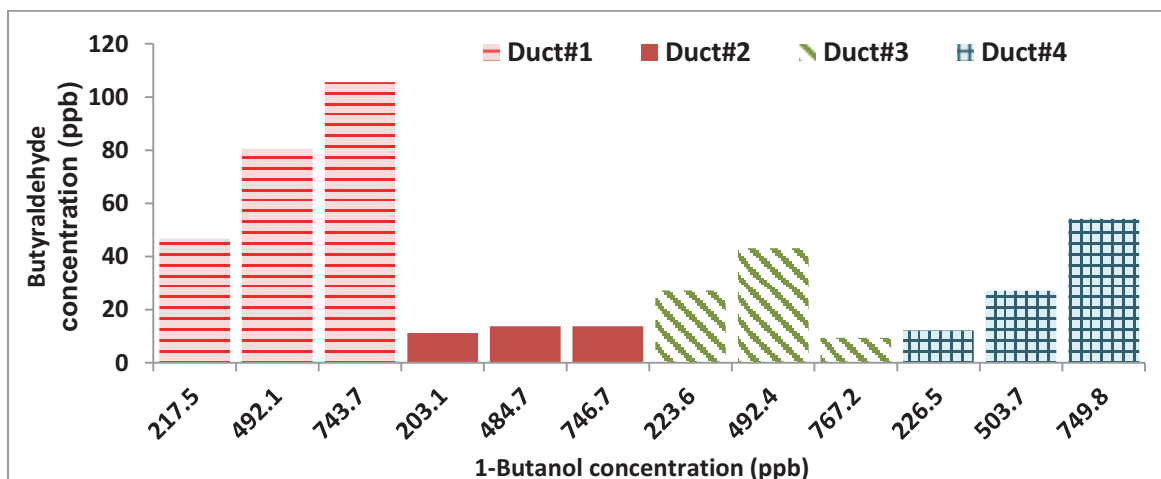


Figure 4-8 Butyraldehyde generation in 1-butanol experiments in each duct.

In photocatalytic oxidation of ethanol, the main by-products were formaldehyde and acetaldehyde. Moreover, negligible amounts of acetone and propionaldehyde are formed in all of the ducts (5-6 ppb) and negligible amounts of crotonaldehyde are generated only in presence of VUV lamps and ozone in Duct # 2, Duct # 3 and Duct # 4. In the case of 1-butanol, major by-products are butyraldehyde, formaldehyde, acetaldehyde and propionaldehyde. A negligible amount of crotonaldehyde (4-6 ppb) is produced only in Duct # 2, Duct # 3 and Duct # 4 with VUV lamps.

Experimental results show that although the removal efficiency decreases with the concentration, the by-product generation increases, which means increment of concentration increases the chance of partial oxidation. For the high concentration experiments, VOC competition for adsorption on catalyst surface is increased. Due to the limitation of active sites on the catalyst surface there is not enough space for all of the contaminants to adsorb. Therefore, chance of partial oxidation and subsequently generation of by-product is increased. Comparison between Duct # 3 and Duct # 1 with VUV and UVC lamps shows that although the removal efficiency of Duct # 3 is higher than Duct # 1 generated by-products concentration in Duct # 3 is lower than Duct # 1. This fact suggests that the presence of ozone prevents by-product generation. Ozone molecules cause chain reactions with by-products and oxidize them in the presence of catalyst substrates. Therefore, by-product concentration decreases.

#### 4.2.2 Alkane VOCs

N-hexane and n-octane oxidation was investigated among the alkane VOCs. In Table 4-2 the environmental test conditions are presented. The removal efficiency of the system for each compound in each duct is reported in Figures 4-9 and 4-10.

Table 4-2 Environmental test conditions for n-hexane and n-octane experiments.

Condition	Flow rate ( CFM )		Relative Humidity ( % )		Temperature ( °C )	
	n-Hexane	Octane	n-Hexane	Octane	n-Hexane	Octane
Upstream	-	-	31.1 ± 1.5	43.2 ± 1.8	25.0 ± 0.2	25.3 ± 0.2
Duct # 1	100.1 ± 4.0	98.2 ± 4.1	31.6 ± 1.5	43.3 ± 1.7	25.6 ± 0.2	25.9 ± 0.2
Duct # 2	104.2 ± 2.5	104.3 ± 2.8	31.4 ± 1.5	43.5 ± 1.8	25.1 ± 0.2	25.4 ± 0.2
Duct # 3	100.7 ± 4.7	100.1 ± 4.3	32.8 ± 1.6	45.4 ± 1.9	24.4 ± 0.2	24.7 ± 0.2
Duct # 4	104.0 ± 2.6	102.9 ± 2.7	30.0 ± 1.3	41.8 ± 1.9	25.3 ± 0.2	25.5 ± 0.2

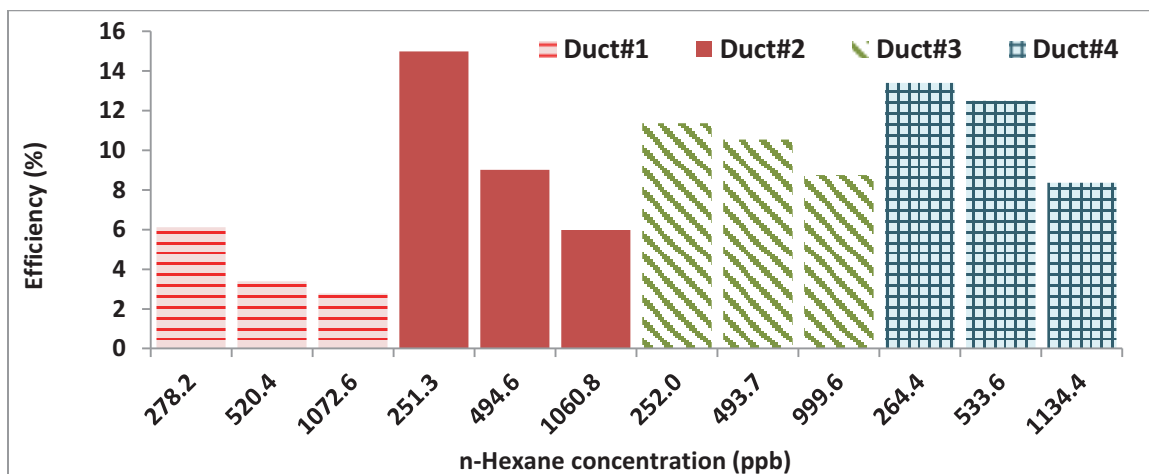


Figure 4-9 Removal efficiency of n-hexane in each duct.

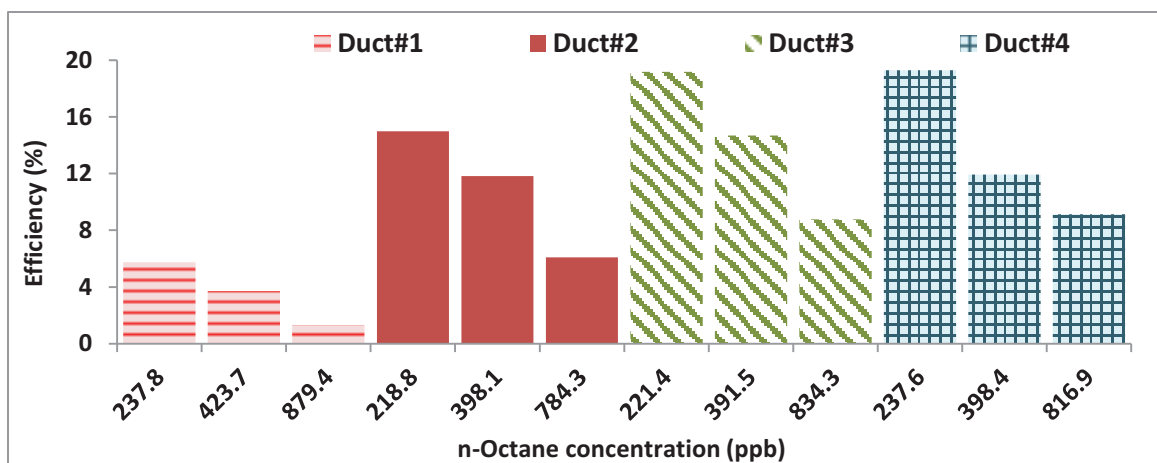


Figure 4-10 Removal efficiency of n-octane in each duct.

For n-hexane and n-octane experiments, the removal efficiency of Duct # 4 tends to be higher than the other ducts. Therefore, the catalyst substrate B had a better removal efficiency compared to the catalyst substrate A. The removal efficiency of Duct # 2 which consists of just VUV lamps was significant compared to Duct # 1 with catalyst and UVC lamps (PCO). Moreover Duct # 3 with VUV lamps shows a better removal efficiency compared to Duct # 1 with UVC lamps which demonstrates that presence of the ozone was in favor of alkane oxidation; considering that ozone concentration in Duct # 3 is 900-1000 ppb while in Duct # 1 is 20 ppb. The removal efficiency of Duct # 2 corroborates the ozone role in the oxidation of alkane, since the ozone concentration in this duct downstream is almost 700 ppb. The removal efficiency reduced with

concentration increment due to the stronger competition between compounds for adsorption on the catalyst surface and oxidation in presence of UV-lamps. Figures 4-11 to 4-13 represent by-products results for n-hexane and n-octane experiments.

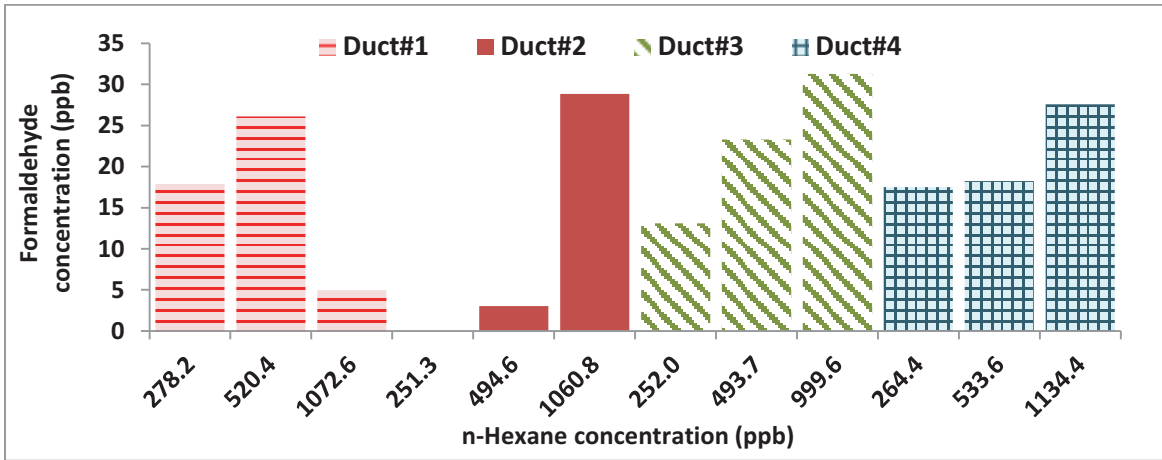


Figure 4-11 Formaldehyde generation in n-hexane experiments in each duct.

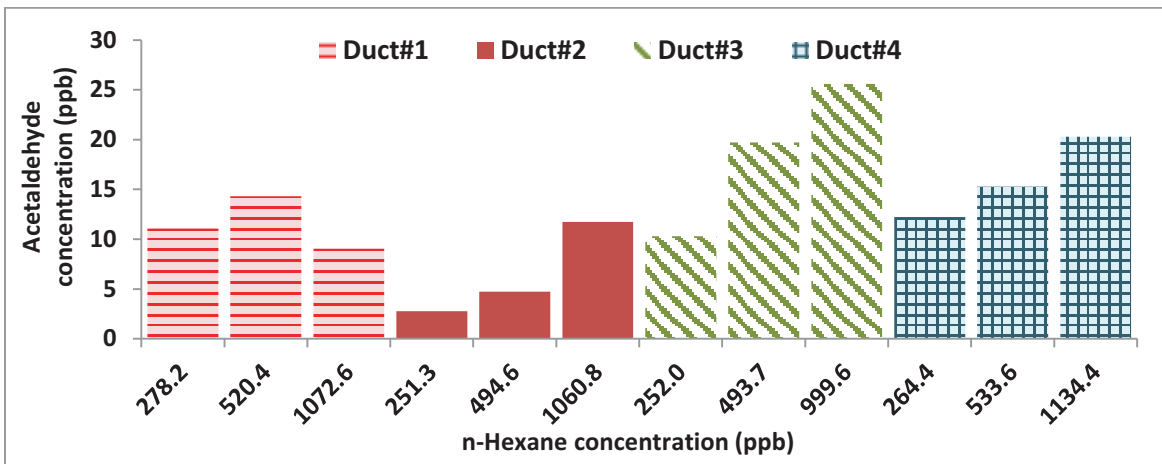


Figure 4-12 Acetaldehyde generation in n-hexane experiments in each duct.

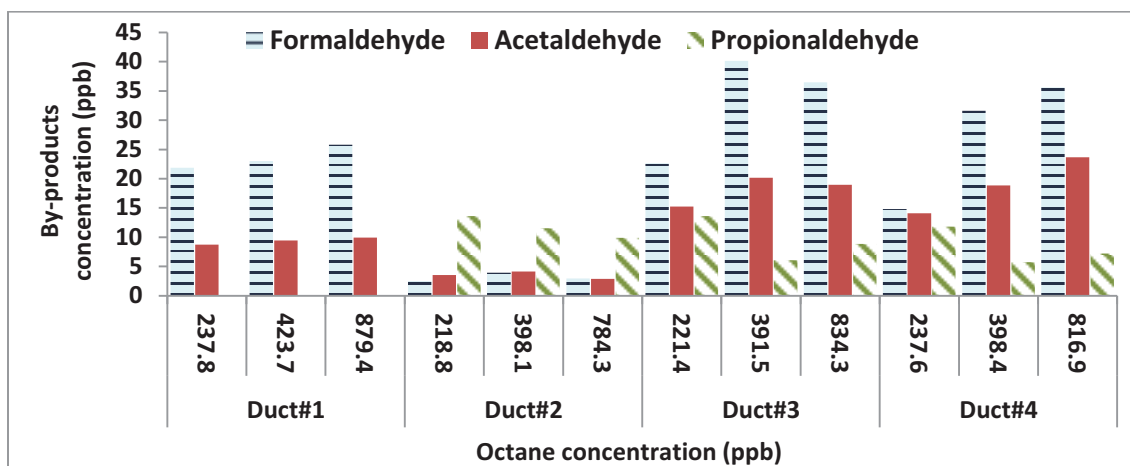


Figure 4-13 By-product generation in n-octane experiments in each duct.

Formaldehyde and acetaldehyde are the main by-products of n-hexane and n-octane. Propionaldehyde, as a main by-product, is generated only in the presence of VUV lamps in n-octane photocatalytic oxidation. Although the removal efficiency decreases with concentration increment, the by-product generation increases, which means concentration increment is in favor of partial oxidation. For high concentration experiments, VOCs competition for adsorption on catalyst surface increases. Due to limitation of active sites on the catalyst surface, there is not enough space for all of the contaminants to adsorb. Therefore, the chance of partial oxidation and more by-products generation increases. The results of n-hexane experiment shows generation of other by-products including acetone, propionaldehyde, butyraldehyde, crotonaldehyde, and hexanal. Concentration of these by-products is 5 ppb to 6 ppb and in Duct # 3 (with higher ozone concentration) is more than the other ducts. In the case of n-octane oxidation, generated by-products with 5 ppb to 6 ppb concentration are acetone crotonaldehyde, hexanal, and valeraldehyde.

### 4.2.3 Ketone VOCs

Acetone and 2-butanone are two major ketones in an indoor environment. Table 4-3 represents the environmental test conditions. Removal efficiency of the system for these compounds in each duct is provided in Figures 4-14 and 4-15.

Table 4-3 Environmental test conditions for acetone and MEK experiments.

Condition	Flow rate ( CFM )		Relative Humidity ( % )		Temperature ( °C )	
	Acetone	MEK	Acetone	MEK	Acetone	MEK
Upstream	-	-	43.7 ± 0.8	21.9 ± 1.4	24.5 ± 0.2	25.5 ± 0.2
Duct # 1	100.9 ± 4.3	101.9 ± 3.7	43.3 ± 0.7	22.3 ± 1.3	25.3 ± 0.2	26.2 ± 0.2
Duct # 2	105.8 ± 2.4	105.5 ± 2.4	43.5 ± 0.8	21.9 ± 1.4	24.7 ± 0.2	25.7 ± 0.2
Duct # 3	97.3 ± 6.4	105.8 ± 4.2	45.5 ± 0.9	22.8 ± 1.4	24.0 ± 0.2	25.0 ± 0.3
Duct # 4	106.8 ± 3.3	103.2 ± 2.7	42.0 ± 0.8	20.4 ± 1.4	24.8 ± 0.2	25.9 ± 0.2

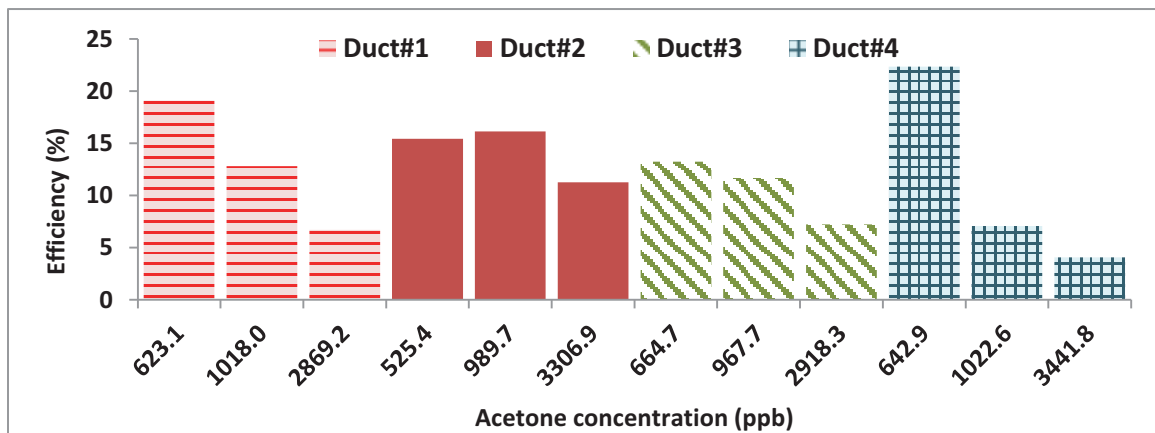


Figure 4-14 Removal efficiency of acetone in each duct.

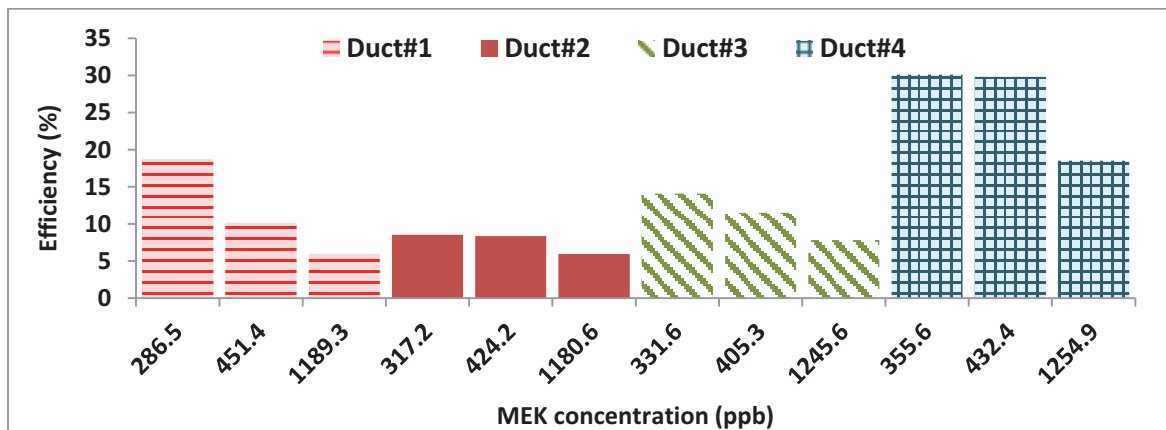


Figure 4-15 Removal efficiency of MEK in each duct.

Ketones removal efficiency decreases for higher pollutant concentrations in all ducts, because lower amounts of molecules can reach the catalyst surface to adsorb and oxidize. Removal efficiency of the ketones in Duct # 3 is not significantly higher than Duct # 1 which demonstrates that ozone reaction with ketones is not significant considering that the ozone concentration in downstream of Duct # 3 is almost 900-1000 ppb while in Duct # 1 is just 20 ppb which is the same as the upstream ozone concentration. Duct # 4 shows a higher removal efficiency compared to the other ducts which shows that the performance of the catalyst substrate B in comparison with catalyst substrate A, although the removal efficiency in case of increment in acetone concentration drastically decreases. Figures 4-16 to 4-19 gives the generated by-products.

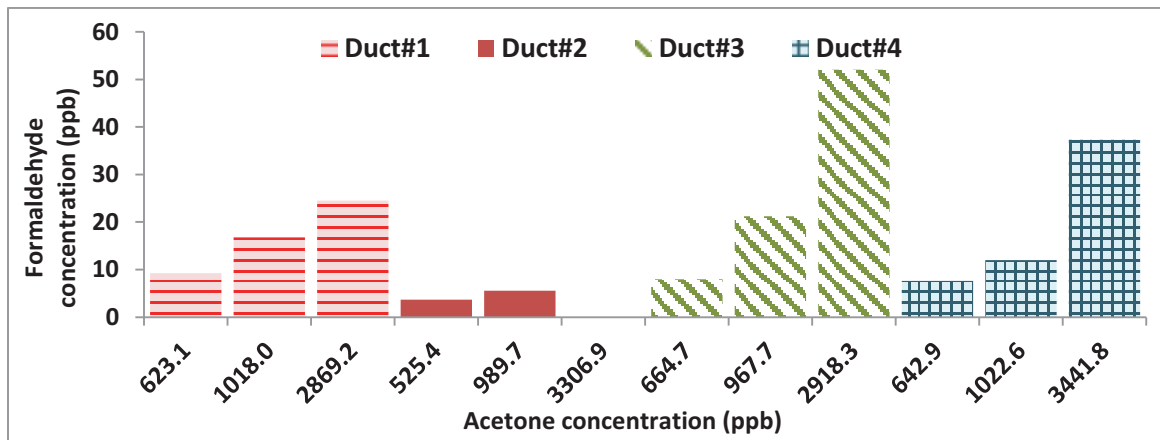


Figure 4-16 Formaldehyde generation in acetone experiments in each duct.

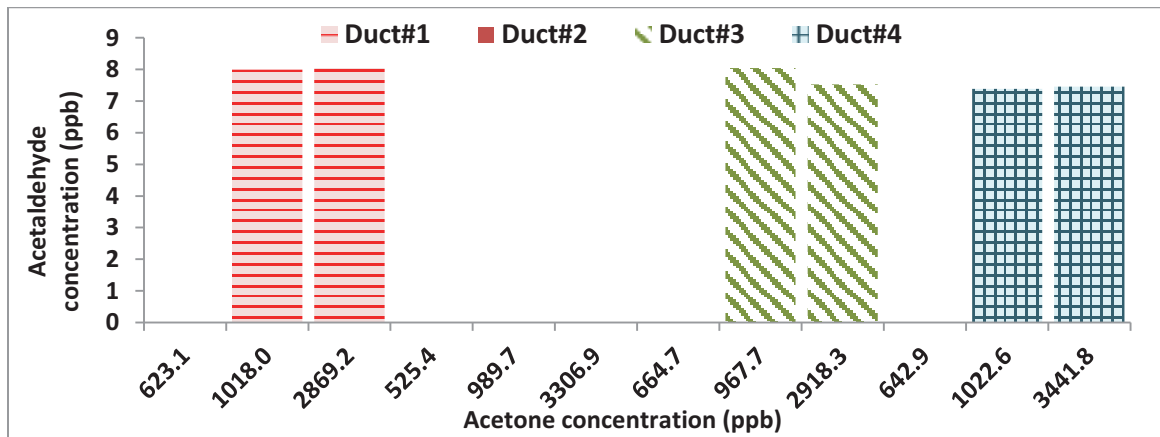


Figure 4-17 Acetaldehyde generation in acetone experiments in each duct.

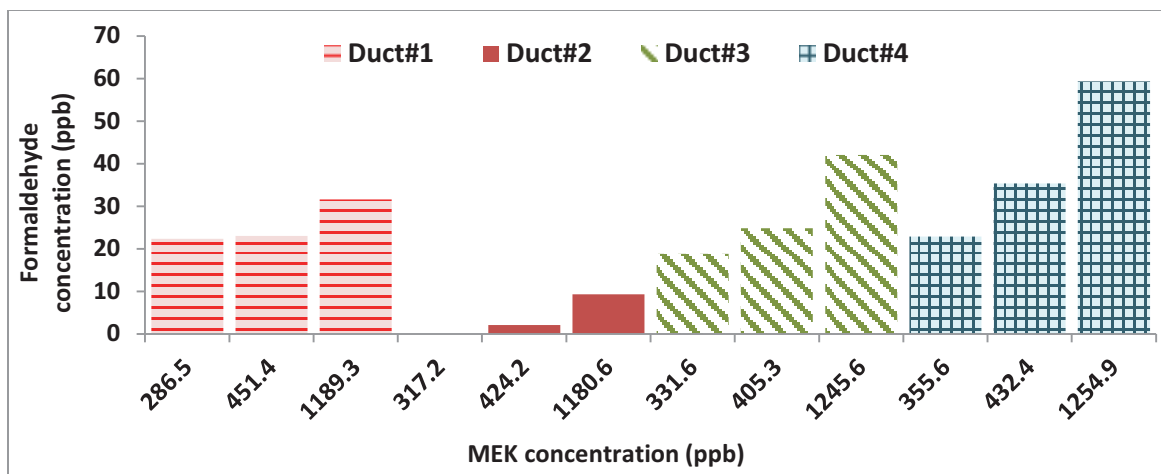


Figure 4-18 Formaldehyde generation in MEK experiments in each duct.

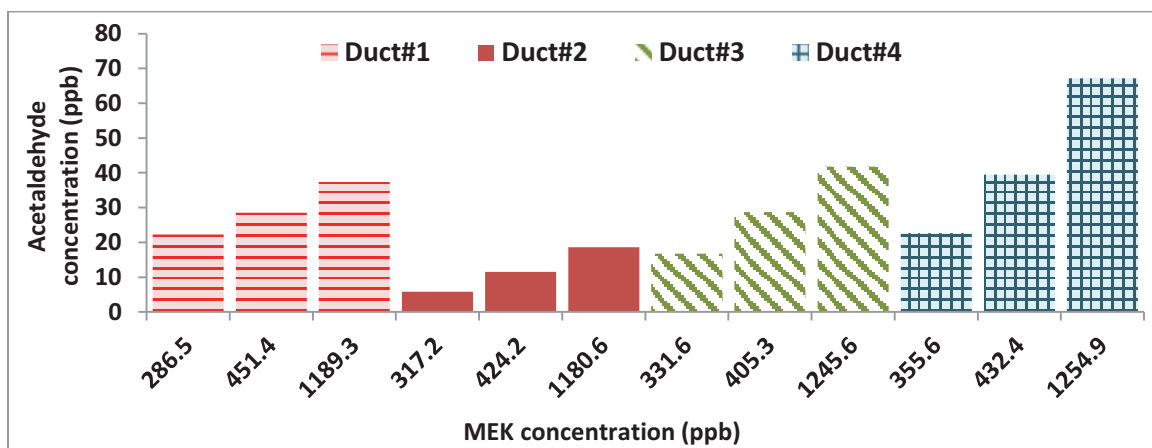


Figure 4-19 Acetaldehyde generation in MEK experiments in each duct.

Formaldehyde and acetaldehyde are the main by-products of ketones, although generation of acetaldehyde in acetone oxidation is less than MEK and acetaldehyde is generated only at a higher concentration (more than 1 ppm) (Figure 4-17). With increment of MEK and acetone concentration, the removal efficiency decreases but the incomplete oxidation rate increases. Therefore, as the concentration increases the by-product generation increase.

#### 4.2.4 Aromatic VOCs

Toluene and p-xylene were selected as contaminants of interest, and Table 4-4 represents the environmental test conditions. The upstream and downstream concentrations were applied to calculate the removal efficiency of the system, (Figures 20 and 21). Figures 4-22 to 4-27 represent the generated by-products of aromatics in the UV-PCO system.

Table 4-4 Environmental test conditions for toluene and p-xylene experiments.

Condition	Flow rate (CFM)		Relative Humidity (%)		Temperature ( °C )	
	Toluene	p-Xylene	Toluene	p-Xylene	Toluene	p-Xylene
Upstream	-	-	44.6 ± 1.2	34.4 ± 1.80	21.4 ± 0.2	23.8 ± 1.1
Duct # 1	102.4 ± 3.4	102.0 ± 3.7	44.6 ± 1.2	34.5 ± 1.78	22.0 ± 0.2	24.5 ± 1.1
Duct # 2	101.9 ± 4.1	102.9 ± 2.5	44.7 ± 1.2	34.3 ± 1.74	21.5 ± 0.2	24.1 ± 1.1
Duct # 3	104.8 ± 5.8	105.8 ± 4.5	46.6 ± 1.2	36.1 ± 1.88	20.9 ± 0.2	23.3 ± 1.1
Duct # 4	97.7 ± 4.2	101.8 ± 2.7	42.9 ± 1.2	32.6 ± 1.69	21.7 ± 0.2	24.2 ± 1.1

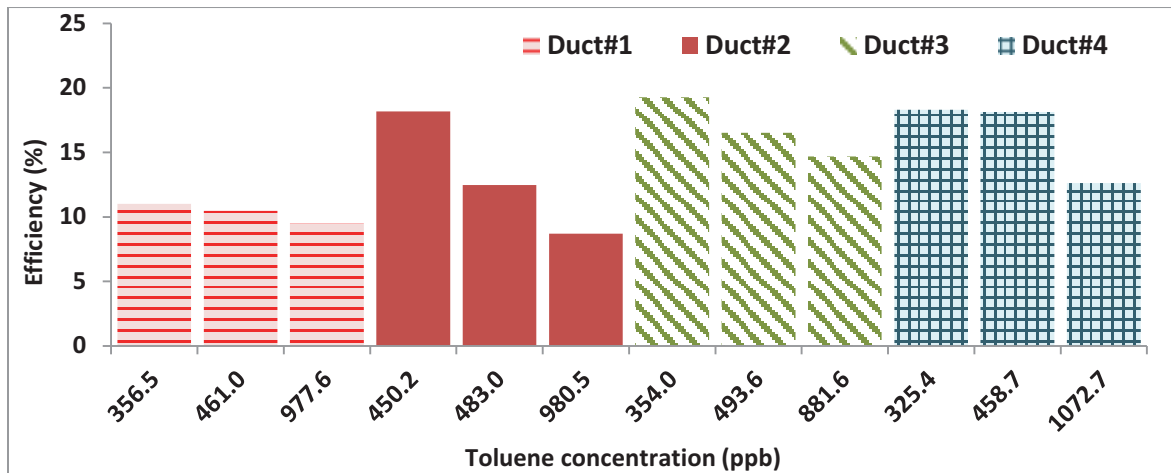


Figure 4-20 Removal efficiency of toluene in each duct.

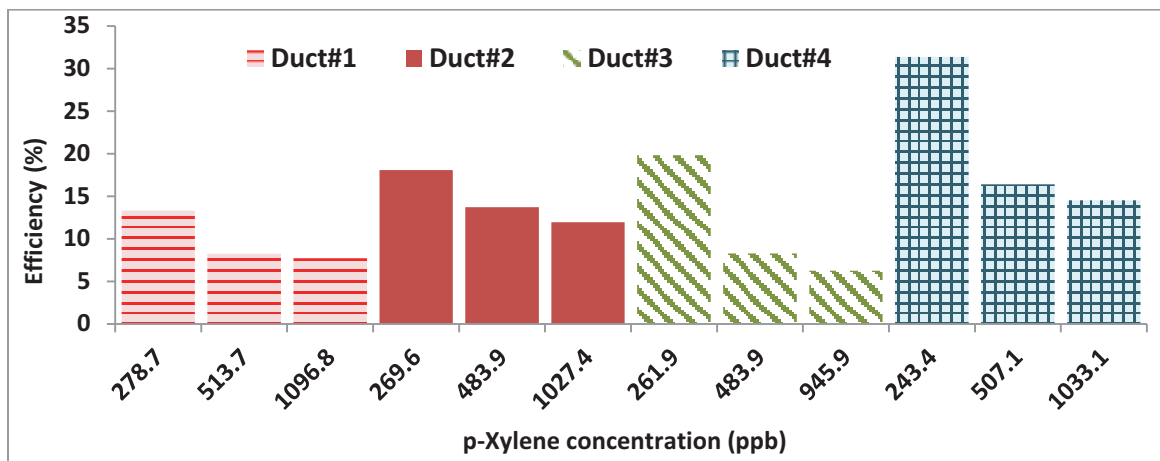


Figure 4-21 Removal efficiency of p-xylene in each duct.

Figures 4-20 and 4-21 show that the removal efficiency of duct # 4 is higher than the other ducts; this indicates that catalyst substrate B has a better performance than catalyst substrate A. Moreover, Duct # 3 has higher removal efficiency than Duct # 1. This could be due to the presence of ozone since the ozone concentration in Duct # 3 is almost 1100 ppb while in Duct # 1, it is 16 ppb to 40 ppb. The removal efficiency of Duct # 2 corroborates the ozone role in the oxidation of aromatics due to 500 ppb and 700 ppb downstream ozone concentration of this duct in toluene and p-xylene degradation respectively. The removal efficiency reduces with concentration increment due to the stronger competition between compounds for adsorption on the catalyst surface and oxidation in the presence of UV-lamps. The role of ozone in the oxidation of aromatics is considerable since in Duct # 2 the removal efficiency of both toluene and p-xylene is higher than Duct # 1. The ozone concentration downstream of Duct # 2 and Duct # 1 is 500 ppb and 16 ppb - 33 ppb in the case of toluene and 700 ppb and 22 ppb - 43 ppb in the case of p-xylene respectively.

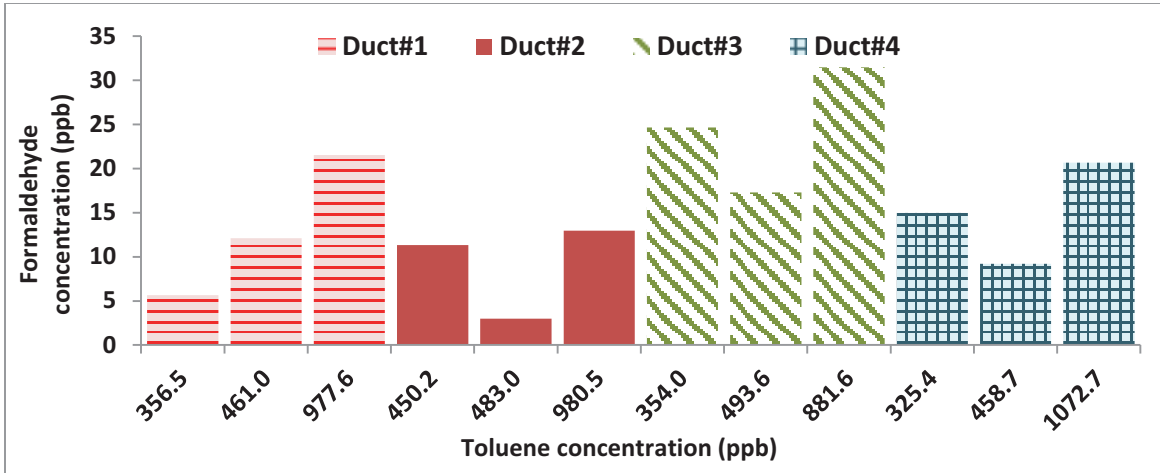


Figure 4-22 Formaldehyde generation in toluene experiments in each duct.

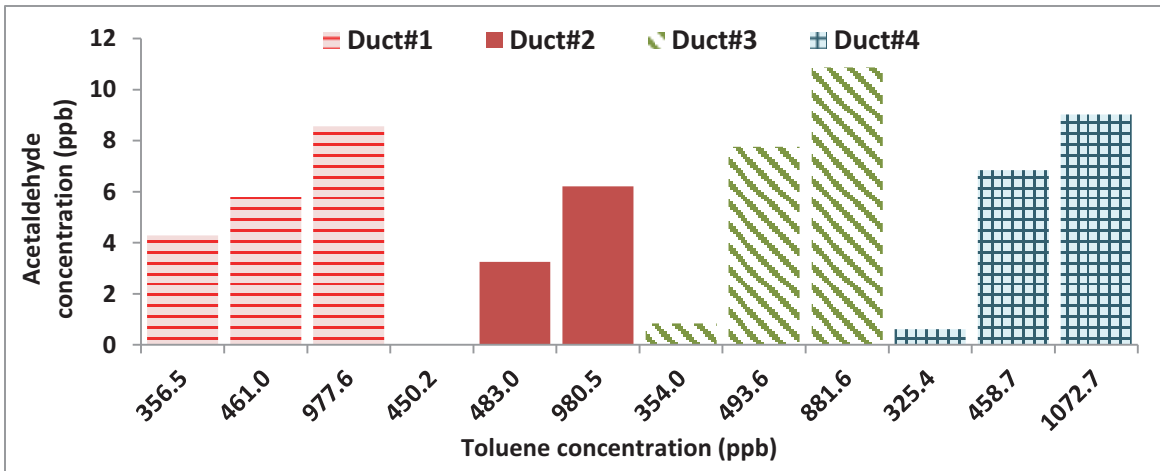


Figure 4-23 Acetaldehyde generation in toluene experiments in each duct.

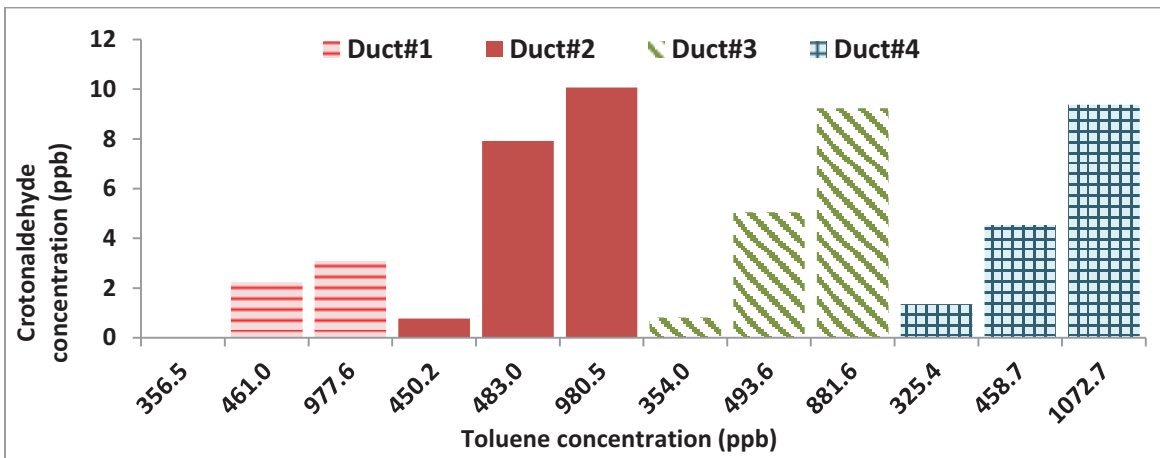


Figure 4-24 Crotonaldehyde generation in toluene experiments in each duct.

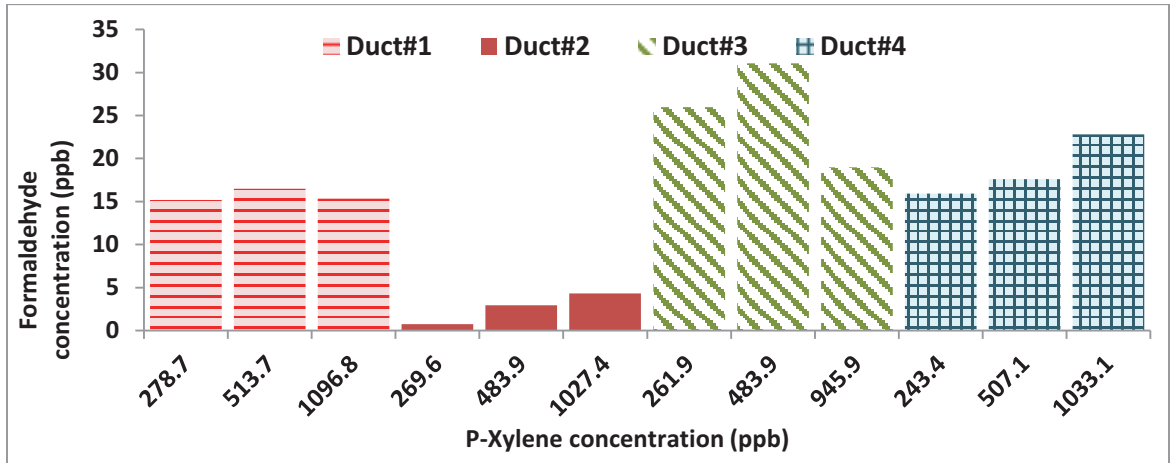


Figure 4-25 Formaldehyde generation in p-xylene experiments in each duct.

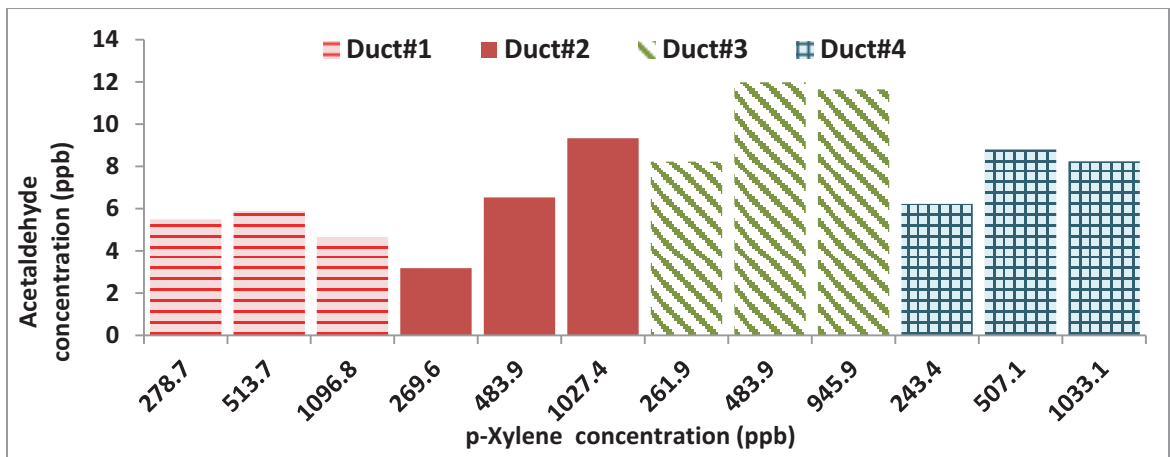


Figure 4-26 Acetaldehyde generation in p-xylene experiments in each duct.

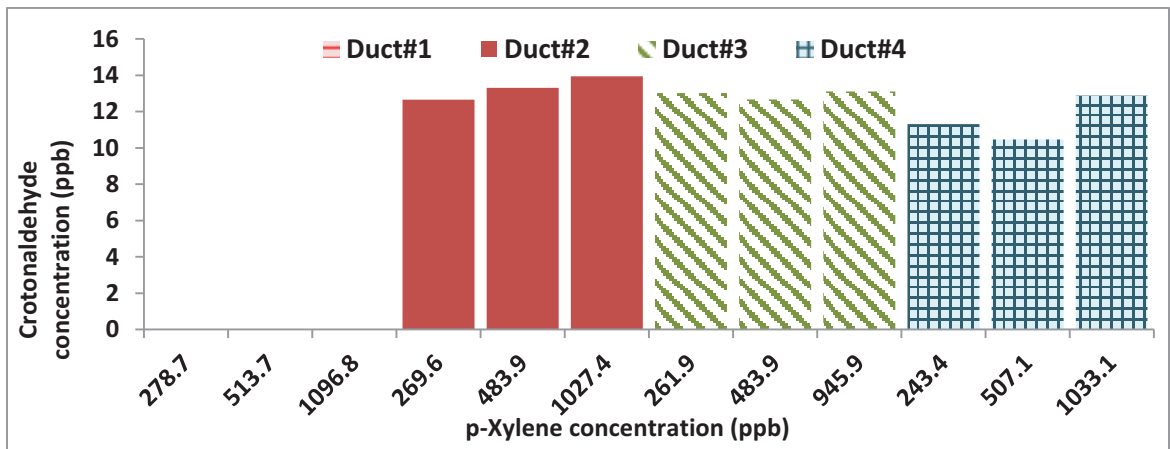


Figure 4-27 Crotonaldehyde generation in p-xylene experiments in each duct.

Formaldehyde, acetaldehyde and crotonaldehyde are the major by-products of toluene and p-xylene. Results show that although the removal efficiency decreases with concentration increment, by-products generation increase, which means concentration increment, is in favor of partial oxidation. For high concentration experiments, VOCs competition for adsorption on catalyst surface increases. Due to the limitation of active sites on the catalyst surface, there is not enough space for all of the contaminants to adsorb. Therefore, chance of partial oxidation and more by-products generation increases. Crotonaldehyde generation mostly depends on the presence of ozone in the system, and in photocatalytic oxidation of p-xylene, this by-product only was generated in the presence of VUV lamps. During photocatalytic oxidation of p-xylene and toluene, some other by-products with less than 7 ppb concentration are formed including butyraldehyde, tolualdehyde, acetone, valeraldehyde, dimethylbenzaldehyde. Also, benzaldehyde was generated only in toluene experiments.

#### **4.2.5 All Groups of VOCs**

The removal efficiency and concentration of commonly generated by-product of all tested compounds at 500 ppb concentration are presented in Figures 4-28 and 4-29. Experiments were done at a  $100 \pm 6$  cfm flow rate,  $23 \pm 2$  °C temperature and  $35\% \pm 10\%$  relative humidity.

Duct # 1 performance for all tested VOCs is as follows: acetone > 1-butanol  $\geq$  ethanol toluene  $\geq$  MEK > p-xylene > n-octane  $\geq$  n-hexane. Duct # 2 performance for all tested VOCs is as the following: acetone > p-xylene  $\geq$  toluene > n-octane > n-hexane > 1-butanol > ethanol. Duct # 3 performance for all tested VOCs: 1-butanol > toluene > n-octane  $\geq$  ethanol  $\geq$  acetone > MEK  $\geq$  n-hexane > p-xylene. Finally, Duct # 4 performance

for all tested VOCs is as the following: 1-butanol > MEK > acetone > ethanol ≥ toluene > p-xylene > n-hexane ≥ n-octane.

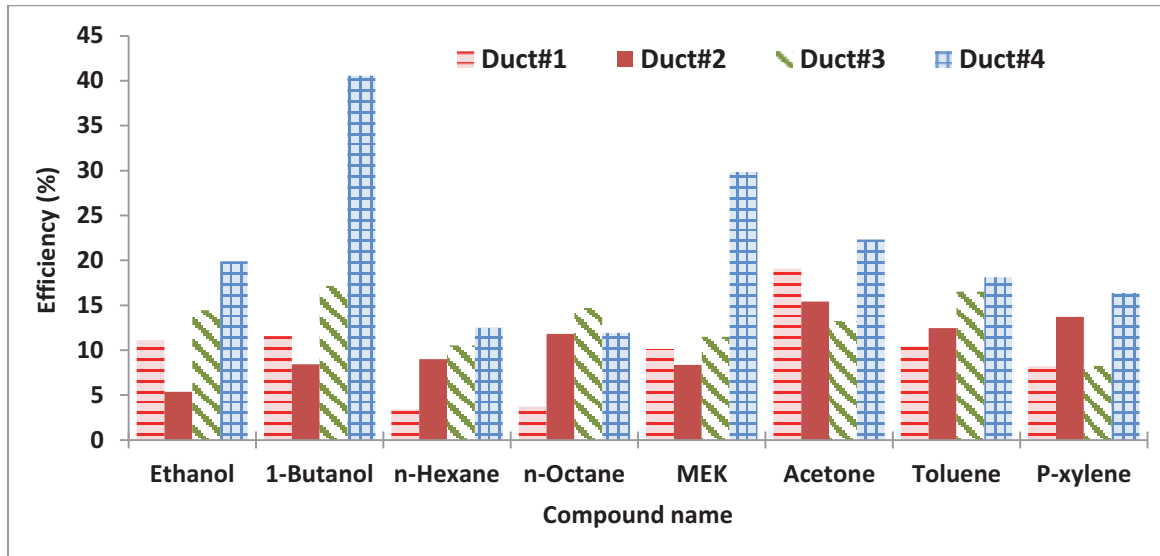


Figure 4-28 Removal efficiency of tested VOCs.

Thus, experimental results show that ozone reacts more with heavier compounds with more stable structure. Catalyst substrate A with UVC lamps has greater performance for oxidation of light compounds while catalyst substrate B has a higher performance for heavier compounds. Both catalyst substrates A and B with UVC and VUV lamps show low performance for alkane compounds. Generally, catalyst substrate B is better than catalyst substrate A and VUV lamps are more efficient than UVC lamps. Figure 4-29 shows the common by-products concentration for the tested VOCs.

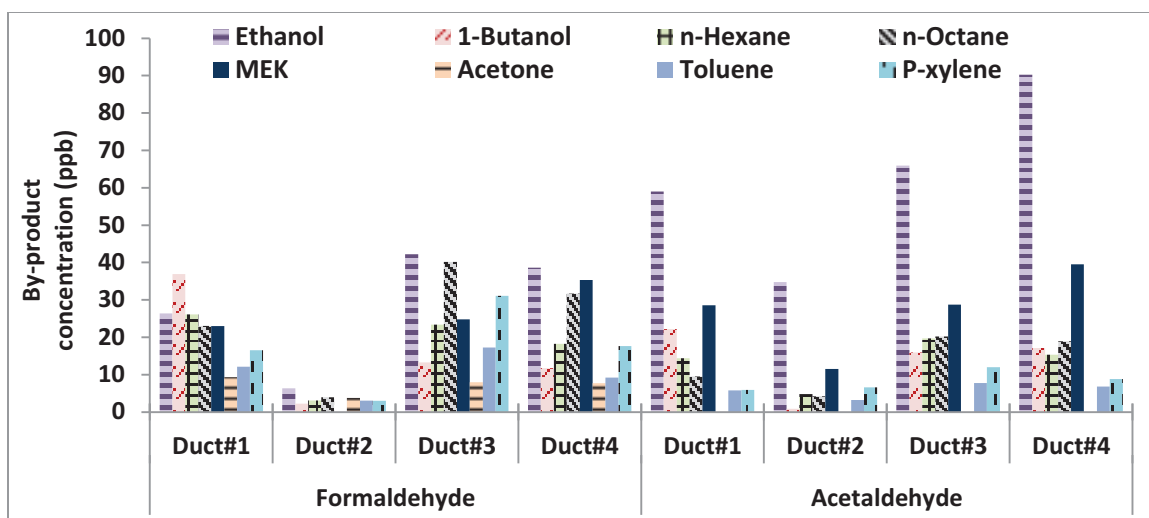


Figure 4-29 Generated by-products of test VOCs with 500 ppb concentration.

Formaldehyde and acetaldehyde are the major by-products of all VOCs using UVC and VUV lamps, and also generation of these by-products depends on ozone concentration and target compound in the system. Ethanol generates the highest amount of acetaldehyde in comparison with other VOCs followed by MEK in the second place. Aromatics including toluene and p-xylene and also acetone generate less acetaldehyde. In the presence of VUV (ozone), first ethanol and then n-octane generate more formaldehyde compared to the others. These compounds are announced as carcinogenic and inhalation toxicants. Environmental Health Hazard Assessment (OEHHA) has recommended Acute Reference Exposure Levels (ARELs) of  $55 \mu\text{g}/\text{m}^3$  (44 ppb) in 3 h for formaldehyde and ARELs of  $470 \mu\text{g}/\text{m}^3$  (261 ppb) for acetaldehyde.

#### 4.3 PARAMETRIC STUDY OF THE UV-PCO SYSTEM

For parametric study of the system ethanol as a target pollutant was chosen. The effect of relative humidity, different numbers of lamps and different numbers of UV-PCO reactors have been considered in this section.

### 4.3.1 Repeatability Test

Experiments on ethanol as a target pollutant with 500 ppb concentration at 100 cfm were done in different days with the same condition to investigate the repeatability of the experiments. Experiments showed good repeatability, and removal efficiency of ducts in are close. In Table 4-5 environmental conditions of the experiments and removal efficiency in each duct are presented.

Table 4-5 Environmental conditions and removal efficiency for the repeatability experiments.

Condition	Flow rate ( CFM )		Relative Humidity ( % )		Temperature ( $^{\circ}$ C )		Removal Efficiency ( % )	
	Test 1	Test 2	Test 1	Test 2	Test 1	Test 2	Test 1	Test 2
Upstream	-	-	15.0 $\pm$ 0.8	14.4 $\pm$ 0.5	22.3 $\pm$ 0.2	25.0 $\pm$ 0.1	-	-
Duct # 1	100.6 $\pm$ 3.1	104.5 $\pm$ 8.2	16.0 $\pm$ 0.8	15.3 $\pm$ 0.4	22.7 $\pm$ 0.2	25.6 $\pm$ 0.4	15.5	18.5
Duct # 2	102.0 $\pm$ 2	106.2 $\pm$ 8.3	15.2 $\pm$ 0.8	14.3 $\pm$ 0.5	22.5 $\pm$ 0.2	25.3 $\pm$ 0.2	6.7	7.0
Duct # 3	99.2 $\pm$ 3.0	105.8 $\pm$ 7.2	16.1 $\pm$ 0.8	15.2 $\pm$ 0.5	21.5 $\pm$ 0.2	24.4 $\pm$ 0.1	22.2	22.3
Duct # 4	100.9 $\pm$ 2.9	105.2 $\pm$ 2.9	13.8 $\pm$ 0.6	13.2 $\pm$ 0.3	22.4 $\pm$ 0.2	25.2 $\pm$ 0.1	36.6	30.0

### 4.3.2 Concentration Effect

This part was discussed in section 4.2.1 using ethanol in three concentrations in an open test rig.

### 4.3.3 Effect of Relative Humidity

For investigation of relative humidity, experiments were done in 4 to 5 different relative humidity levels in each duct with 500  $\pm$  20 ppb ethanol as a target pollutant at 100  $\pm$  6 CFM flow rate and 21  $\pm$  2  $^{\circ}$ C. Duct # 1 at 9%, 15%, 20%, 42% and 60%; Duct # 2 at 9%, 15%, 20%, 30% and 42%; Duct # 3 at 9%, 15%, 30%, 42% , 60% and Duct # 4 at 9%, 15%, 30%, 42%, and 60%. Figure 4-30 represents the effect of relative humidity on removal efficiency in each duct. Generated by-products at different relative humidity are provided in Figures 4-31 and 4-32.

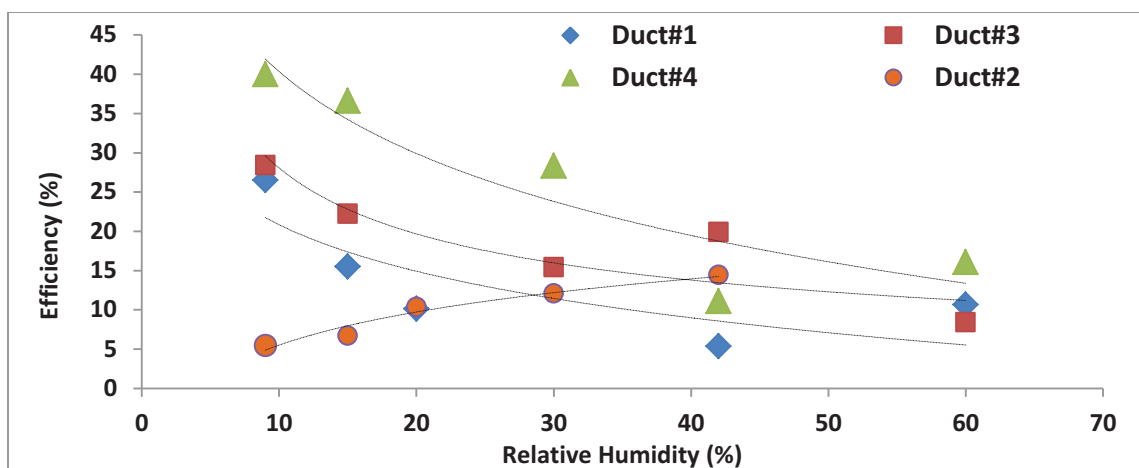


Figure 4-30 Effect of relative humidity on removal efficiency of ethanol in each duct.

In Ducts # 1, 3, and 4 of the UV-PCO system, when the relative humidity increases, removal efficiency decreases. An increase of water vapor molecules increases the competition of water and VOCs molecules for adsorption on the catalyst surface. Due to the acidic structure of  $\text{TiO}_2$  and preference for adsorbing water vapor molecules compared to VOCs with less polarity, at higher relative humidity, lower amounts of VOC molecules adsorb on the surface to oxidize. Therefore, removal efficiency decreases. In Duct # 2, the removal efficiency increases with relative humidity which is because of the generation of radicals including OH radicals at higher amounts for oxidization of VOCs.

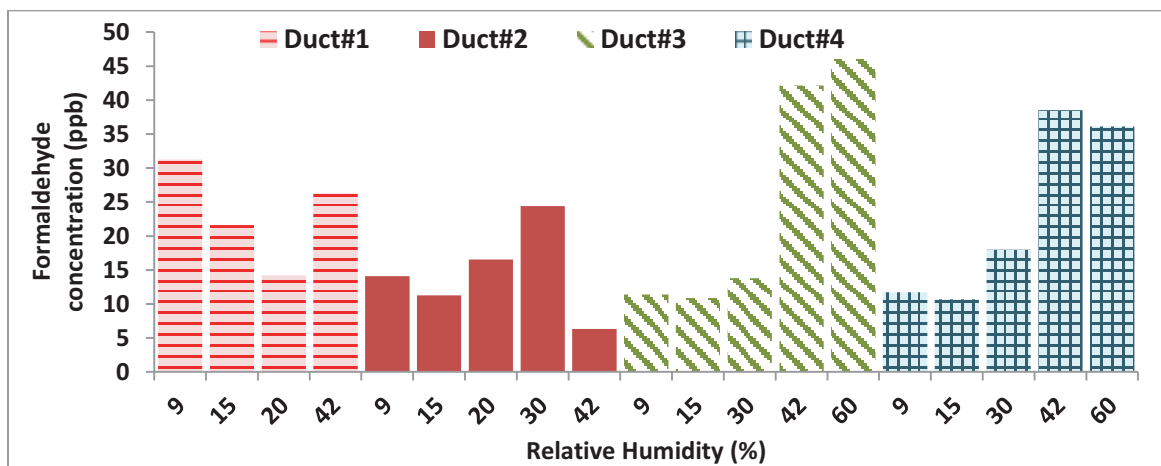


Figure 4-31 Formaldehyde generation in different relative humidity in each duct.

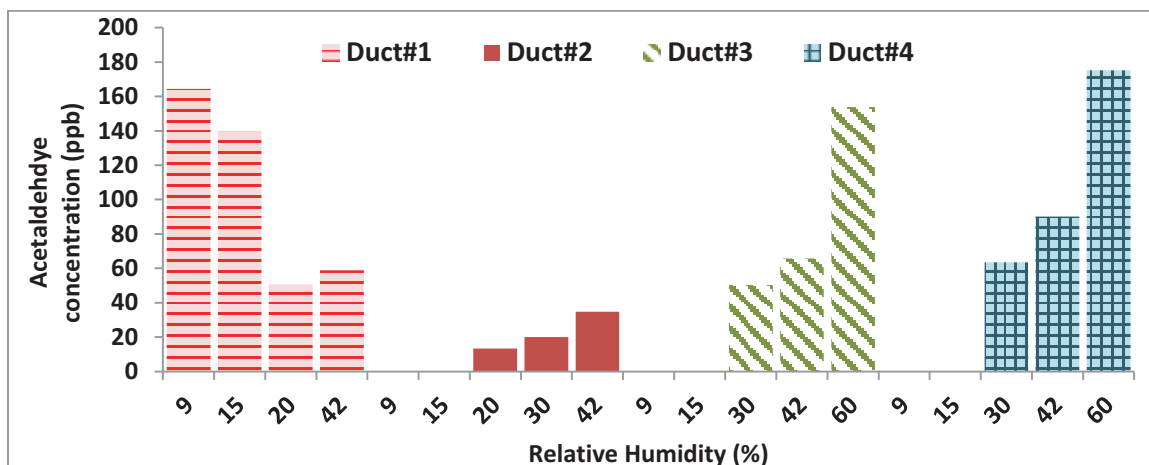


Figure 4-32 Acetaldehyde generation in different relative humidity in each duct.

Increase of relative humidity favors by-product generation in Duct # 2, 3, and 4 since presence of ozone (Duct # 2, 3, and 4) causes more radical production especially OH radicals. Due to enhancement of radical generation, partial oxidation in the presence of catalyst increases. Therefore, although the removal efficiency decreases, the by-product generation increases which means most of the reactions lead to partial oxidation. Formaldehyde generation drastically increases in presence of ozone and high relative humidity. In the case of Duct # 1, by-products generation decreases at higher relative humidity since the removal efficiency decreases and there are no ozone molecules in the system to promote radical generation. Reduction of by-products concentration in high relative humidity means that, in the absence of ozone, complete oxidation will happen.

#### 4.3.4 Effect of Flow Rate

The flow rate is one of the main parameters which affect the performance of UV-PCO technology. Experiments were carried out at  $500 \pm 20$  ppb ethanol and  $45 \pm 10\%$  relative humidity and  $22 \pm 2$  °C. Figure 4-33 shows the removal efficiency trend versus the flow rate in each duct. When the flow rate increases, the residence time in the reaction part decreases, and removal efficiency will decrease. Duct # 1 with catalyst substrate A shows

less dependency on the flow compared to the others while Duct # 4 removal efficiency drastically decreases with flow rate increment.

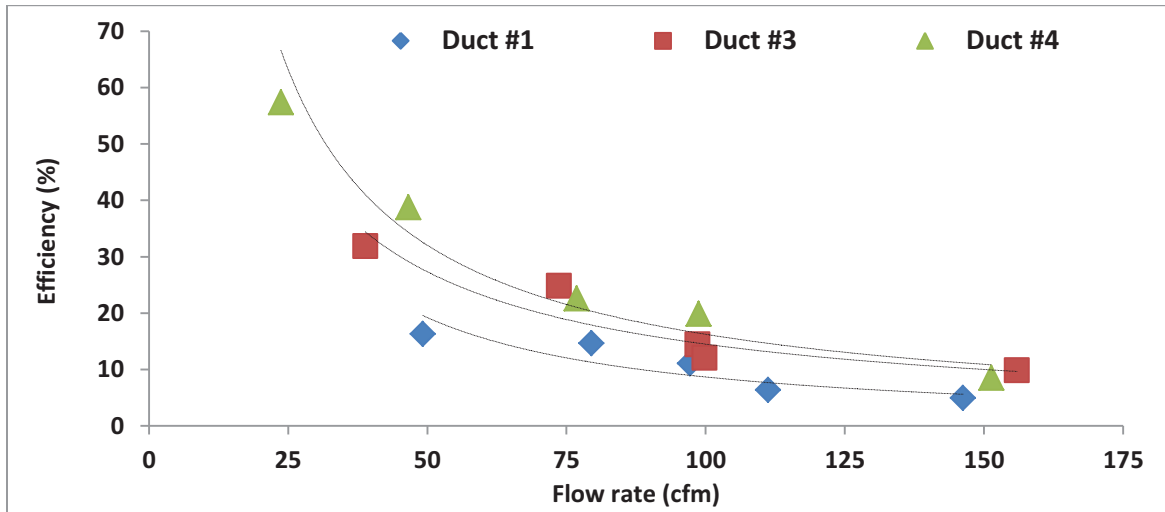


Figure 4-33 Effect of flow rate on removal efficiency of ethanol in each duct.

Figures 4-34 and 4-35 show the generated by-products in ethanol oxidation under different flow rates. Samples for by-products only were taken at three flow rates which are around 75, 100 and 150 cfm.

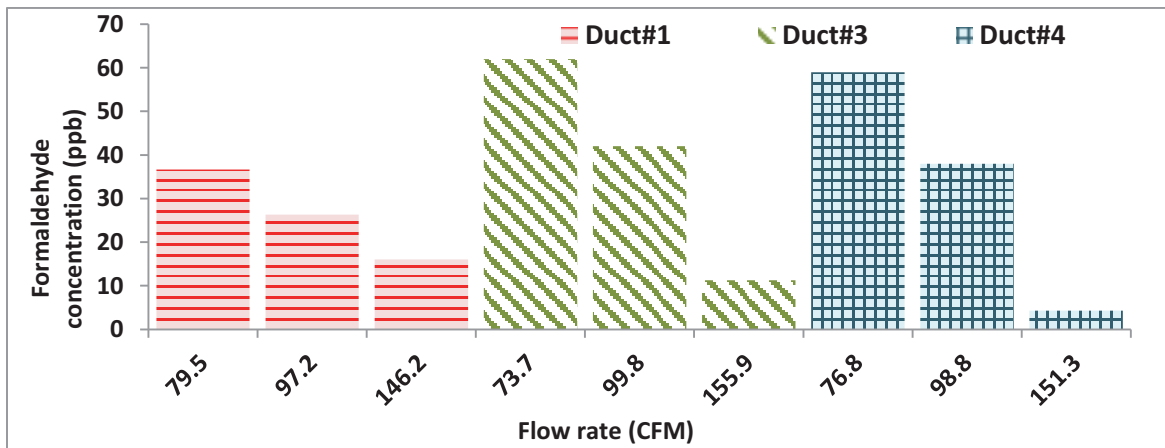


Figure 4-34 Effect of flow rate on formaldehyde generation in photocatalytic oxidation of ethanol in each duct.

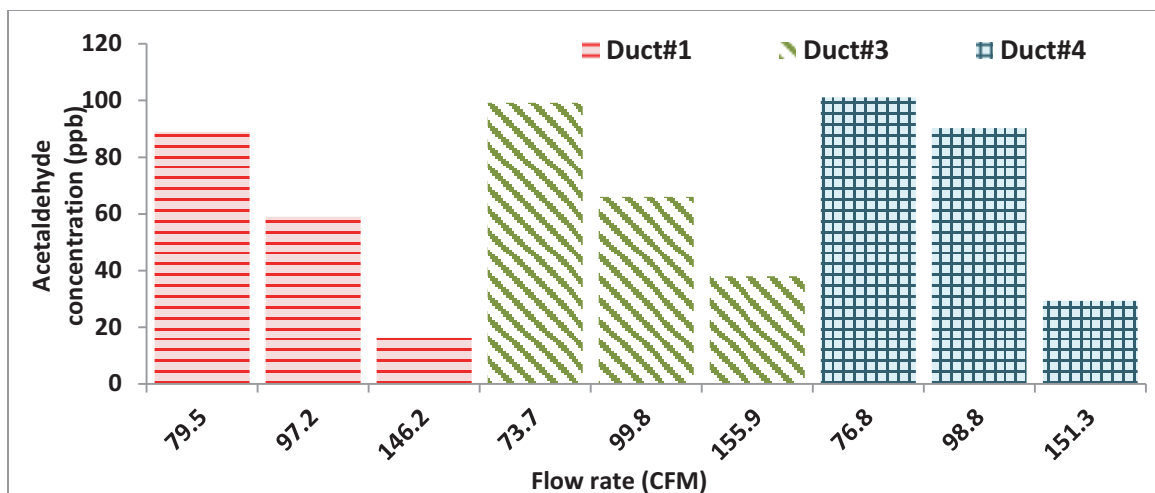


Figure 4-35 Effect of flow rate on acetaldehyde generation in photocatalytic oxidation of ethanol in each duct.

The results show with an increment in the flow rate, by-product generation decreases due to the reduction of removal efficiency in each duct.

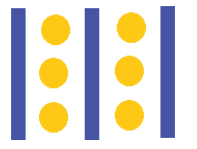
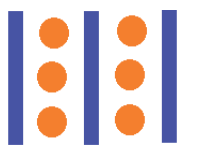
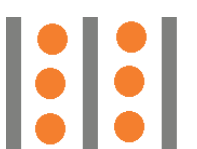
#### 4.3.5 Effect of Number of Lamps (Irradiance)

In order to study the effect of UV-Lamps on UV-PCO performance, experiments with  $500 \pm 20$  ppb concentration ethanol as a target pollutant at  $100 \pm 6$  cfm flow rate and  $35 \pm 5\%$  relative humidity and  $21 \pm 1$  °C with 1 and 3 UV-lamps have been carried out in each duct. The experimental procedure is the same as section 3.8; except for the change in the number of the lamps in the duct. Removal efficiency and generated by-products concentration are provided in Table 4-6. The configuration and description of the reaction section in each duct is provided in Table 4-7.

Table 4-6 Removal efficiency and concentration of generated by-products for each duct in irradiance experiments.

Duct No.	Removal efficiency (%)		Formaldehyde concentration (ppb)		Acetaldehyde concentration (ppb)	
	1 Lamp	3 Lamps	1 Lamp	3 Lamps	1 Lamp	3 Lamps
Duct # 1	13.6	15	9	14.8	12.7	32.0
Duct # 3	12.6	19.9	13.9	23.0	31.7	54.7
Duct # 4	12.8	21.8	8.7	24.4	445	40.8

Table 4-7 Configuration of reaction section in each duct in irradiance experiments.

Duct No.	1 Lamp test configuration	3 Lamps test configuration	Descriptions
Duct # 1			Catalyst substrate A UVC lamps
Duct # 3			Catalyst substrate A VUV lamps
Duct # 4			Catalyst substrate B VUV lamps
Duct # 2	Empty	Empty	-

Removal efficiency increases with the number of UV-Lamps, and consequently by-product generation increases. The number of UV-lamps in Duct # 1 does not affect the removal efficiency significantly, while in Duct # 3 and Duct # 4 it is considerable, which is a sign of the ozone effect on pollutant oxidation.

#### 4.3.6 Removal Efficiency Improvement

Since removal efficiency is one of the basic parameters for evaluation of UV-PCO technology, improvement of this parameter is of high importance. Therefore, an experiment with a new configuration based on the described procedure in section 3.8 was performed. Ethanol concentration in an indoor building is close to 250 ppb. Therefore, the experiment was carried out at  $250 \pm 25$  ppb concentration at a  $100 \pm 5$  cfm flow rate,  $50 \pm 5\%$  relative humidity and  $21 \pm 2$  °C. The configuration and description of the reaction section are presented in Table 4-8. Removal efficiency and by-products concentration are provided in Table 4-9.

Table 4-8 Configuration and description of the reaction section in removal efficiency improvement experiment.

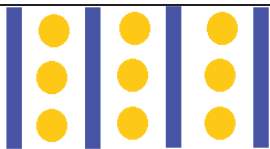
Duct No.	Reaction section configuration	Descriptions
Duct # 1		Catalyst substrate A UVC lamp
Duct # 3		Catalyst substrate A VUV lamps
Duct # 4		Catalyst substrate B VUV lamps
Duct # 2	Empty	-

Table 4-9 Removal efficiency and by-products concentration of removal efficiency improvement experiment.

Duct No.	Removal efficiency (%)	Formaldehyde concentration (ppb)	Acetaldehyde concentration (ppb)
Duct # 1	36.3	93.9	3.6
Duct # 3	37.3	60.8	0.0
Duct # 4	59.7	50.0	4.3

Experimental results in Table 4-9 demonstrate that this configuration increases the removal efficiency. Duct # 4 shows a higher removal efficiency and lower by-products generation compared to other ducts; therefore, catalyst substrate B has a better performance. Duct # 3 shows the same removal efficiency but lower by-products generation in comparison with Duct # 1 which means that VUV lamps performance is better than UVC lamps for pollutants oxidation in UV-PCO technology. Formaldehyde generation in this configuration is higher than acetaldehyde. Since this compound is one of the carcinogenic compounds, finding methods for its removal must be considered.

# CHAPTER 5 CONCLUSIONS AND FUTURE WORK

## 5.1 SUMMARY

The main objective of this study is to evaluate UV-PCO performance and identify and quantify possible by-products for different groups of VOCs. Moreover, the impact of relative humidity, flow rate, number of lamps and UV-PCO reactors on the removal efficiency and generated by-products concentration using ethanol as a target were investigated. To fully investigate the UV-PCO performance for mineralization of VOCs, an open loop mode test rig with four parallel ducts was designed and implemented. Each duct has a 0.3 m × 0.3 m cross-sectional area. Four groups of VOCs, including alcohol, alkane, aromatic, and ketones and two compounds from each group were selected: Ethanol and 1-butanol from alcohols, n-hexane and n-octane from alkanes, toluene and p-xylene from aromatics and acetone and MEK from ketones. All objectives were achieved in this study.

Based on collected experimental results, the performance of UV-PCO technology and its limitations were investigated and discussed. A repeatability test for ethanol was conducted to examine the reliability of the developed method.

## 5.2 CONCLUSIONS AND MAJOR FINDINGS

The conclusions of this study are as follows:

- ✓ The repeatability of the developed method was verified for ethanol as a target compound. The results obtained from the repeatability tests with identical conditions were in agreement.

- ✓ The extension of the reaction section to three lamps and four catalyst substrates (three UV-PCO reactors) in ethanol test increased the irradiance and contact with catalyst and consequently improved the removal performance of the system.
- ✓ The removal capacity of the UV-PCO technology decreases if the catalyst is not activated. For this purpose, after each test the catalyst was activated by emission of UV-lamps and a flow of fresh air through the duct.
- ✓ Based on the experimental data from this study, ozone reacted more with heavier compounds with a more stable structure. Catalyst substrate A with UVC lamps had more preference for oxidation of light compounds while catalyst substrate B performed better for heavier compounds although both of them in the case of ethanol showed very good performance.
- ✓ Both catalyst substrates A and B with UVC and VUV lamps showed low performance for alkane compounds.
- ✓ Generally, catalyst substrate B is better than catalyst substrate A and VUV lamps are more efficient than UVC lamps
- ✓ It was found that among different groups of VOCs, ethanol generates more by-products, especially acetaldehyde, during photocatalytic oxidation.
- ✓ All VOCs had a common behavior when their concentration increased. They all showed a decrease in removal efficiency and increase in generated by-products concentration. This phenomenon was due to the fact that when the concentration of VOCs increases the competition for adsorption on catalyst surface increases and

lower amounts of target compounds can reach the catalyst and adsorb UV light for oxidation, and partial oxidation rate will increase.

- ✓ Formaldehyde and acetaldehyde were the major by-products of all VOCs. This conclusion is in agreement with results reported in previous studies. Environmental Health Hazard Assessment (OEHHA) has recommended Acute Reference Exposure Levels (ARELs) of  $55 \mu\text{g}/\text{m}^3$  (44 ppb) in 3h for formaldehyde and ARELs of  $470 \mu\text{g}/\text{m}^3$  (261 ppb) for acetaldehyde. Therefore, it would be necessary to decrease generation of these compounds and their level of concentration either by improvement of UV-PCO technology or combination of this technology with other technologies.
- ✓ In photocatalytic oxidation of 1-butanol, major by-products are butyraldehyde, formaldehyde, acetaldehyde and propionaldehyde. A negligible amount of crotonaldehyde was produced only in Duct # 2, Duct # 3 and Duct # 4 with VUV lamps; while in ethanol degradation only formaldehyde and acetaldehyde were formed.
- ✓ In photocatalytic oxidation of n-hexane other by-products including acetone, propionaldehyde, butyraldehyde, crotonaldehyde, and hexanal were generated and in case of n-octane oxidation, generated by-products were acetone crotonaldehyde, hexanal, and valeraldehyde.
- ✓ Formaldehyde, acetaldehyde and crotonaldehyde are the major by-products of toluene and p-xylene. During photocatalytic oxidation of p-xylene and toluene, some other by-products including butyraldehyde, tolualdehyde, acetone, valeraldehyde,

and dimethylbenzaldehyde were produced. Also benzaldehyde was generated just in toluene experiments.

- ✓ Ethanol degradation and consequently by-products generation decreased when the flow rate increased. When the flow rate increases, residence time in the reaction part decreases and therefore, removal efficiency will decrease.
- ✓ Generation of some by-products mostly depends on the presence of ozone in the system; for instance, crotonaldehyde and propionaldehyde mostly were generated in the presence of  $O_3/UV/TiO_2$ .
- ✓ A significant difference was found in ethanol photocatalytic oxidation when the relative humidity increased. In Duct # 1, 3, and 4 of the UV-PCO system, when the relative humidity increased, removal efficiency decreased. Increment of water vapor molecules increases the completion of water and VOC molecules for adsorption on the catalyst surface. Due to the acidic structure of  $TiO_2$  and a stronger desire for adsorbing water vapor molecules compared to VOCs with less polarity, at higher relative humidity lower amounts of VOC molecules adsorb on the surface to oxidize, and removal efficiency decreases. In Duct # 2, removal efficiency increased with relative humidity which is because of the higher generation of radicals including OH radicals for oxidization of VOCs.
- ✓ Removal efficiency increased with increment of UV-lamps, and consequently by-products generation increased. Increment of UV-lamps in Duct # 1 did not affect the removal efficiency significantly while in Duct # 3 and Duct # 4 was considerable which demonstrates the effect of ozone on pollutant oxidation.

### **5.3 LIMITATIONS OF THE PRESENT STUDY**

- Among the VOCs chosen, acetone and 1-butanol were tested in different concentration compared to the others since acetone showed a lower sensitivity to B&K and 1-butanol condensates in the tubing which made it impossible to continue the experiment at the same concentrations of the other compounds.
- One of the difficulties of the system was to have a constant background concentration of laboratory air. The system was sensitive to the variation in air ventilation. Therefore, even a slight variation in the pressure influenced the challenge compound concentration in the duct.
- Catalyst deactivation was one of the concerns which was observed in the preliminary test. Therefore, the catalyst activation process was needed based on the previous experiment duration and compound structure (Heavier compounds need more time to desorb from catalyst surface).
- It was not possible to control the humidity in the laboratory. Therefore, experiments were done in different days in which relative humidity are almost equal.

### **5.4 RECOMMENDATIONS FOR FUTURE WORK**

Based on the findings of this study, recommendations for future research on the application of UV-PCO technology for the removal of indoor VOCs are as follows:

- Establishing a standard apparatus for UV-PCO technology, test conditions, test procedure and reporting format (similar to ASHRAE Std 145.1 for sorbent media) for catalyst performance evaluation.
- Preparing a VOCs index with removal efficiency and generated by-products, considering both type and concentration levels with their acceptable levels for occupants in indoor buildings based on their odors, irritation and health effects.
- Conducting more detailed investigations on mechanisms for generation of specific compounds that lead to harmful by-products.
- A mathematical model is needed to predict the UV-PCO performance and by-product concentration for different VOCs based on the flow rate, light intensity, wavelength, ozone concentration, temperature and relative humidity.
- Performing experiments either on a single or mixture of VOC in each group to identify possible by-products and study the UV-PCO system.
- Conducting experiments to find the best conditions for less by-product generation with a high removal efficiency of the target pollutants.
- More investigations on removal of generated by-products using UV-PCO or other technologies for design of air cleaner with less side effects and a high removal efficiency for having immune indoor buildings.
- Improvement of the  $\text{TiO}_2$  catalyst for less deactivation, higher removal efficiency and the possibility of application under visible light.

## REFERENCES

ASHRAE. 2011. ASHRAE Std. SPC 145.2: "Method of testing gaseous contaminant air-cleaning devices for removal efficiency", American Society of Heating, Refrigerating and Air-Conditioning Engineers, Inc.

ASHRAE. 2008. ASHRAE Std. 145.1: "Laboratory test method of assessing the performance of gas-phase air cleaning media", American Society of Heating, Refrigerating and Air-Conditioning Engineers, Inc.

ASHRAE Handbook, Chapter 28, Air Cleaners for Particulate Contaminants. Heating, Ventilating, and Air-Conditioning: Systems and Equipment: 2008. American Society of Heating, Refrigerating and Air-Conditioning Engineers, Inc.

Alberici, R.M. and Jardim, W.F. 1997. "Photocatalytic destruction of VOCs in the gas-phase using titanium dioxide." *Applied Catalysis B: Environmental* 14:55-68.

Amama, P.B., Itoh, K., and Murabayashi, M. 2004. "Photocatalytic degradation of trichloroethylene in dry and humid atmospheres: role of gas-phase reactions." *Journal of Molecular Catalysis A: Chemical* 217:109-115.

Anpo, M. and Takeuchi, M. 2003. "The design and development of highly reactive titanium oxide photocatalysts operating under visible light irradiation." *Journal of Catalysis* 216:505-516.

Ao, C.H. and Lee, S.C. 2003. "Enhancement effect of TiO<sub>2</sub> immobilized on activated carbon filter for the photodegradation of pollutants at typical indoor air level." *Applied Catalysis B: Environmental* 44:191-205.

Ao, C.H. and Lee, S.C. 2004. "Combination effect of activated carbon with TiO<sub>2</sub> for the photodegradation of binary pollutants at typical indoor air level." *Journal of Photochemistry and Photobiology A: Chemistry* 161:131-140.

Avila, P., Bahamonde, A., Blanco, J., Sanchez, B., Cardona, A.I. and Romero, M. 1998. "Gas-phase photo-assisted mineralization of volatile organic compounds by monolithic titania catalysts." *Applied Catalysis B: Environmental* 17:75-88.

Belver, C., Bellod, R., Fuerte, A., and Fernandez-Garcia, M. 2006. "Nitrogen-containing TiO<sub>2</sub> photocatalysts: Part 1. Synthesis and solid characterization." *Applied Catalysis B: Environmental* 65:301-308.

Bellu, E. 2007, "Detection, analysis, and photocatalytic destruction of the freshwater taint compound geosmin", Doctoral Thesis, Robert Gordon University.

Bhatkhande, D.S., Pan

garkar, V.G. and Beenackers, A.A. 2002. "Photocatalytic degradation for environmental

- applications—a review." *Journal of Chemical Technology & Biotechnology* 77:102-116.
- Bhowmick, M. and Semmens, M.J. 1994. "Ultraviolet photooxidation for the destruction of VOCs in air." *Water Research* 28:2407-2415.
- Bickley, R.I. and Jayanty, R.K.M. 1974. "Photo-adsorption and photo-catalysis on titanium dioxide surfaces. Photo-adsorption of oxygen and the photocatalyzed oxidation of isopropanol." *Faraday Discuss. Chem. Soc.* 58:194-204.
- Birnie, M., Riffat, S., and Gillott, M. 2006a. "Photocatalytic reactors: design for effective air purification." *International Journal of Low-Carbon Technologies* 1:47.
- Blount, M.C. and Falconer, J.L. 2001. "Characterization of adsorbed species on TiO<sub>2</sub> after photocatalytic oxidation of toluene." *Journal of Catalysis* 200:21-33.
- Blount, M.C. and Falconer, J.L. 2002. "Steady-state surface species during toluene photocatalysis." *Applied Catalysis B: Environmental* 39:39-50.
- Bouzaza, A., Vallet, C. and Laplanche, A. 2006. "Photocatalytic degradation of some VOCs in the gas phase using an annular flow reactor: Determination of the contribution of mass transfer and chemical reaction steps in the photodegradation process." *Journal of Photochemistry and Photobiology A: Chemistry* 177:212-217.
- Brown, S.K, Sim, M.R., Abramson, M.J. and Gray, C.N. 1994. "Concentrations of volatile organic compounds in indoor air—a review." *Indoor Air* 4:123-134.
- Buckley, P.T. and Birks, J.W. 1995. "Evaluation of visible-light photolysis of ozone-water cluster molecules as a source of atmospheric hydroxyl radical and hydrogen peroxide." *Atmospheric Environment* 29:2409-2415.
- Cao, L., Gao, Z., Suib, S.L., Obee, T.N., Hay, S.O., and Freihaut, J.D. 2000. "Photocatalytic oxidation of toluene on nanoscale TiO<sub>2</sub> catalysts: studies of deactivation and regeneration." *Journal of Catalysis* 196:253-261.
- Carlier, P., Hannachi, H. and Mouvier, G. 1986. "The chemistry of carbonyl compounds in the atmosphere-A review." *Atmospheric Environment (1967)* 20:2079-2099.
- Chang, C.P., Chen, J.N. and Lu, M.C. 2003. "Heterogeneous photocatalytic oxidation of acetone for airpurification by near UV-irradiated titanium dioxide." *Journal of Environmental Science & Health Part A* 38:1131-1143.
- Chen, D.H., Ye, X. and Li, K. 2005. "Oxidation of PCE with a UV LED photocatalytic reactor." *Chemical engineering & technology* 28:95-97.
- Cheng, M., Brown, S.K. 2003. "VOCs identified in Australian indoor air and product emission environments". Proceedings of National Clean Air Conference: 23–7

Newcastle.

Chin, P., Yang, L.P., and Ollis, D.F. 2006. "Formaldehyde removal from air via a rotating adsorbent combined with a photocatalyst reactor: Kinetic modeling." *Journal of Catalysis* 237:29-37.

d'Hennezel, O., Pichat, P. and Ollis, D.F. 1998a. "Benzene and toluene gas-phase photocatalytic degradation over H<sub>2</sub>O and HCL pretreated TiO<sub>2</sub>: by-products and mechanisms." *Journal of Photochemistry and Photobiology A: Chemistry* 118:197-204.

Demeestere, K., Dewulf, J., and Langenhove, H.V. 2007. "Heterogeneous Photocatalysis as an Advanced Oxidation Process for the Abatement of Chlorinated, Monocyclic Aromatic and Sulfurous Volatile Organic Compounds in Air: State of the Art." *Critical Reviews in Environmental Science and Technology* 37:489-538.

Dibble, L.A. and Raupp, G.B. 1992. "Fluidized-bed photocatalytic oxidation of trichloroethylene in contaminated air streams." *Environmental Science & Technology* 26:492-495.

Doucet, N., Bocquillon, F., Zahraa, O., and Bouchy, M. 2006. "Kinetics of photocatalytic VOCs abatement in a standardized reactor." *Chemosphere* 65:1188-1196.

Einaga, H., Futamura, S. and Ibusuki, T. 2001. "Complete oxidation of benzene in gas phase by platinized titania photocatalysts." *Environmental science & technology* 35:1880-1884.

EPA TO-11a method for carbonyl compounds: <http://www.epa.gov/ttn/amtic/files/ambient/airtox/to-11a.pdf>).

Frank, S.N. and Allen, J.B. 1977. "Heterogeneous photocatalytic oxidation of cyanide and sulfite in aqueous solutions at semiconductor powders." *The Journal of Physical Chemistry* 81:1484-1488.

Frazer, L. 2001. "Titanium dioxide: Environmental white knight?" *Environmental Health Perspectives*, 109(4): A174-A177.

Fogler, H.S. 2006. *Elements of Chemical Reaction Engineering*, Fourth Edition, Pearson Education, Inc.

Fujishima, A. and Honda, K. 1972. "Electrochemical photolysis of water at a semiconductor electrode." *Nature* 238:37-38.

Gravelle, P.C., Juillet, F., Meriaudeau, P., and Teichner, S.J. 1971. "Surface reactivity of reduced titanium dioxide." *Discussions of the Faraday Society* 52:140-148.

Ginestet, A., Pugnet, D., Rowley, J., Bull, K. and Yeomans, H. 2005. "Development of a new photocatalytic oxidation air filter for aircraft cabin." *Indoor Air* 15: 326-334.

Hager, S. and Bauer, R. 1999. "Heterogeneous photocatalytic oxidation of organics for air purification by near UV irradiated titanium dioxide." *Chemosphere* 38:1549-1559.

Haghighat, F., Lee, Ch.S., Pant, B., , G., Lakdawala, N. and Bastani, A. 2008. "Evaluation of various activated carbons for air cleaning - Towards design of immune and sustainable buildings." *Atmospheric Environment* 42:8176-8184.

Hegedüs, M., and Dombi, A. 2004a. "Comparative study of heterogeneous photocatalytic decomposition of tetrachloroethene and trichloroethene in the gas phase." *Applied Catalysis A: General* 271:177-184.

Hoffmann, M.R., Martin, S.T., Choi, W.Y. and Bahnemann, D.W. 1995. "Environmental applications of semiconductor photocatalysis." *Chemical Reviews* 95:69-96.

Hodgson, A.T. and Levin, H. 2003. "Volatile organic compounds in indoor air – a review of concentrations measured in north American since 1990". Lawrence Berkeley National Laboratory (LBNL), No.51715.

Hodgson, A.T., Sullivan, D.P, and Fisk, W.J. 2005a. "Evaluation of ultra-violet photocatalytic oxidation (UV-PCO) for indoor air applications: conversion of volatile organic compounds at low part-per-billion concentrations". Lawrence Berkeley National Laboratory (LBNL) Report, No. 58936.

Hodgson, A.T., Sullivan, D.P. and Fisk, W.J. 2005b. "Parametric evaluation of an innovative ultra-violet photocatalytic oxidation (UVPCO) air cleaning technology for indoor applications." Lawrence Berkeley National Laboratory (LBNL) Report, No. 59074.

Hodgson, A.T. and Levin, H. 2003. "Volatile organic compounds in indoor air: a review of concentrations measured in North America since 1990, Lawrence Berkeley National Laboratory (LBNL) Report, No. 51715.

Hung, Ch.H. and Marifas, B.J. 1997a. "Role of chlorine and oxygen in the photocatalytic degradation of trichloroethylene vapor on TiO<sub>2</sub> films." *Environmental Science & Technology* 31:562-568.

Hugo I.D.L., Salaices, M., Serrano, B. 2005. "Photocatalytic reaction engineering". Springer-Verlag New York Inc., 110-150.

International Organization for Standardization. 1992. *Water quality: evaluation of the aerobic biodegradability of organic compounds in an aqueous medium: semi-continuous activated sludge method (SCAS) = Qualite de l'eau : evaluation, en milieu aqueux, de la biodegradabilite aerobie des composes organiques : methode semi-continue par boues actives (Methode SCAS)*. [Geneva]: ISO.

Jacoby, W.A., Blake, D.M., Fennell, J.A., Boulter, J.E., Vargo, L.M., George, M.C. and

- Dolberg, S.K. 1996. "Heterogeneous photocatalysis for control of volatile organic compounds in indoor air." *Journal of the Air & Waste Management Association* 46:891-898.
- Jeong, J., Sekiguchi, K. and Sakamoto, K. 2004. "Photochemical and photocatalytic degradation of gaseous toluene using short-wavelength UV irradiation with TiO<sub>2</sub> catalyst: comparison of three UV sources." *Chemosphere* 57:663-671.
- Kim, S.B., Hwang, H.T. and Hong, S.C. 2002. "Photocatalytic degradation of volatile organic compounds at the gas-solid interface of a TiO<sub>2</sub> photocatalyst." *Chemosphere* 48:437-444.
- Kim, S.B., and Hong, S.C. 2002. "Kinetic study for photocatalytic degradation of volatile organic compounds in air using thin film TiO<sub>2</sub> photocatalyst." *Applied Catalysis B: Environmental* 35:305-315.
- Kittrell, J.R., Dupre, C.R., and Gerrish, D.A. 2006. "Advances in photocatalytic remediation technology." *Remediation Journal* 16:81-91.
- Larson, S.A. and Falconer, J.L. 1997. "Initial reaction steps in photocatalytic oxidation of aromatics." *Catalysis letters* 44:57-65.
- Lam, Ch.W. 2007. "Development of photocatalytic oxidation technology for purification of air and water." Thesis for the degree of Master of Philosophy at the University of Hong Kong.
- Li, X.Z., Li, F.B., Xie, Y.B., 2005. "Photocatalytic oxidation using lanthanide ion-doped titanium dioxide catalysts for water and wastewater treatment." *Trends in Water Pollution Research*, 31-74.
- Lichtin, NN, Avudaithai, M., Berman, E. and Grayfer, A. 1996. "TiO<sub>2</sub>-photocatalyzed oxidative degradation of binary mixtures of vaporized organic compounds." *Solar energy* 56:377-385.
- Linsebigler, A.L., Lu, G. and Yates, J.T. 1995. "Photocatalysis on TiO<sub>2</sub> surfaces: principles, mechanisms, and selected results." *Chemical Reviews* 95:735-758.
- Ma, C.M. and Ku, Y. 2006. "Photocatalytic oxidation of gaseous trichloroethylene by UV/TiO<sub>2</sub> process." *Reaction Kinetics and Catalysis Letters* 89:293-301.
- Menzies, D., Pasztor, J., Rand, T., and Bourbeau, J. 1999. "Germicidal ultraviolet irradiation in air-conditioning systems: effect on office worker health and wellbeing: A pilot study." *Occupational and Environmental Medicine*. 56: 397-402.
- Minnesota Department of Health. 2009. "Volatile organic compounds (VOCs) in your home". Retrieved 02/20, 2009, from <http://www.health.state.mn.us/divs/eh/indoorair/voc/>

Mo, J., Zhang, Y., Xu, Q., Lamson, J.J., and Zhao, R. 2009. "Photocatalytic purification of volatile organic compounds in indoor air: A literature review." *Atmospheric Environment* 43:2229-2246.

Muggli, D.S., Ding, L. and Odland, M.J. 2002a. "Improved catalyst for photocatalytic oxidation of acetaldehyde above room temperature." *Catalysis Letters* 78:23-31.

Nimlos, M.R., Jacoby, W.A., Blake, D.M. and Milne, T.A. 1993. "Direct mass spectrometric studies of the destruction of hazardous wastes. 2. Gas-phase photocatalytic oxidation of trichloroethylene over titanium oxide: products and mechanisms." *Environmental Science & Technology* 27:732-740.

Obee, T.N. and Hay, S.O. 1997. "Effects of moisture and temperature on the photooxidation of ethylene on titania." *Environmental science & technology* 31:2034-2038.

Ohko, Y., Fujishima, A. and Hashimoto, K. 1998. "Kinetic analysis of the photocatalytic degradation of gas-phase 2-pmpanoi under mass transport-limited conditions with a TiO<sub>2</sub> film photocatalyst," *The Journal of Physical Chemistry*. B 102:1724-1729.

Office of Environmental Health Hazard Assessment (OEHHA):[http://oehha.ca.gov/tcdb/index .asp](http://oehha.ca.gov/tcdb/index.asp)

Pengyi, Z., Fuyan, L., Gang, Y., Qing, C. and Wanpeng, Z. 2003. "A comparative study on decomposition of gaseous toluene by O<sub>3</sub>/UV, TiO<sub>2</sub>/UV and O<sub>3</sub>/TiO<sub>2</sub>/UV." *Journal of Photochemistry and Photobiology A: Chemistry* 156:189-194.

Peral, J., Domènech, X., and Ollis, D.F. 1997. "Heterogeneous photocatalysis for purification, decontamination and deodorization of air." *Journal of Chemical Technology & Biotechnology* 70:117-140.

Peral, J. and Ollis, D.F. 1997a. "TiO<sub>2</sub> photocatalyst deactivation by gas-phase oxidation of heteroatom organics." *Journal of Molecular Catalysis A: Chemical* 115:347-354.

Piera, E., Ayllón, J.A., Doménech, X. and Peral, J. 2002. "TiO<sub>2</sub> deactivation during gas-phase photocatalytic oxidation of ethanol." *Catalysis Today* 76:259-270.

Raupp, G.B., Nico, J.A., Annangi, S., Changrani, R., and Annapragada, R. 1997. "Two flux radiation field model for an annular packed bed photocatalytic oxidation reactor." *AIChE Journal* 43:792-801.

Ray, M.B. 2000. "Photodegradation of the volatile organic compounds in the gas phase: a review." Department of Chemical and Environmental Engineering, The National University of Singapore, 405-439.

Sattler, M.L. and Liljestrang, H.M. 2003. "Method for predicting photocatalytic oxidation rates of organic compounds." *Journal of the Air & Waste Management Association* 53:3-

12.

Shen, Y. S. and Ku, Y. 2002. "Decomposition of gas-phase trichloroethene by the UV/TiO<sub>2</sub> process in the presence of ozone." *Chemosphere* 46:101-107.

Sánchez, B., Cardona, A.I., Romero, M., Avila, P. and Bahamonde, A. 1999. "Influence of temperature on gas-phase photo-assisted mineralization of TCE using tubular and monolithic catalysis." *Catalysis Today* 54:369-377.

Sun, Y.X., Fang, L., Wyon, D.P., Wisthaler, A., Lagercrantz, L., and Tejsen, P.S. 2005. "Experimental research on photocatalytic oxidation air purification technology applied to aircraft cabins", Proceedings of Indoor Air 2005 Conference.

Teichner, S.J. and Formenti, M. 1985. "Heterogeneous photocatalysis in photoelectrochemistry, photocatalysis and photoreactors", ed. M. Schiavello. Reidel Publishing Company, 457-89

Thad, G. 2001. "Indoor Environmental Quality". Lewis Publishers.

Tompkins, D.T., Lawnicki, B.J., Zeltner, W.A., and Anderson, M.A. 2005. "Evaluation of photocatalysis for gas-phase air cleaning—Part 1: Process, technical and sizing considerations." *ASHRAE transactions* 111:60-84.

U.S. EPA. 2009. An introduction to indoor air quality - organic gases (volatile organic compounds-VOCs). Retrieved 01/28, 2009, from <http://www.epa.gov/iaq/voc.html>.

U.S. EPA. 2007. Residential air cleaning devices. Retrieved 01/03, 2009, from <http://www.epa.gov/iaq/pubs/residair.html>

VanOsdell, D.W. 1994. *Evaluation of test methods for determining the effectiveness and capability of gas-phase air filtration equipment for indoor air applications-phase I: literature review and test recommendations*. ASHRAE Trans. 100: 511-523

Vorontsov, A.V., Lion, Cl., Savinov, E.N. and Smirniotis, P.G. 2003. "Pathways of photocatalytic gas phase destruction of HD simulant 2-chloroethyl ethyl sulfide." *Journal of Catalysis* 220:414-423.

Vorontsov, A.V., Savinov, E.V., Davydov, L. and Smirniotis, P.G. 2001. "Photocatalytic destruction of gaseous diethyl sulfide over TiO<sub>2</sub>." *Applied Catalysis B: Environmental* 32:11-24.

Waki, K., Wang, L., Nohara, K. and Hidaka, H. 1995. "Photocatalyzed mineralization of nitrogen-containing compounds at TiO<sub>2</sub>/H<sub>2</sub>O interfaces." *Journal of Molecular Catalysis A: Chemical* 95:53-59.

Wang, K.H., Hsieh, Y.H., Lin, C.H., and Chung, C.Y. 1999. "The study of the photocatalytic degradation kinetics for dichloroethylene in vapor phase." *Chemosphere*

39:1371-1384.

Wang, S., Ang, H.M. and Tade, M.O. 2007. "Volatile organic compounds in indoor environment and photocatalytic oxidation: state of the art." *Environment international* 33:694-705.

Wang, W., Chiang, L.W. and Ku, Y. 2003. "Decomposition of benzene in air streams by UV/TiO<sub>2</sub> process." *Journal of hazardous materials* 101:133-146.

Wekhof, A. 1991. "Treatment of Contaminated Water, Air and Soil with UV Flashlamps." *Environmental Progress IO* 4: 241-247.

Xu, W. and Raftery, D. 2001. "In situ solid-state nuclear magnetic resonance studies of acetone photocatalytic oxidation on titanium oxide surfaces." *Journal of Catalysis* 204:110-117.

Xu, Y. and Schoonen, M.A.A. 2000. "The absolute energy positions of conduction and valence bands of selected semiconducting minerals." *American Mineralogist* 85:543.

Yamashita, H., Anpo, M., 2004. "Application of an ion beam technique for the design of visible light-sensitive, highly efficient and highly selective photocatalysts: ion-implantation and ionized cluster beam methods." *Catalysis surveys from Asia* 8: 35-45.

Yung-Shuen, S. and Young, K. 1998. "Decomposition of gas-phase chloroethenes by UV/O<sub>3</sub> process", *Water Resources*, 32(9): 2669-2679.

Ye, X., Chen, D., Gossage, J. and Li, K. 2006. "Photocatalytic oxidation of aldehydes: Byproduct identification and reaction pathway." *Journal of Photochemistry and Photobiology A: Chemistry* 183:35-40.

Zhang, Y., Yang, R. and Zhao, R. 2003. "A model for analyzing the performance of photocatalytic air cleaner in removing volatile organic compounds." *Atmospheric Environment* 37:3395-3399.

Zhong, L., Haghghat, F., Blondeau, P., and Kozinski, J. 2010a. "Modeling and physical interpretation of photocatalytic oxidation efficiency in indoor air applications." *Building and Environment* 45:2689-2697.

Zhou, L., Zhu, B. 2006. "Oxidation processes for degradation of organic pollutants in water, literature review" *Report for Smart Water Project*, Institute of Sustainability and Innovation Victoria University.

## Appendix A: VOCs Injection Rate Calculation Using Syringe System Injection

Compound Name	C (ppb)	C (ppm)	Mw (g/mole)	T (h)	Factor (kg/m <sup>3</sup> )	C (mg/m <sup>3</sup> )	D (g/ml)	D (mg/ul)	C (ul/m <sup>3</sup> )	Q <sub>in duct</sub> (l <sup>3</sup> /min)	Q (m <sup>3</sup> /min)	Injection rate (ul/min)
Toluene	1000	1	92.14	296.15	3.79	3.79	0.867	0.867	4.37	400	11.33	49.54
	500	0.5	92.14	296.15	3.79	1.90	0.867	0.867	2.19	400	11.33	24.77
	250	0.25	92.14	296.15	3.79	0.95	0.867	0.867	1.09	400	11.33	12.38
p-Xylene	1000	1	106.16	296.15	4.37	4.37	0.866	0.866	5.04	400	11.33	57.14
	500	0.5	106.16	296.15	4.37	2.18	0.866	0.866	2.52	400	11.33	28.57
	250	0.25	106.16	296.15	4.37	1.09	0.866	0.866	1.26	400	11.33	14.29
n-Hexane	1000	1	86.18	296.15	3.55	3.55	0.656	0.656	5.41	400	11.33	61.24
	500	0.5	86.18	296.15	3.55	1.77	0.656	0.656	2.70	400	11.33	30.62
	250	0.25	86.18	296.15	3.55	0.89	0.656	0.656	1.35	400	11.33	15.31
n-Octane	1000	1	114.23	296.15	4.70	4.70	0.703	0.703	6.69	400	11.33	75.74
	500	0.5	114.23	296.15	4.70	2.35	0.703	0.703	3.34	400	11.33	37.87
	250	0.25	114.23	296.15	4.70	1.18	0.703	0.703	1.67	400	11.33	18.93
Butanone (MEK)	1000	1	72.11	296.15	2.97	2.97	0.8	0.8	3.71	400	11.33	42.02
	500	0.5	72.11	296.15	2.97	1.48	0.8	0.8	1.85	400	11.33	21.01
	250	0.25	72.11	296.15	2.97	0.74	0.8	0.8	0.93	400	11.33	10.50
Acetone	2000	2	58.08	296.15	2.39	4.78	0.788	0.788	6.07	400	11.33	68.71
	1000	1	58.08	296.15	2.39	2.39	0.788	0.788	3.03	400	11.33	34.36
	500	0.5	58.08	296.15	2.39	1.20	0.788	0.788	1.52	400	11.33	17.18
Ethanol	1000	1	46.07	296.15	1.90	1.90	0.785	0.785	2.42	400	11.33	27.36
	500	0.5	46.07	296.15	1.90	0.95	0.785	0.785	1.21	400	11.33	13.68
	250	0.25	46.07	296.15	1.90	0.47	0.785	0.785	0.60	400	11.33	6.84
1-Butanol	800	0.8	74.12	296.15	3.05	2.44	0.808	0.808	3.02	400	11.33	34.21
	500	0.5	74.12	296.15	3.05	1.53	0.808	0.808	1.89	400	11.33	21.38
	250	0.25	74.12	296.15	3.05	0.76	0.808	0.808	0.94	400	11.33	10.7

C: Concentration, Mw: Molecular weight, T: Temperature, D: Density, Q: Flow rate.

## *Appendix B: HPLC and B&K Calibration Equations*

### *B&K Calibration Equations:*

Toluene:	$y=1.1501x - 1.1658$	p-Xylene:	$y=0.6533x - 0.4847$
n-Hexane:	$y=0.1668x - 0.1708$	n-Octane:	$y=0.1322x - 0.0867$
Ethanol:	$y=0.5124x - 0.4817$	1-Butanol:	$y=0.2684x - 0.2851$
Acetone:	$y=2.0547x - 1.84$	MEK:	$y=0.7316x - 0.7727$

*x: B&K Respond    y: Actual Concentration (ppm)*

### *HPLC Calibration Curves:*

Formaldehyde: $y=2.90 \times 10^{-05}x - 0.4393$	Acetaldehyde: $y=3.86 \times 10^{-05}x - 0.6429$
Acrolein: $y=3.41 \times 10^{-05}x + 1.9120$	Acetone: $y=6.26 \times 10^{-05}x - 5.6148$
Propionaldehyde: $y=5.34 \times 10^{-05}x - 1.6360$	Crotonaldehyde: $y=5.62 \times 10^{-05}x - 0.4802$
Butyraldehyde: $y=5.98 \times 10^{-05}x + 1.2372$	Benzaldehyde: $y=8.28 \times 10^{-05}x - 0.5071$
Isovaleraldehyde: $y=6.97 \times 10^{-05}x + 0.1900$	Valeraldehyde: $y=7.01 \times 10^{-05}x + 2.3971$
o-Tolualdehyde: $y=9.56 \times 10^{-05}x + 0.6782$	m-Tolualdehyde: $y=9.41 \times 10^{-05}x + 0.5761$
p-Tolualdehyde: $y=1.12 \times 10^{-05}x - 4.3515$	Hexanal: $y=4.76 \times 10^{-05}x - 0.5020$
Dimethylbenzaldehyde: $y=4.76 \times 10^{-05}x - 0.2702$	

*x: HPLC Respond    y: Compound Mass(ng)*

## *Appendix C: Ozone Concentration in Downstream of Ducts*

Section in Thesis	Test Name	Target Compound & Ozone Concentration	Duct No.											
			Duct#1 or Upstream	Duct#2	Duct#3	Duct#4	Duct#5	Duct#6	Duct#7	Duct#8				
4.2.1	Ethanol Concentration Test	Ethanol concentration(ppb)	293.29	462.78	966.24	320.95	466.25	761.89	293.17	469.03	734.88	283.77	472.26	1017.97
		Ozone concentration(ppb)	15.59	21.57	21.14	2065.85	1999.51	2047.61	1180.92	1111.16	1110.93	1262.95	1268.29	1267.15
		1-Butanol concentration(ppb)	217.48	492.07	743.71	203.11	484.69	746.75	223.62	492.39	767.24	226.46	503.70	749.79
4.2.1	1-Butanol Concentration Test	Ozone concentration(ppb)	20.00	22.91	23.87	687.34	720.64	712.77	1032.74	1060.03	1110.93	1390.96	1396.53	1393.17
		n-Hexane concentration(ppb)	278.15	520.40	1072.60	251.28	494.56	1060.85	252.04	493.66	999.56	264.42	533.58	1134.39
		Ozone concentration(ppb)	6.91	19.67	21.03	648.05	709.88	693.43	995.53	1053.18	990.95	1312.24	1322.78	1300.48
4.2.2	n-Octane Concentration Test	n-Octane concentration(ppb)	237.85	423.70	879.38	218.76	398.14	784.33	221.36	391.53	834.28	237.64	398.36	816.94
		Ozone concentration(ppb)	19.18	22.86	24.39	706.76	743.55	710.37	927.33	975.09	931.72	1340.51	1326.32	1332.10
		Acetone concentration(ppb)	623.09	1017.96	2869.24	525.44	989.68	3306.93	664.70	967.67	2918.30	642.95	1022.58	3441.76
4.2.3	Acetone Concentration Test	Ozone concentration(ppb)	16.92	22.24	27.85	614.90	628.32	638.46	939.61	1063.47	976.71	1192.76	1191.46	1255.91
		MEK concentration(ppb)	286.49	451.40	1189.28	317.20	424.22	1180.62	331.62	405.28	1245.62	355.56	432.43	1254.94
		Ozone concentration(ppb)	17.11	19.63	22.29	806.21	766.34	790.25	991.99	952.93	971.81	1428.15	1409.10	1399.60
4.2.3	MEK Concentration Test	Toluene concentration(ppb)	356.53	461.00	977.59	450.18	483.04	980.46	353.98	493.58	881.60	325.44	458.69	1072.69
		Ozone concentration(ppb)	16.36	26.27	33.62	500.61	486.39	490.83	1102.82	1070.76	1114.69	1068.41	1053.39	1060.07
		P-Xylene concentration(ppb)	278.74	513.68	1096.82	269.60	483.94	1027.36	261.88	483.94	945.90	243.35	507.11	1033.09
4.2.4	Toluene Concentration Test	Ozone concentration(ppb)	22.83	27.96	43.92	757.49	709.68	681.89	1126.76	1055.84	1003.17	1286.90	1257.89	1149.26
		p-Xylene Concentration Test												

Section in Thesis	Test Name	Target Compound & Ozone Concentration	Duct No.			
			Duct#1 or Upstream	Duct#2	Duct#3	Duct#4
4.3.1	Repeatability Test	Ethanol concentration(ppb)	500.00			
		Ozone concentration(ppb) Test 4 April 12	23.57	2188.13	2381.48	1055.43
		Ozone concentration(ppb) Test 7 May 12	21.57	1999.51	1111.16	1268.29

Section in Thesis	Test Name	Target Compound	Duct No.	Relative Humidity (%)	Ozone concentration (ppb)
4.3.3	Effect of Relative Humidity	Ethanol 500 ppb	Duct#1 or Upstream	9	20.60
				15	23.57
				20	13.16
				42	13.88
				60	38.42
				9	2248.84
			Duct#2	15	2188.13
				20	2014.29
				30	516.44
				42	760.75
				9	2368.83
				15	2381.48
			Duct#3	30	1322.99
				42	1018.40
				60	904.43
				9	1015.85
				15	1055.43
				30	1117.75
			Duct#4	42	1439.71
				60	1076.50

Section in Thesis	Test Name	Target Compound	Duct No.	Flow Rate (cfm)	Ozone concentration (ppb)
4.3.4	Effect of Flow Rate	Ethanol 500 ppb	Duct#1 or Upstream	49.2	14.50
				79.5	12.44
				97.17	19.80
				111.2	20.00
				146.24	20.63
				38.9	4318.80
			Duct#3	73.7	2379.45
				98.57	1322.99
				99.82	1098.60
				155.92	837.36
				23.7	9926.80
				46.6	3864.50
Duct#4	76.82	1657.52			
	98.77	1117.75			
			151.32	1327.73	

Section in Thesis	Test Name	Target Compound & Ozone Concentration	Duct No.					
4.3.5	Effect of Number of UV-Lamps	Ethanol concentration(ppb)	500					
			Duct No.		Duct#3		Duct#4	
			3 Lamps		11amps		3 Lamps	
			17.45		15.33		2185.91	
			3 Lamps		11amps		917.46	
			17.45		15.33		2185.91	
4.3.6	Efficiency Improvement	Ozone concentration(ppb)	250					
			Duct No.		Duct#3		Duct#4	
			3 Lamps		3		3	
			8.08		5835.16		2183.60	
			3 Lamps		3		3	
			8.08		5835.16		2183.60	

## ***Appendix D: Light Intensity of the UV-lamps in Catalyst Surface***

For measuring light intensity of the UV-lamps in UV-PCO system, 254 nm and 185 nm wavelength sensors were applied. Two UV-lamps together were measured since in each UV-PCO reactor two lamps were installed. Light intensity was measured 2 inches away from the lamps for 10 minutes and average of the reading in different point of the catalyst surface was taken as that point adsorbed light intensity.

1	2	3
4	5	6
7	8	9

<i>Light intensity measured by 254 nm wavelength sensor 2 inches away from the lamps in catalyst surface place (mW/cm<sup>2</sup>)</i>										
	<b>Point 1</b>	<b>Point 2</b>	<b>Point 3</b>	<b>Point 4</b>	<b>Point 5</b>	<b>Point 6</b>	<b>Point 7</b>	<b>Point 8</b>	<b>Point 9</b>	<b>Average of all points</b>
<b>Duct # 1</b>	0.195	0.131	0.195	7.66	4.04	5.99	3.36	2.06	2.02	2.850
<b>Duct # 3</b>	0.713	0.118	0.343	7.6	3.28	8.08	2.39	1.71	3.8	3.115
<b>Duct # 4</b>	0.378	0.125	0.382	6.33	3.97	7.68	4.2	2.1	3.24	3.156

<i>Light intensity measured by 185nm wavelength sensor 2 inches away from the lamps in catalyst surface place (mW/cm<sup>2</sup>)</i>	
<b>Duct No.</b>	<b>Average of all points</b>
<b>Duct # 1</b>	-
<b>Duct # 3</b>	0.88
<b>Duct # 4</b>	0.99